Pacific Northwest
NATIONAL LABORATORY
Proudly Operated by Battelle Since 1965

Nuclear Waste Glass Corrosion

JD VIENNA

Pacific Northwest National Laboratory, Richland, WA

ICTP-IAEA International School on Nuclear Waste
Actinide Immobilization, September 10-14, Trieste, Italy

PNNL-SA-138258

Outline

- Vitrification as a technology to immobilize radioactive wastes
- General glass corrosion
- Reaction rates
- Residual rates
- Acceleration or Stage III behavior
- Glass as a barrier
- Current models for prediction of glass corrosion
- Radiation impacts
- References

Nuclear Waste Glasses

Nuclear Waste Glasses Worldwide

- Vitrification is the reference technology to immobilize highly radioactive nuclear wastes worldwide
- **Examples** of sites producing alkali-borosilicate glasses for waste immobilization are listed

Site	Operated	Melter Tech	Produced Glass Mass, t	Disposal Glass Mass, t	Planned Disposal
Pamela, Belgium	1985-1989	JHCM	650	650	Clay
AVM, France	1978-2012	HWIM	1,220	1,220	Clay
LaHague, France	1989-Present	HWIM,CCIM	7,032*	NR	Clay
Karlsruhe, Germany	2010-2012	JHCM	208	6,450*	Salt or Clay
Tokai, Japan	1995-Present	JHCM	700	NR	TBD
Rokkasho, Japan	TBD	JHCM	0	NR*	TBD
Sellafield, UK	1990-Present	HWIM	2,500*	2,700	TBD
WVDP, US	1996-2002	JHCM	574	574	TBD
DWPF, US	1996-Present	JHCM	7,200	13,867	TBD
WTP HLW, US	TBD	JHCM	0	32,000	TBD
WTP LAW, US	TBD	JHCM	0	527,838	Sand

JHCM- Joule-heated ceramic melter
HWIM- Hot-walled induction melter
CCIM- Cold-crucible induction melter

Based on Gin et al. 2013

Silicate Glass Structure

- Glass: an amorphous, metastable, solid
- Structure dependent on composition and temperature history

Example Crystal

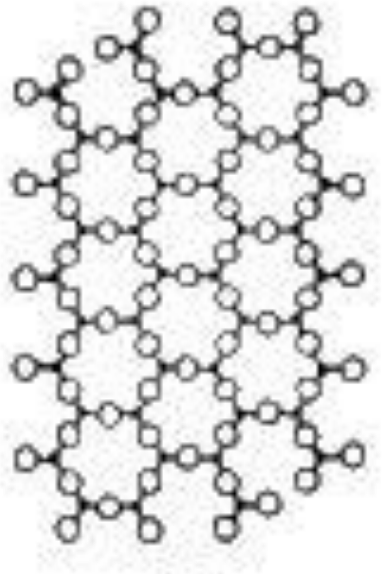

(a)

Example Glass

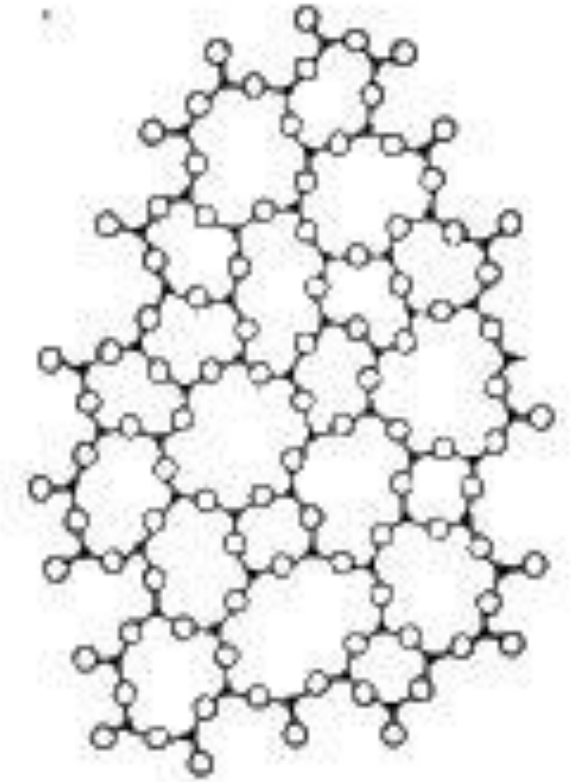

(b)

Silicate Glass Structure, cont.

- $[SiO_4]^{4-}$ tetrahedra form the primary “network”
- Additives and waste components chemically bound within solid
  - Network formers (e.g., Si^{4+}, B^{3+}, P^{5+})
    - linking or “polymerizing” the anion complexes (e.g., SiO_4^{4-}) leads to a 3D network
    - coordination number of 3 or 4 (generally)
  - Network modifiers (e.g., Na^{+}, Ca^{2+})
    - breakup or “depolymerize” the network
    - coordination number 6 to 8 (generally)
  - Intermediates (e.g., Al^{3+}, Fe^{3+})
    - can either reinforce the network (coordination number of 4) or depolymerize the network (typically for coordination number of 6 to 8)

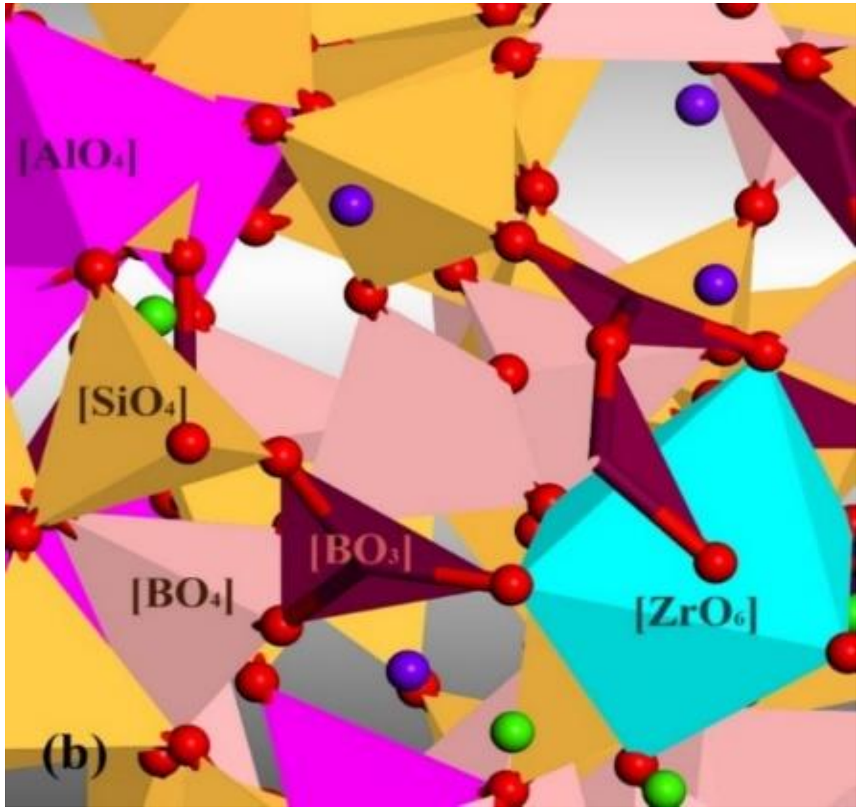

Modeled structure of ISG
Du and Rimsza 2017

Glass Structure, cont.

▶Rings and Cages

- SiO_4^{4-}, BO_4^{5-} and AlO_4^{5-} form three-dimensional network structure with ring size centered at around 6.

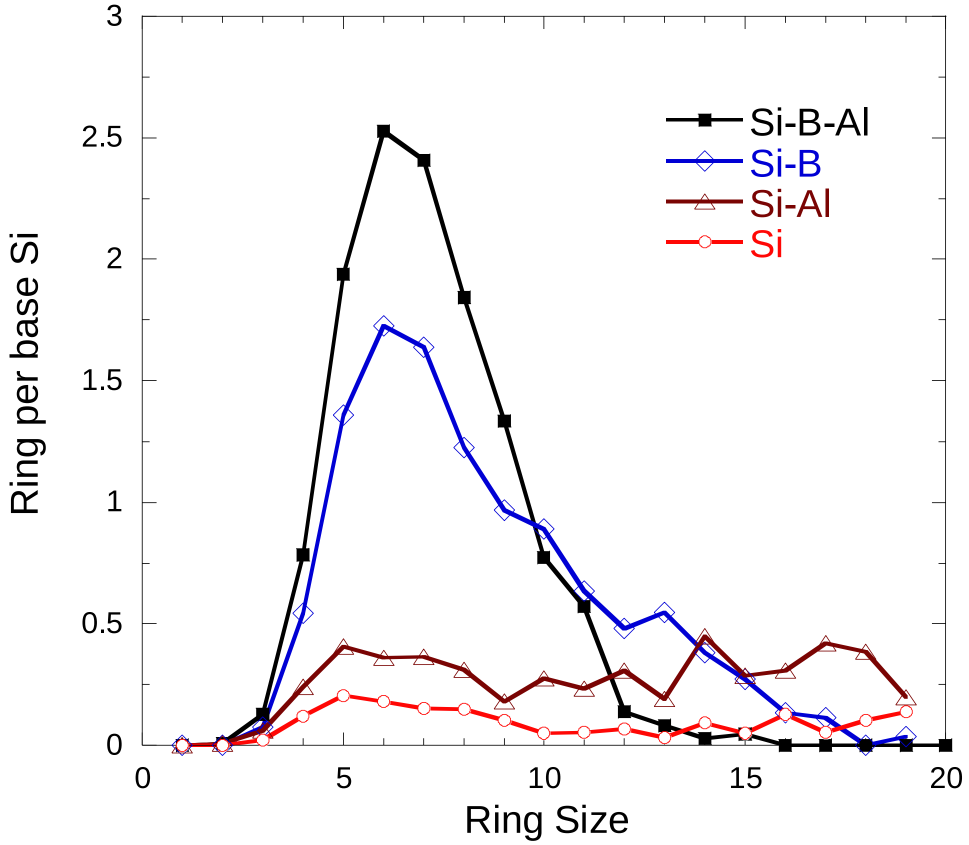

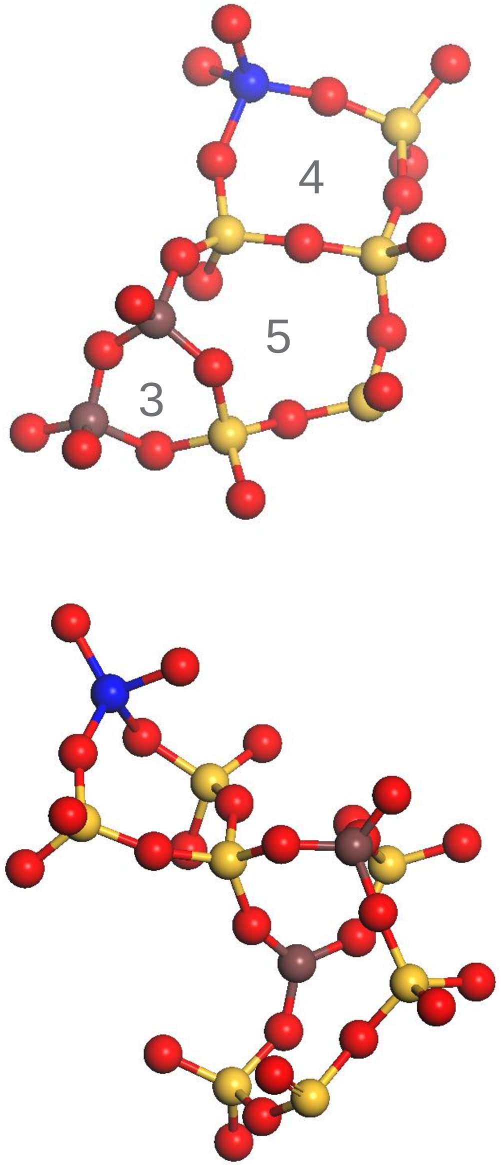

Xiang. et al. 2013

Composition Effects on Properties Important to U.S. Waste Glasses

Oxide	Al_2O_3	B_2O_3	CaO	Cr_2O_3	Fe_2O_3	K_2O	Li_2O	MgO	Na_2O	SiO_2	ZnO	ZrO_2	Other
Viscosity	↑	↓	↓	↔	↔	↓	↓	↓	↓	↑	↔	↑	
EC	↔	↔	↔	↔	↔	↑	↑	↔	↑	↓	↔	↔	
T_L, C_T (spinel)	↑	↓	↓	↑	↑	↓	↓	↔	↓	↓	↑	↑	NiO, MnO↑
PCT	↓↑	↓↑	↔	↔	↔	↑	↑	↑	↑	↓	↔	↓	
VHT	↓↑	↓↔	↔	↔	↔	↑	↑	↔↑	↑	↓	↔	↓	
Nepheline	↑	↓	↑	↔	↔	↑	↑	↔	↑	↓	↔	↔	
Salt	↑	↓	↓	↑	↔	↓	↓	↔	↓	↑	↔	↔	SO_3, Cl ↑, V_2O_5↓
TCLP	↓	↑	↔	↔	↔	↑	↑	↔	↑	↓	↑	↓	MnO↑
Corrosion	↓	↔	↔	↓	↓	↑	↑	↔	↑	↓	↓	↓	NiO↓

↑ - Increase property
↓ - Decrease property
↔ - Small effect on property
multiple arrows are for non-linear effects, first is for lower concentrations

Glass Composition Design

- A range of glass compositions are generated
- Glasses are designed to meet specific physical, chemical, and regulatory compliance constraints
- Glasses are designed specifically for waste compositions to be immobilized, examples:
    - US tank waste primarily composed of cold chemicals with high composition variability and low radioactivity
    - French UOx HLW is primarily fission products and high radioactivity
- Performance related properties used in glass formulation are typically responses to one or more standardized durability test, examples:
    - 100°C Soxhlet
    - 7-day, 90°C, Product Consistency Test (PCT)
    - 28-day, 90°C, Materials Char. Center test 1 (MCC1)
    - 200°C Vapor Hydration Test (VHT)

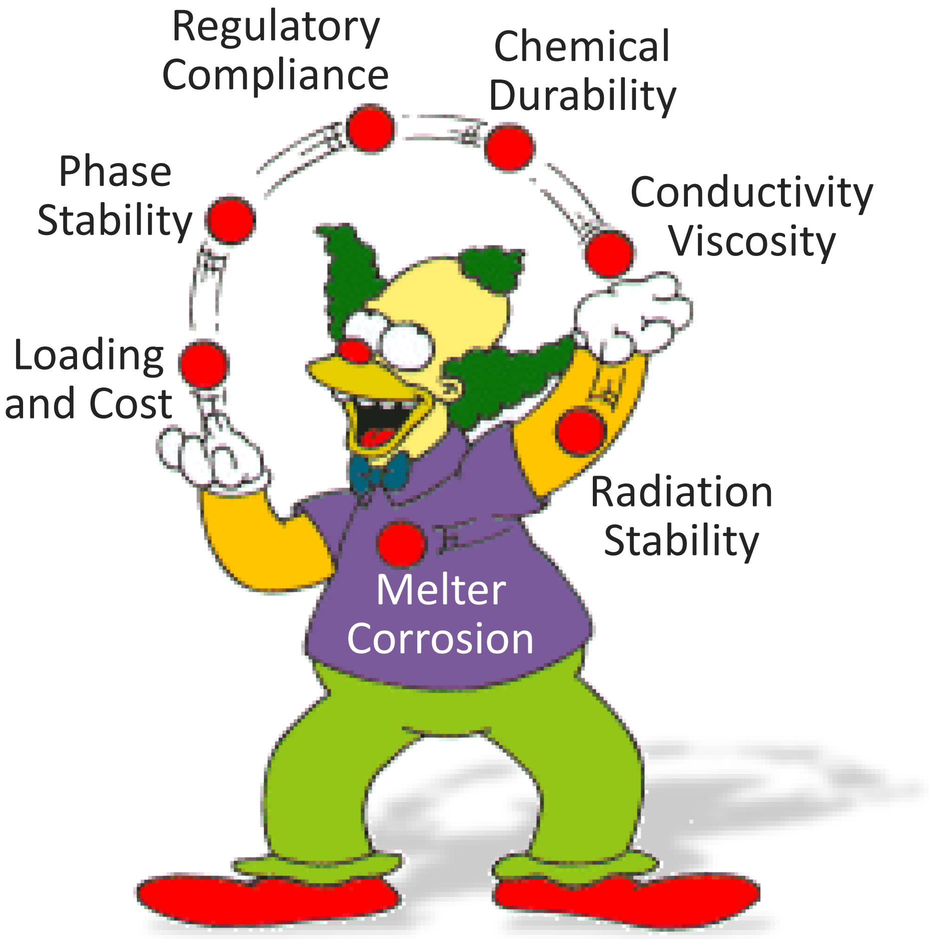

Vienna 2014 & The Simpsons

Glass Compositions, wt%

Oxide	France		Japan	UK			Belgium		DWPF		WTP HLW		WTP LAW	
	R7/T7	AVM	P0798	Magnox	AGR	Blend	Pamela	WVDP	Min	Max	Min	Max	Min	Max
Al_2O_3	4.9	9.7	5.0	5.1	<0.1	1.9	20.2	6.0	4.3	9.8	2.0	18.9	6.1	6.1
B_2O_3	14.0	17.0	14.2	16.8	18.0	18.3	25.6	12.9	4.3	8.3	4.0	20.0	10.0	10.0
BaO	0.6	0.3	0.5	0.5	0.6	1.2	-	0.2	-	-	-	-	0	0
CaO	4.0	0.2	3.0	-	-	-	5.0	0.5	0.5	1.4	0	3.1	2.0	7.0
Cs_2O	1.4	0.7	0.8	1.1	1.1	1.6	0	-	-	-	-	-	0	0
Fe_2O_3	2.9	1.9	2.0	1.7	0.7	1.9	0.5	12.0	8.2	12.6	1.9	17.4	5.5	5.5
K_2O	-	-	-	-	-	-	-	5.0	-	-	0	2.6	0.01	3.4
Li_2O	2.0	0.4	3.0	4.0	4	4.8	3.5	3.7	3.5	5.6	0	6.0	0	4.3
MgO	-	3.6	0	5.6	<0.1	1.3	-	0.9	0.3	2.2	-	-	1.5	2.8
MoO_3	1.7	0.8	1.5	1.6	1.9	2.0	0	-	-	-	-	-	-	-
Na_2O	9.9	17.7	10.0	8.3	8.9	8.1	8.8	8	11.3	13.6	4.1	21.4	5.4	21.0
P_2O_5	-	1.2	-	0.2	0.1	-	-	1.2	0.2	0.6	0	2.5	0.0	1.4
SiO_2	45.5	41.4	46.6	46.0	49.2	46.3	35.3	41.0	44.8	54.6	31.0	53.0	43.3	50.1
TiO_2	-	-	-	-	-	-	-	0.8	0.0	0.7	0	0.1	1.4	1.4
ZnO	2.5	-	3.0	-	-	-	0	-	-	-	0	4.0	3.5	3.5
ZrO_2	2.7	1.0	1.5	1.6	1.8	2.4	0.1	1.3	0.1	0.2	0	13.5	3.0	3.0
$[Ln,An]_2O_3$	4.9	3.1	6.1	4.2	10.1	8.4	0	4.6	1.0	3.5	0	8.5	-	-
Minors	3.0	1.1	2.9	3.3	3.6	1.7	1.6	1.9	1.7	10.0	3	11.6	0	0.2

General Aspects of Silicate Glass Corrosion

General Observations

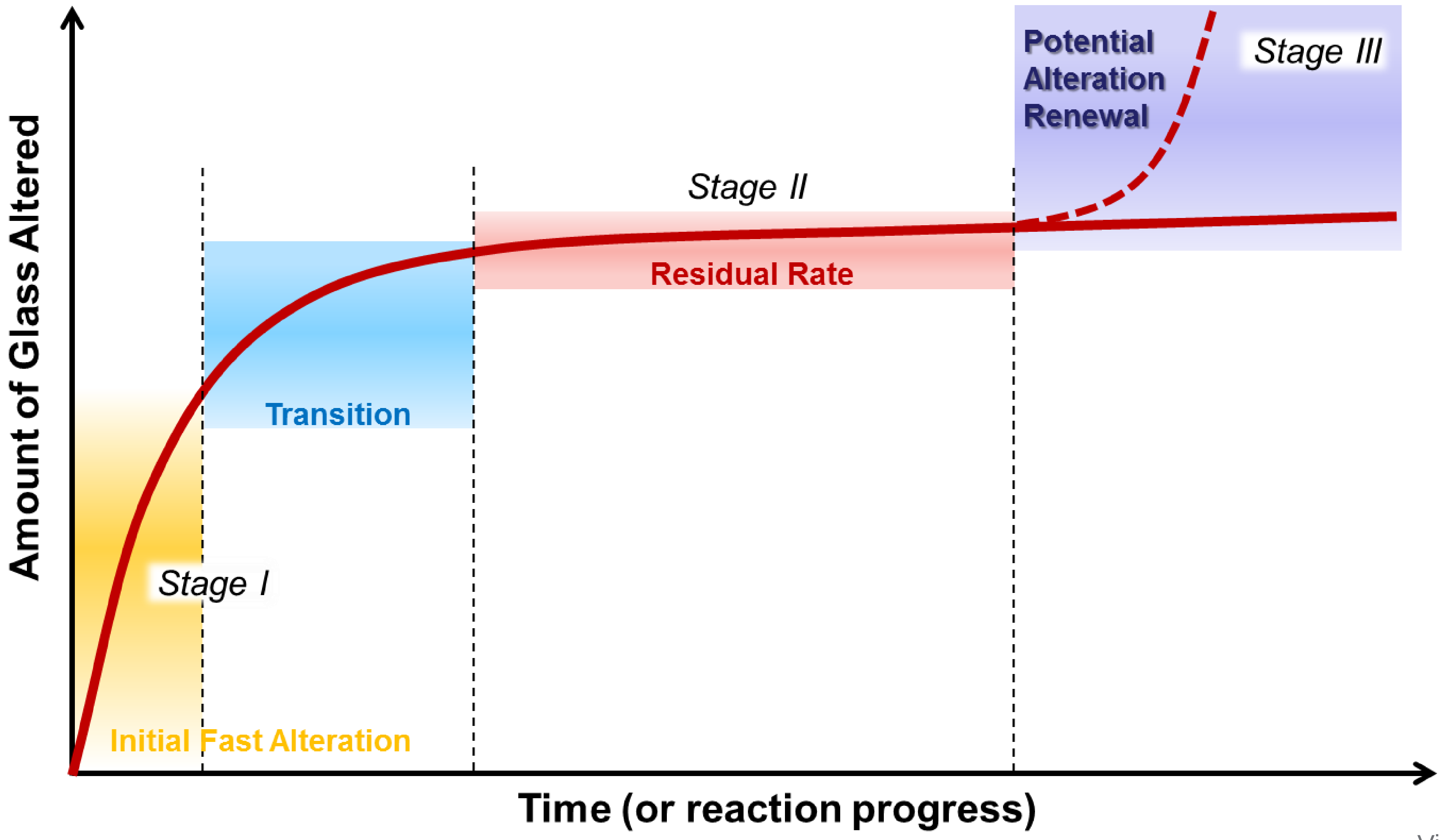

Vienna et al. 2013

General Observations, cont.

Reactive Behaviors

- Selective dissolution of glass network
- Restructuring of glass to form gel (dissolution reprecipitation under some conditions)
- Evolution of gel structure
- Dissolution of gel
- Precipitation of 2nd phases

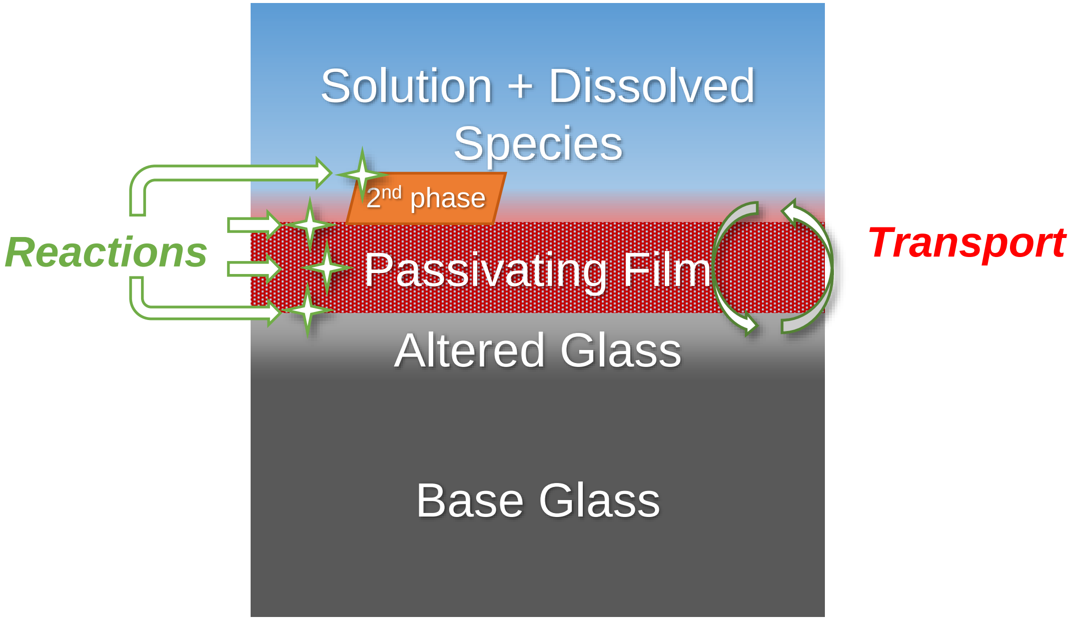

Transport Behaviors

- Reactive transport of water and dissolved species through tortuous passivating film
- Ion exchange in altered material

General Observations, Cont.

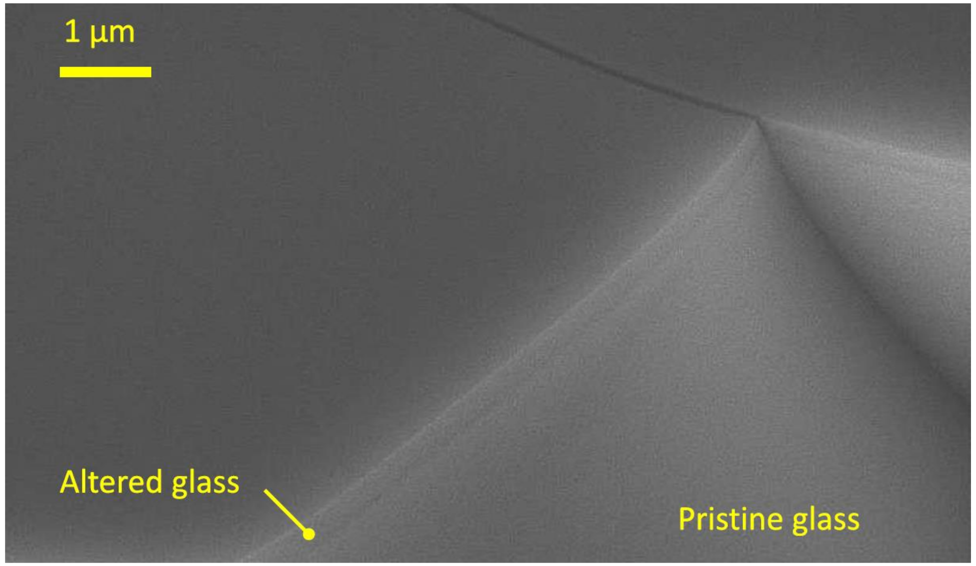

Gin et al. 2017

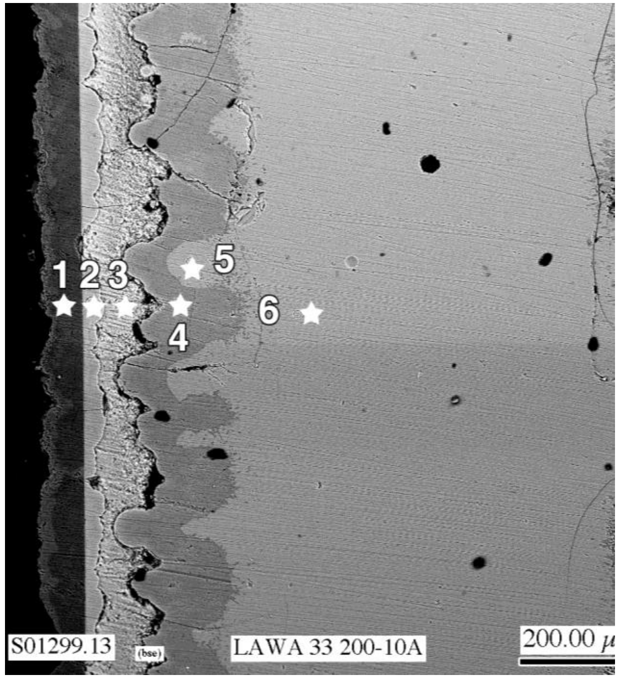

Vienna et al. 2001

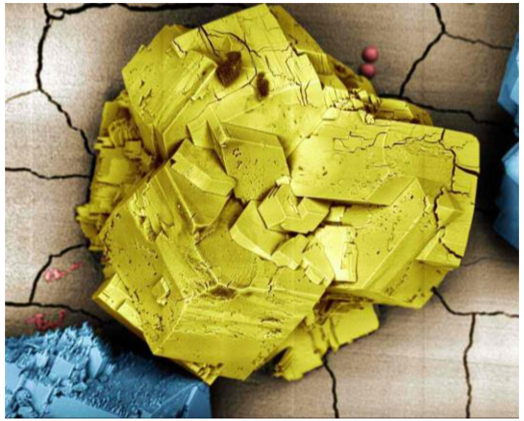

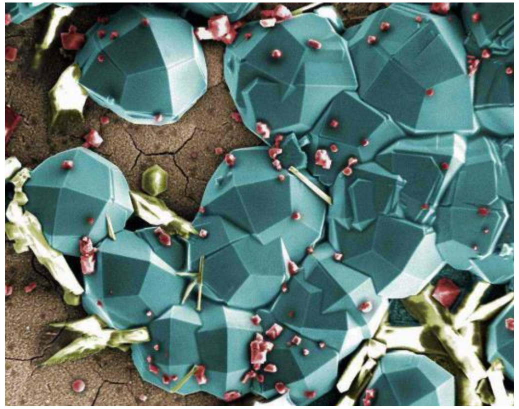

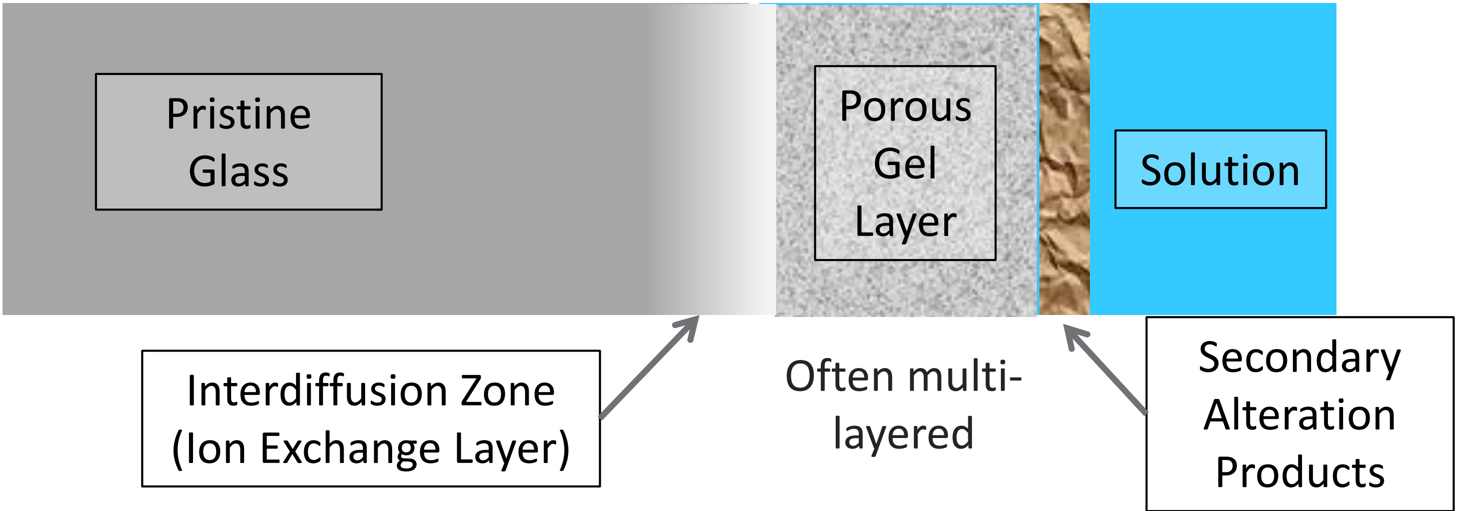

Pristine Glass

Porous Gel Layer

Solution

Interdiffusion Zone (Ion Exchange Layer)

Often multi-layered

Secondary Alteration Products

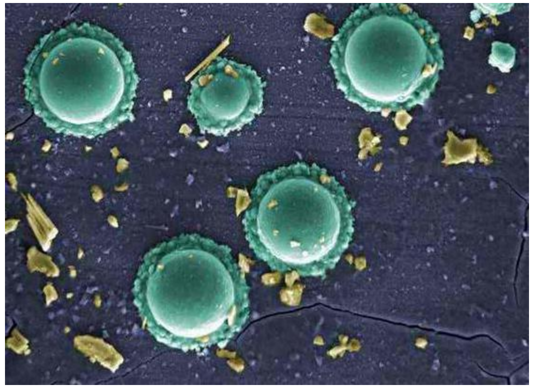

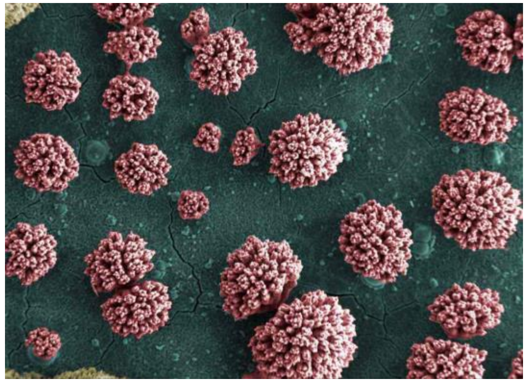

Research Challenges

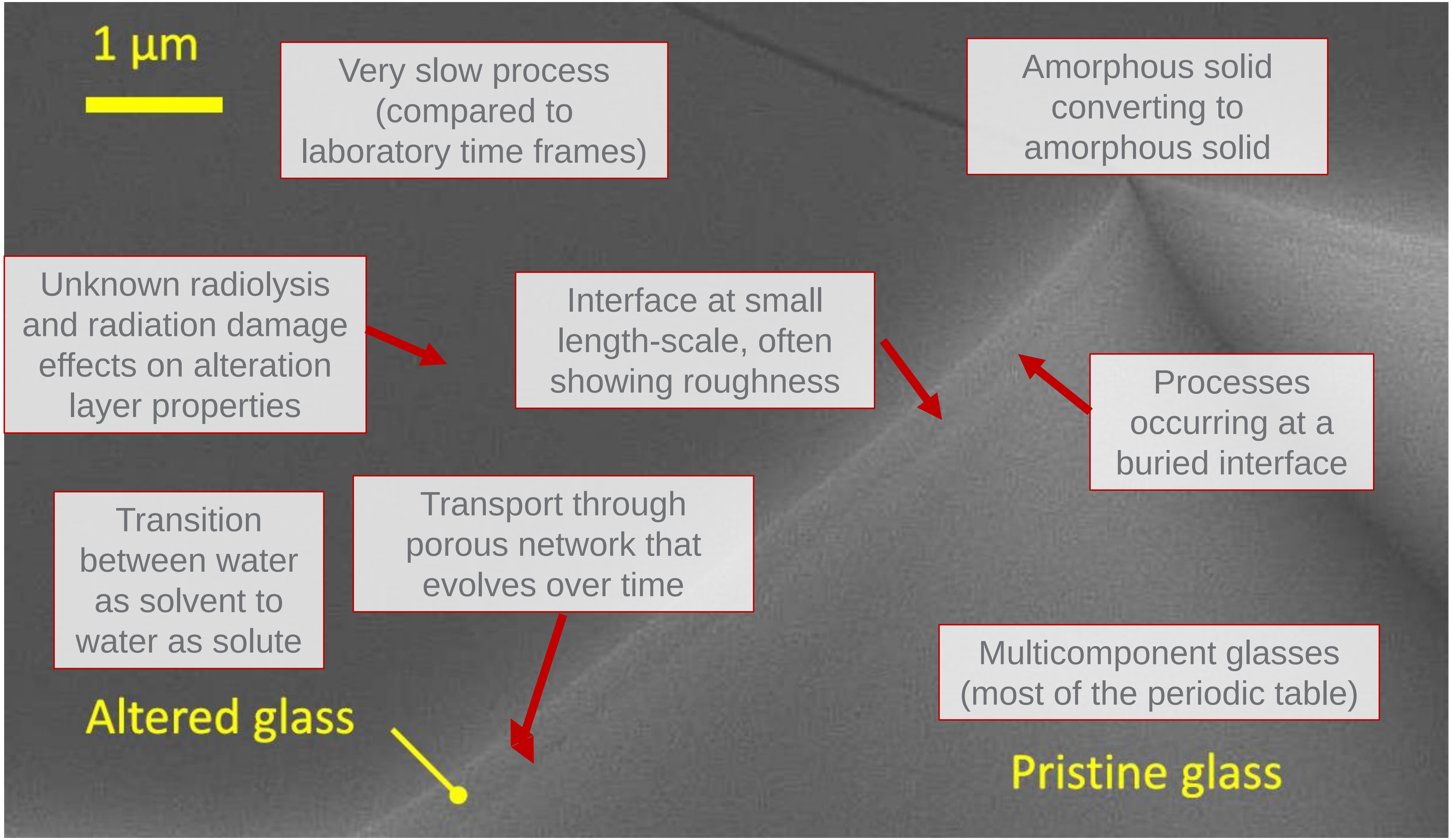

Very slow process (compared to laboratory time frames)

Amorphous solid converting to amorphous solid

Unknown radiolysis and radiation damage effects on alteration layer properties

Interface at small length-scale, often showing roughness

Processes occurring at a buried interface

Transition between water as solvent to water as solute

Transport through porous network that evolves over time

Multicomponent glasses (most of the periodic table)

Focus on Reaction Rates

Example Chemical Reactions

Ion Exchange

Hydrolysis

Condensation

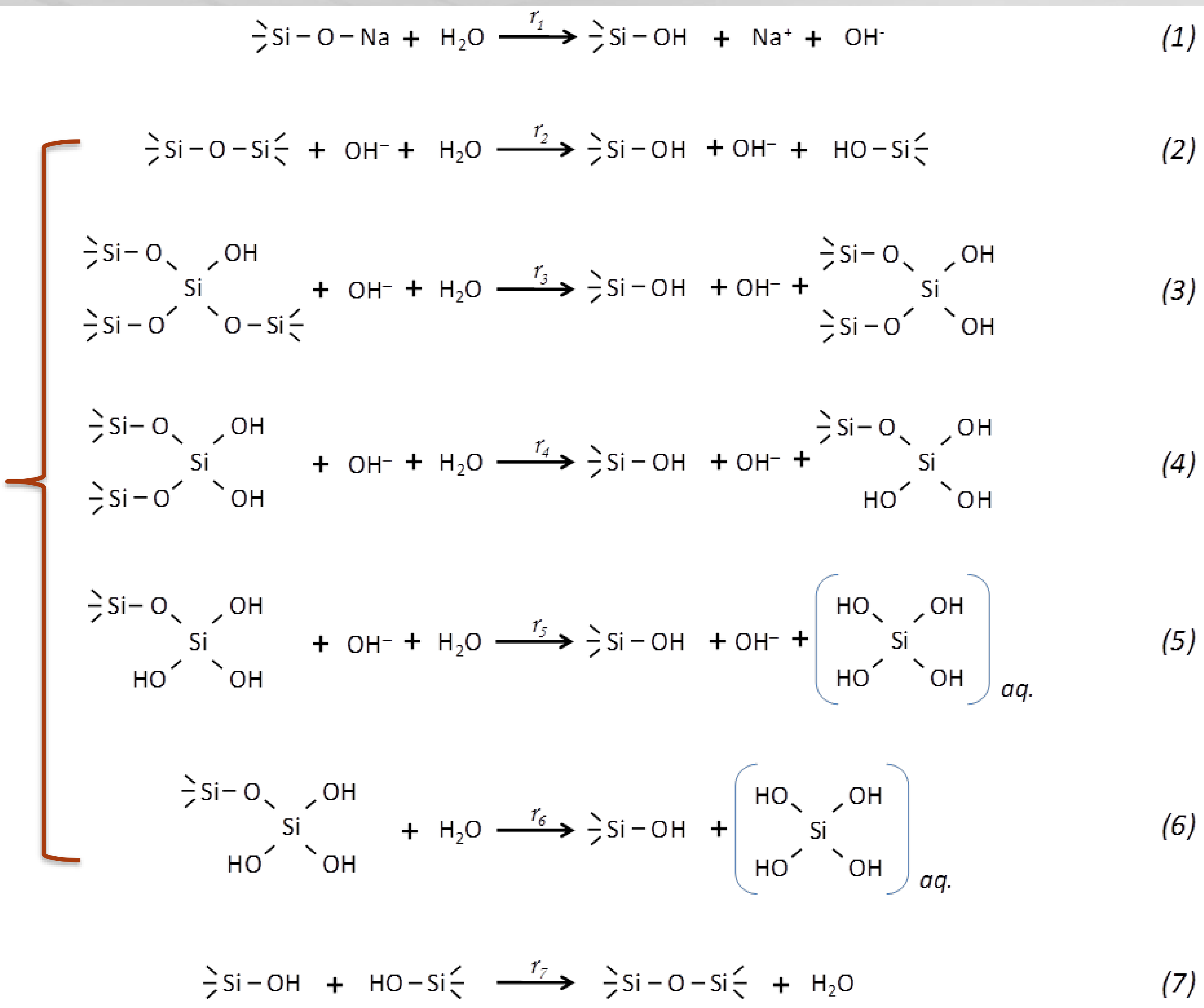

$$\equiv Si-O-Na + H_2O \xrightarrow{r_1} \equiv Si-OH + Na^+ + OH^- \quad (1)$$

$$\equiv Si-O-Si\equiv + OH^- + H_2O \xrightarrow{r_2} \equiv Si-OH + OH^- + HO-Si\equiv \quad (2)$$

$$\equiv Si-OH + HO-Si\equiv \xrightarrow{r_7} \equiv Si-O-Si\equiv + H_2O \quad (7)$$

Rieke et al. 2014

Example Reaction Rate Model (without transport)

- Forward dissolution rate, r_f = the rate at which glass dissolves into solution at specific values of the T and pH in the absence of back reactions
- Dissolution rate most likely to be directly impacted by structure and composition of glass

$$\cancelto{r_f}{r_i} = v_i k_0 a_{H^+}^{\pm\eta} \exp\left(\frac{-E_a}{RT}\right) \cancelto{1}{\left[1-\left(\frac{Q}{K_g}\right)^{\sigma}\right]} + \begin{matrix}\text{potential}\\ \text{other terms}\end{matrix}$$

r_i = normalized glass dissolution rate
(based on element *i*), g m^{-2} d^{-1}
r_f = *forward glass dissolution rate,* g m^{-2} d^{-1}
v_i = stoichiometric coefficient for element *i* in glass
k_0 = intrinsic rate constant, g m^{-2} d^{-1}
a_{H+} = hydrogen ion activity
η = pH power law coefficient (dependent on pH regime)

E_a = apparent activation energy, J mol^{-1}
R = gas constant, J mol^{-1} K^{-1}
T = absolute temperature, K
Q = ion-activity product of rate controlling species
K_g = pseudo-equilibrium constant for glass
σ = reaction order (Temkin coefficient)

Isolation of Individual Effects

- Single-pass flow-through test (SPFT, ASTM C1662) can be used to measure effects of individual parameters
- Measure impacts of pH, T, $[H_4SiO_4]$ and $[Al(OH)_4^-]$
- Avoid feed-back effects by high flow rate/surface area (q/s)

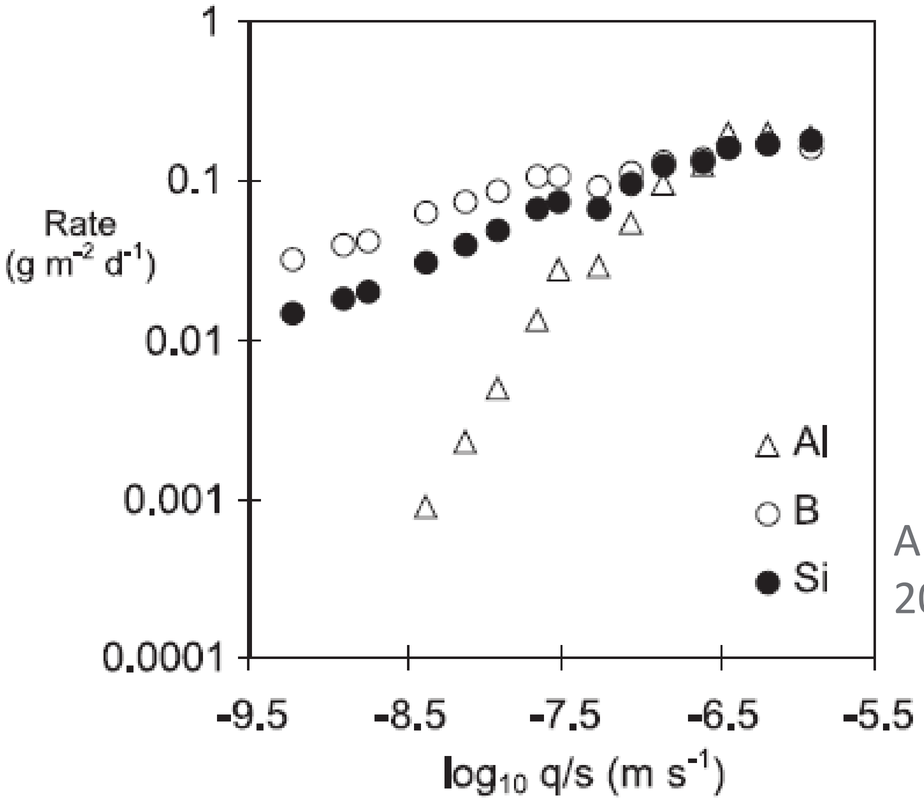

Abraitis et al. 2000

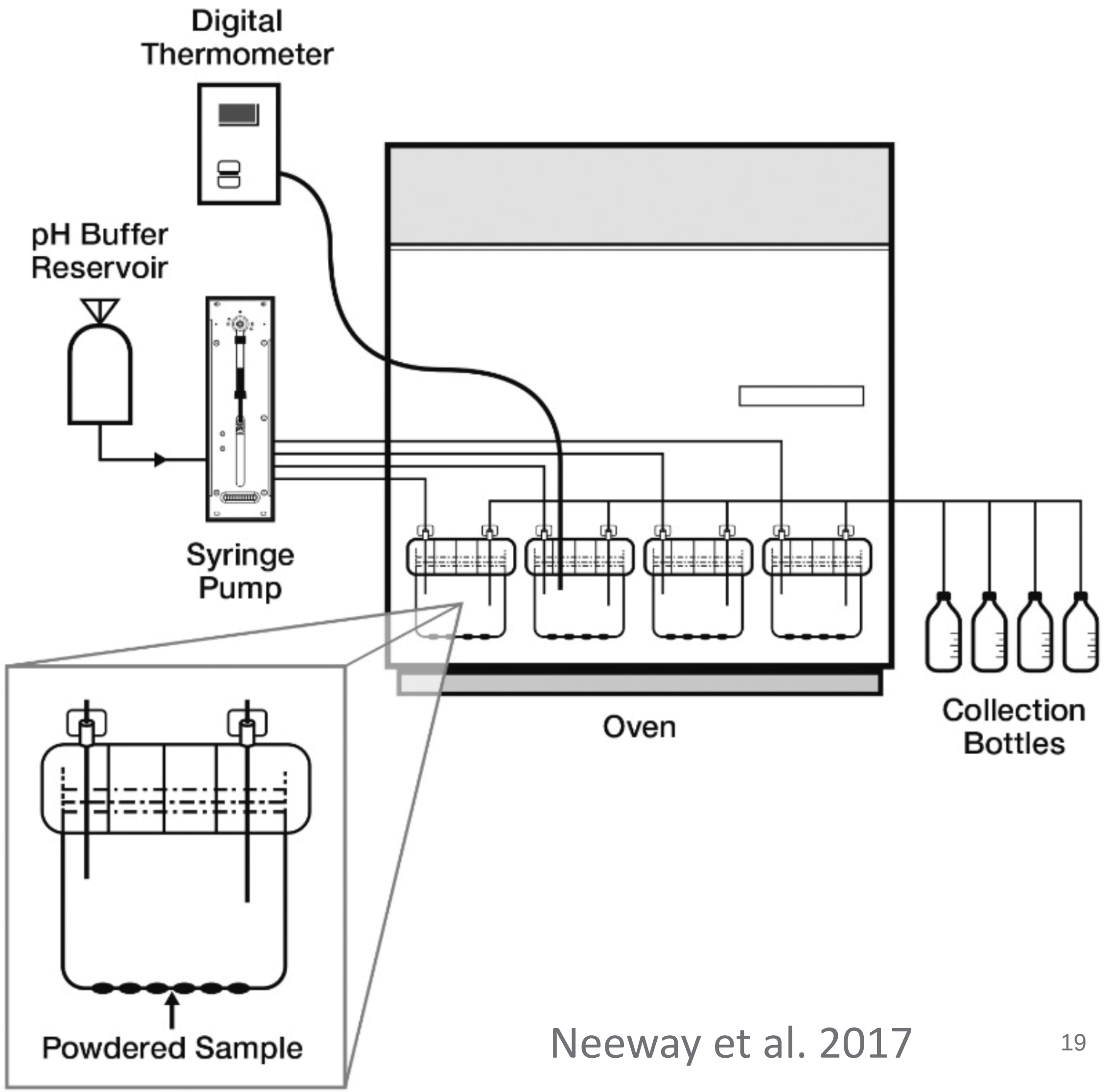

Neeway et al. 2017

pH Impacts

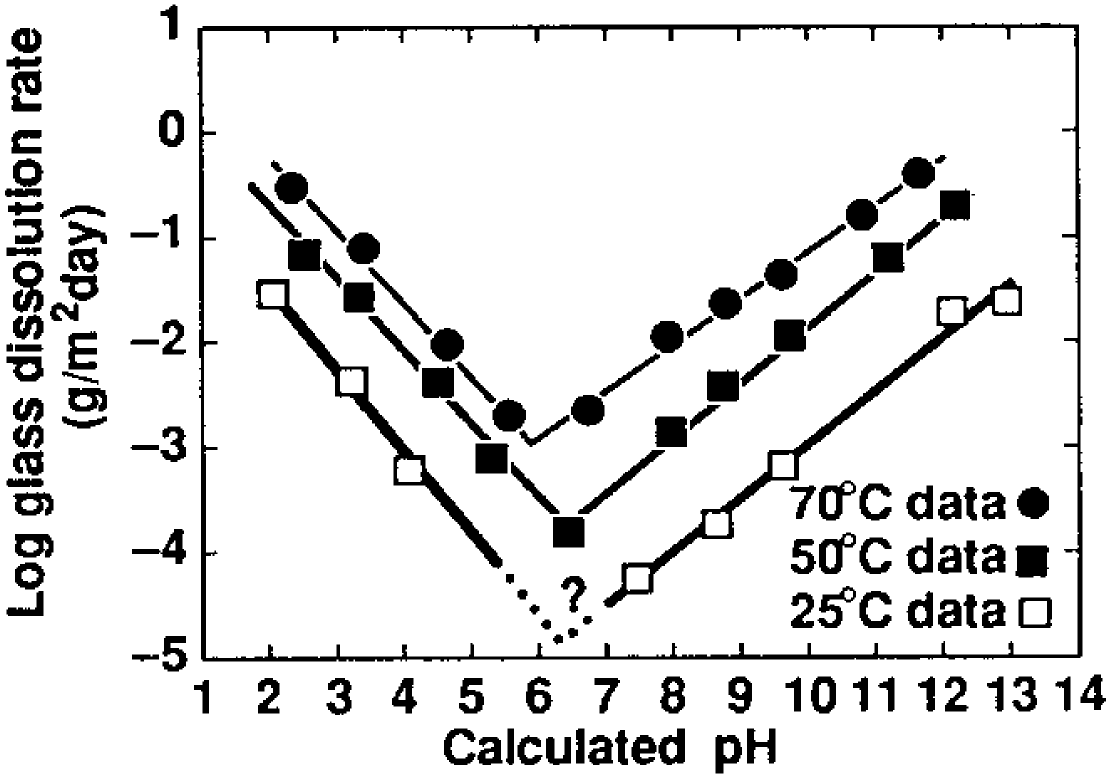

- Hydrolysis rate depends on:
  - Bond length and bond angle (stretched O-Si-O bonds favors hydrolysis)
  - Site protonation (high or low pH)

Knauss et al. 1990

Temperature Impacts

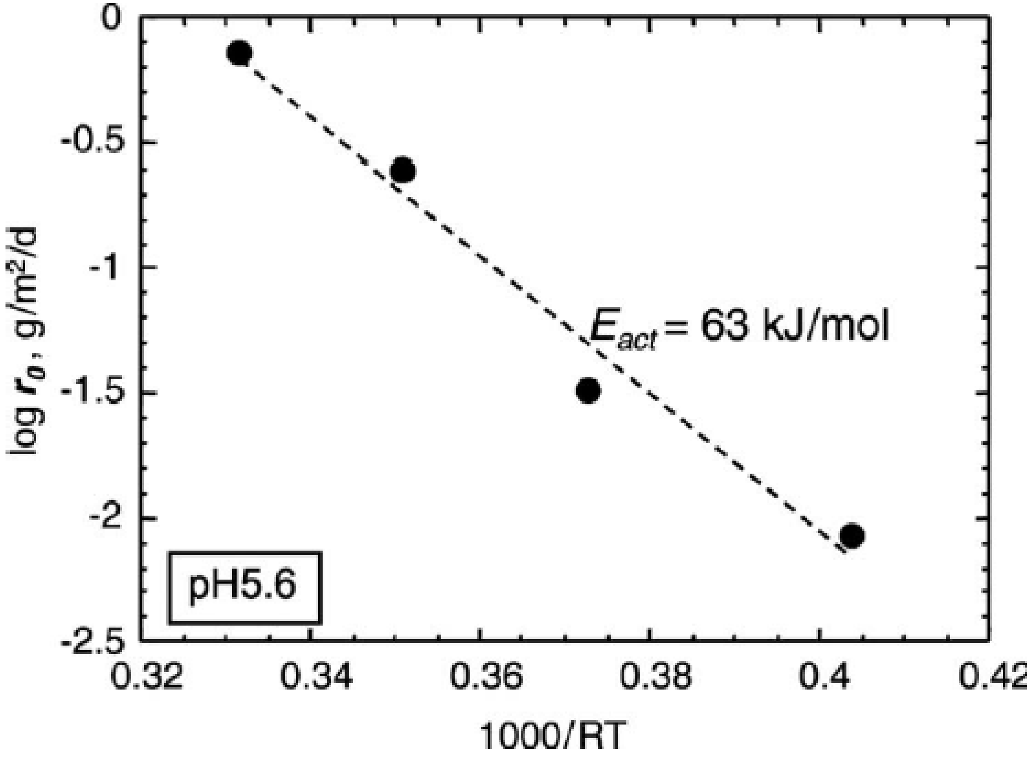

Inagaki et al. 2012

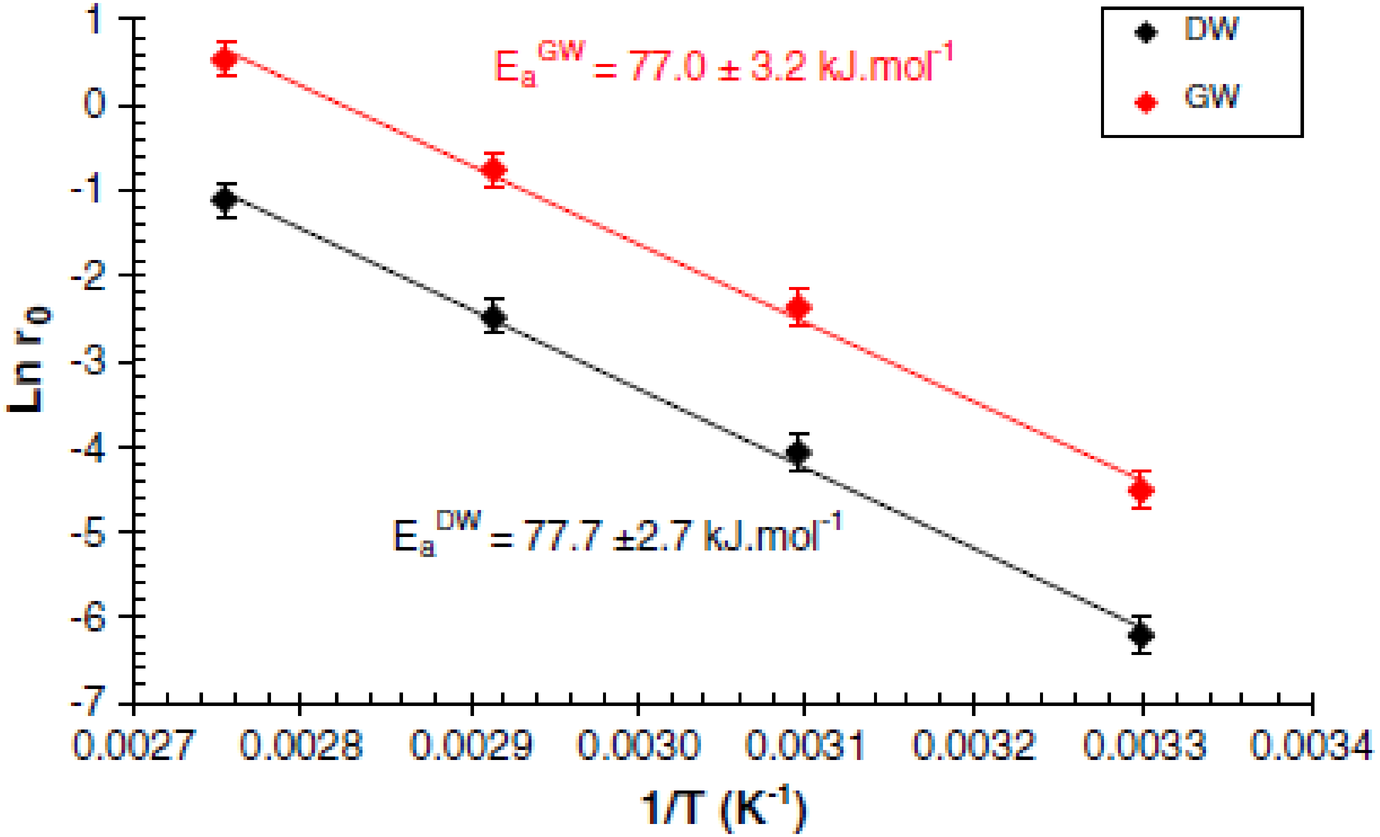

Jollivet et al. 2012

H_4SiO_4 Concentration Impacts

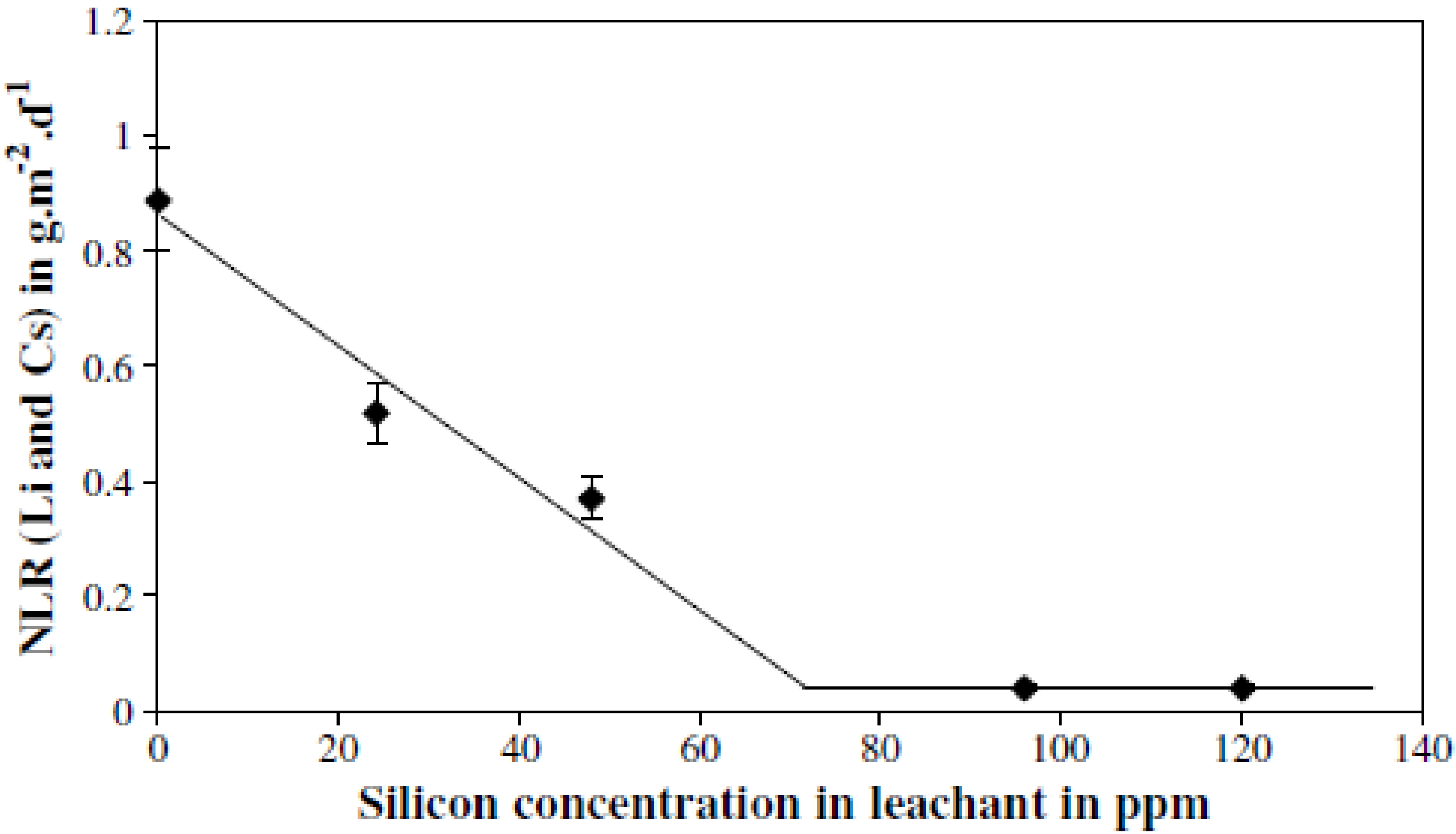

Ferrand et al. 2006

Aluminate Effects

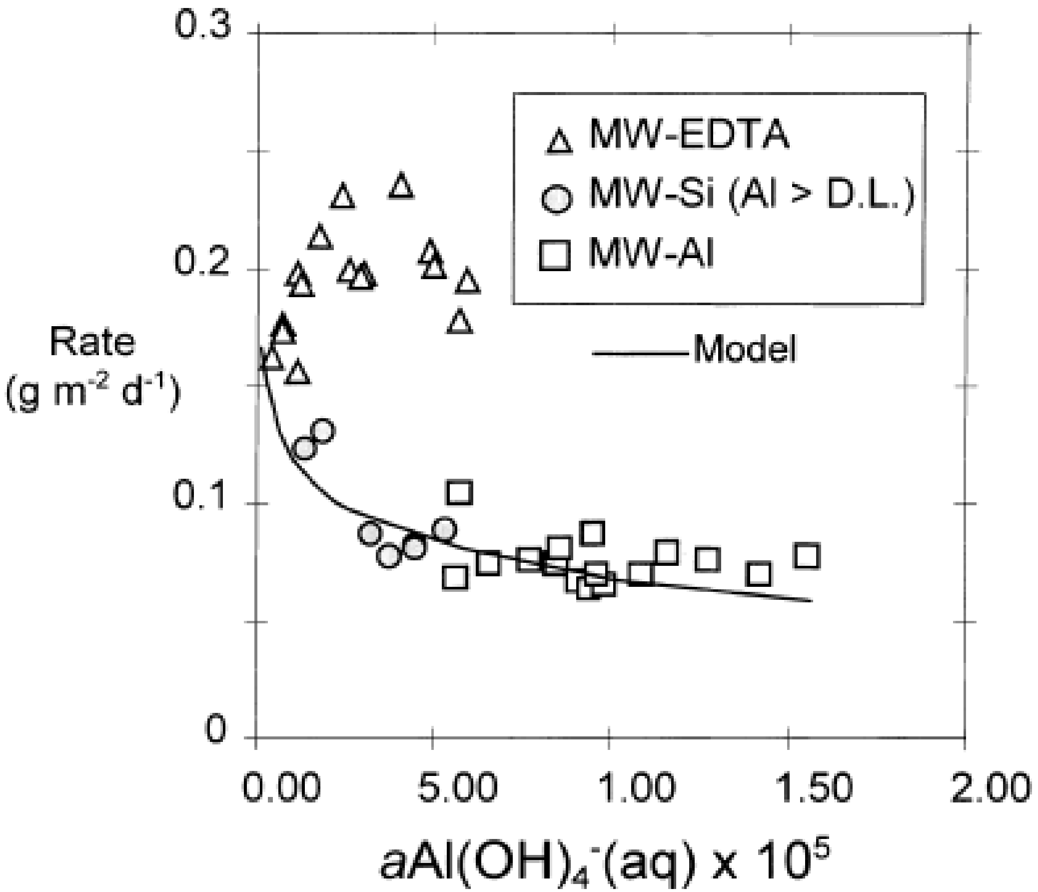

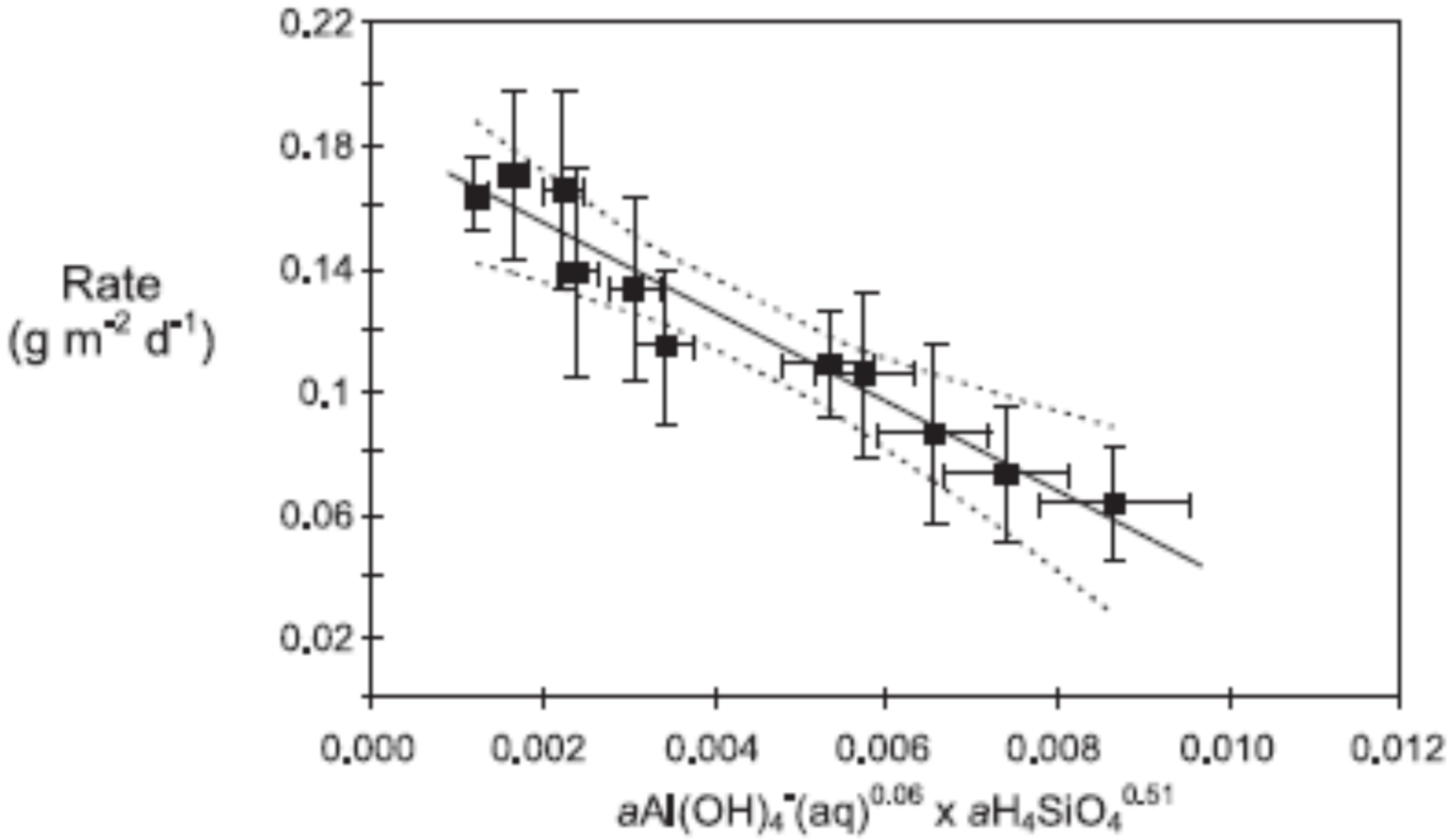

Abraitis et al. 2000ab

What is New?

Glass Composition Effects on Forward Rate

- 19 glasses all measured by SPFT with systematic variation in pH (7 to 13) and T (23° to 90°C)
- Include broad range of compositions (US HLW glasses, US LAW glasses, International glasses)

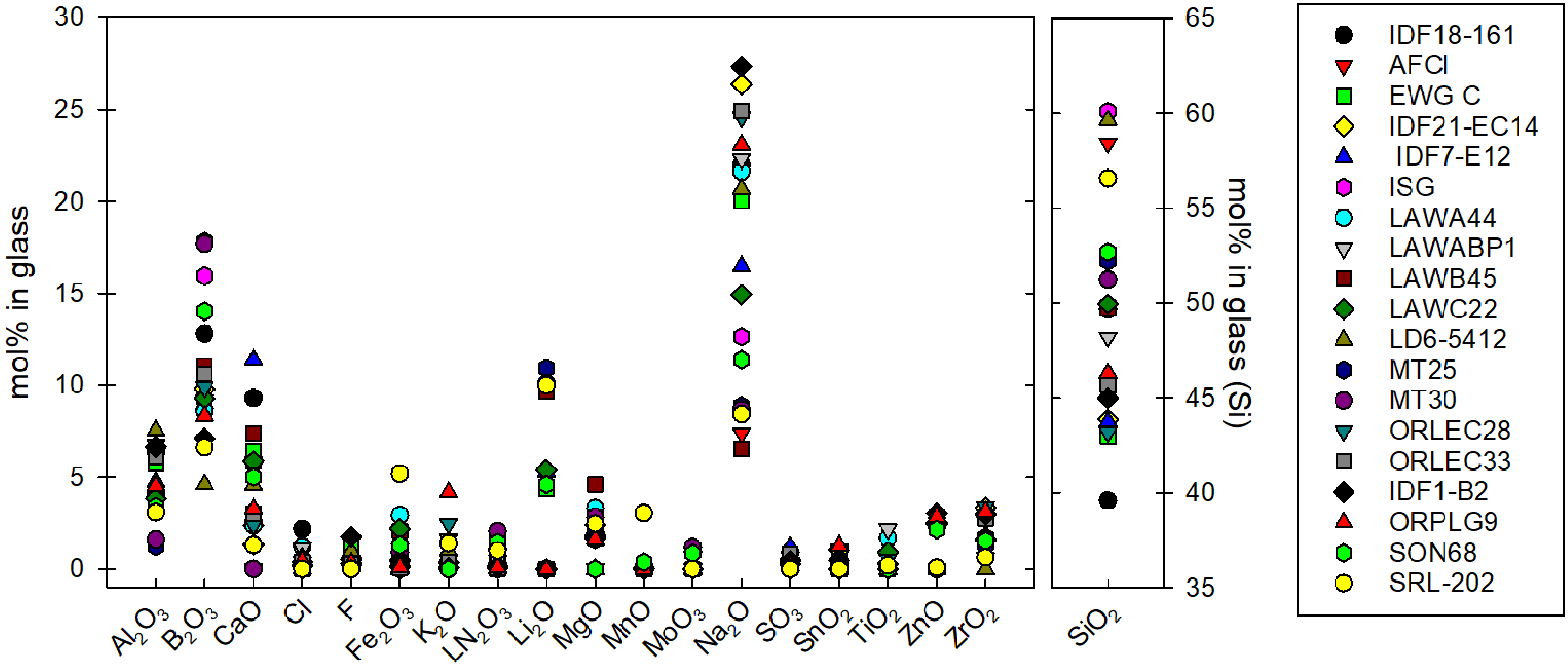

Modeling the Data for Individual Glass

- Measure r_f of glass with systematic variation in pH and T
- Fit data to linear equation:

$$\log[r_f] = \log[k_0] + \eta \cdot pH - E_a \cdot \frac{\log[e]}{RT}$$

$\mathrm{Log}[k_0] = 8.37 \pm 0.92\ \mathrm{gm^{-2}d^{-1}}$
$\eta = 0.396 \pm 0.060$
$E_a = 81.6 \pm 6.1\ \mathrm{kJmol^{-1}}$
$R^2 = 0.983$
RMSE = 0.141

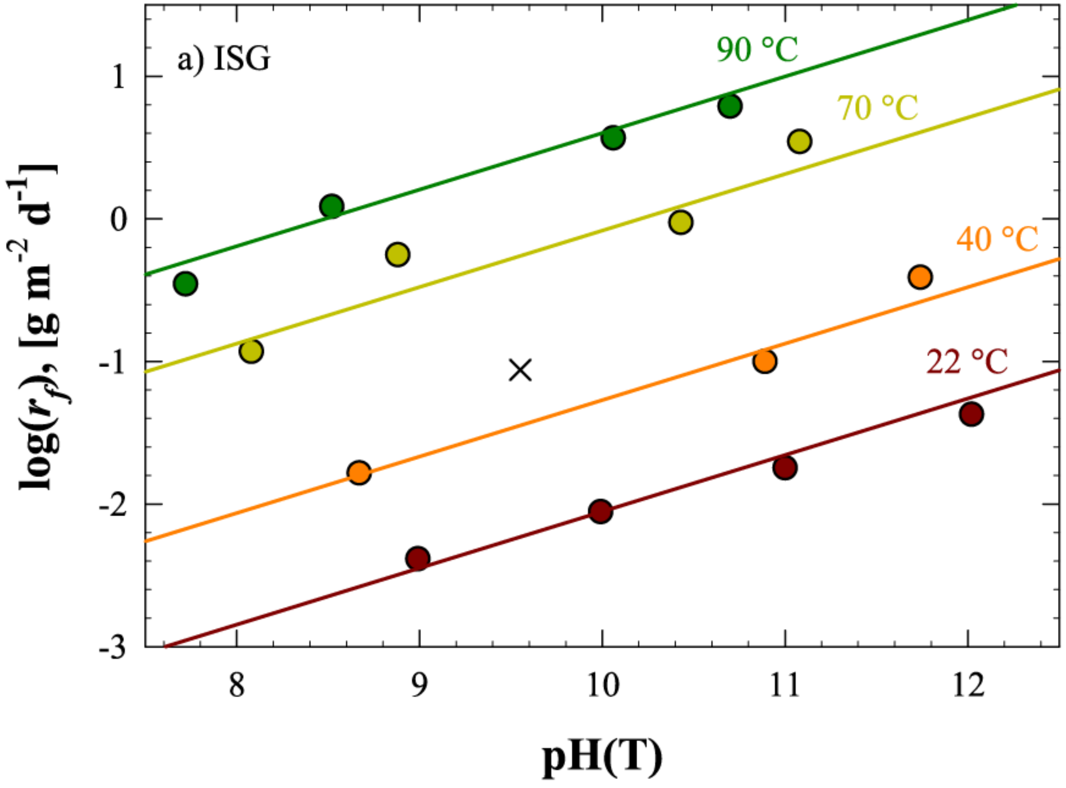

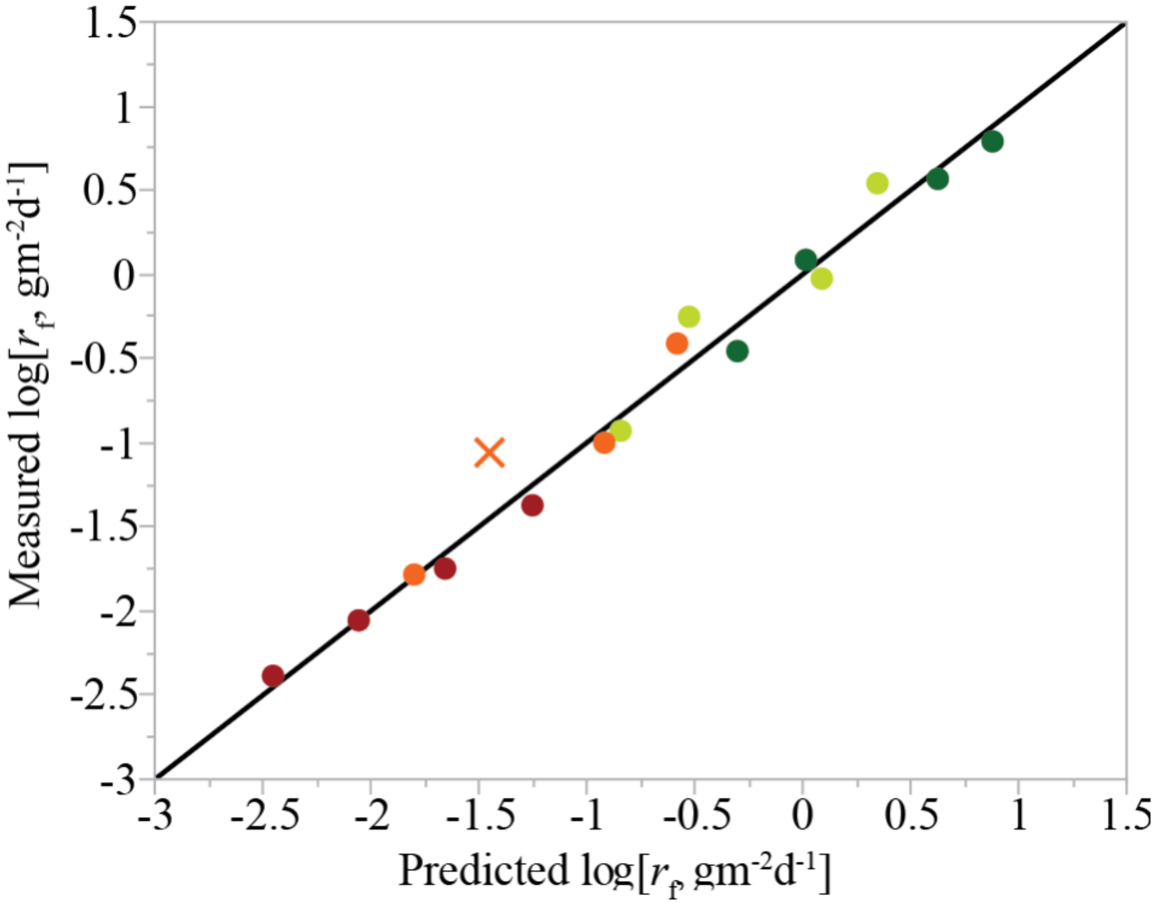

Simultaneously Fit r_f to pH, T, and Composition

- Model explaining 90% of variation in log[r_f] data obtained with no composition effects (R^2_{fit} = 0.896, R^2_{val} = 0.894, RMSE = 0.323)
- Three glasses have noticeably higher log[r_f]
- Composition effects only found in log[k_0] term
- Composition effects model shows most significant composition effect is estimated fraction tetrahedra from $^{[4]}$B ($f^{[4]}$B)
  - Effect non-linear, best modeled by step-function change

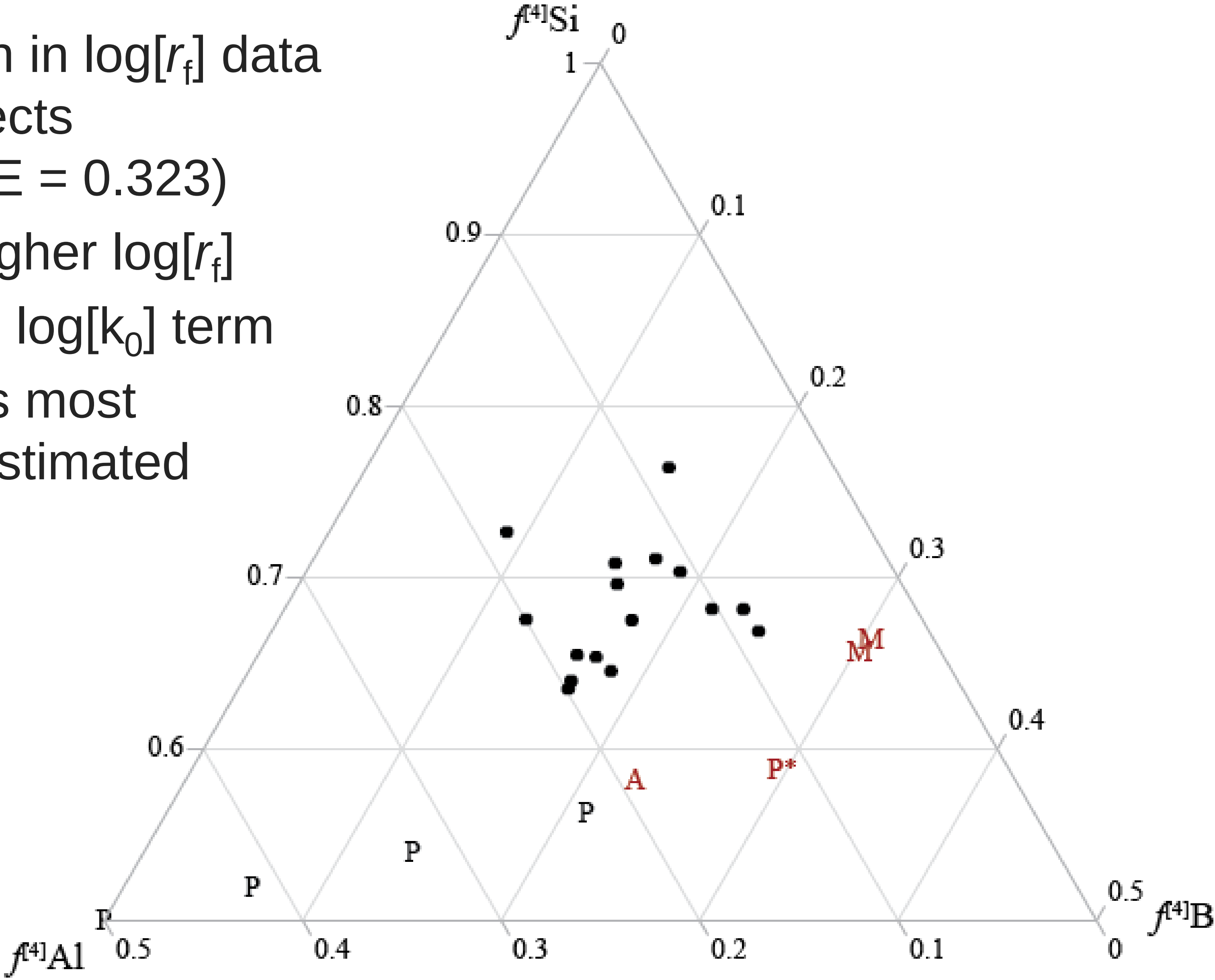

Summary of Modeling Results

- Composition effects on r_f in caustic solution are relatively small over a broad composition space
- They are best modeled using a $f^{[4]}$B = 0.22 threshold with rate being composition independent above and below the threshold
- The exact location of the threshold and any composition effects outside of the regions tested here are uncertain

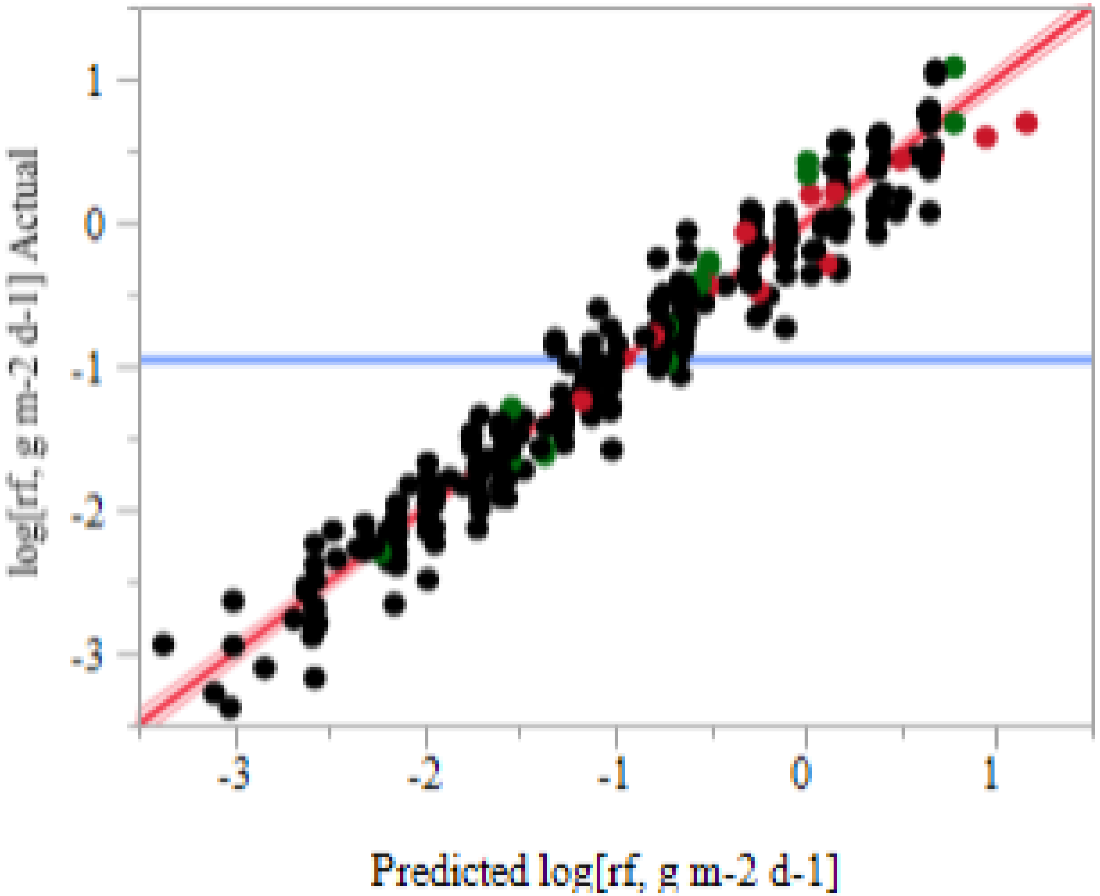

End Result

$$\log[r_f(g \cdot m^{-2} \cdot d^{-1})] = \left\{ \begin{array}{l} \text{below threshold} \Rightarrow 7.09 + 0.421 pH_{(T)} - 76,200 \dfrac{\log(e)}{RT} \\ \text{above threshold} \Rightarrow 7.86 + 0.421 pH_{(T)} - 76,200 \dfrac{\log(e)}{RT} \end{array} \right\}$$

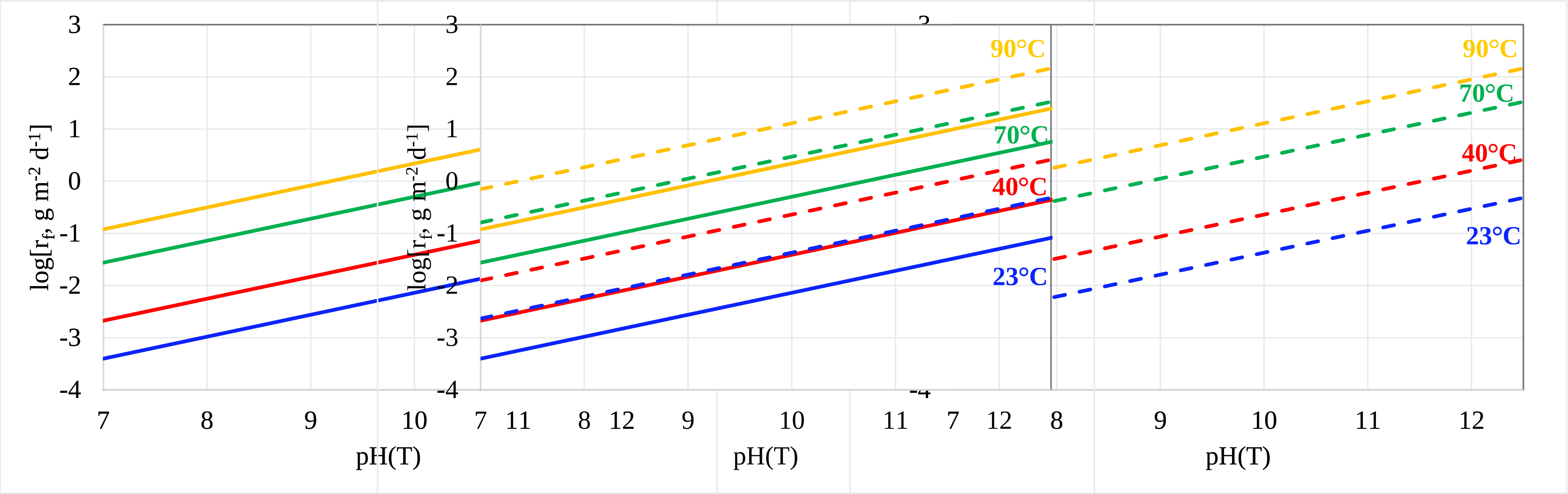

Vienna et al. 2018

Residual Rate

How Do We Measure Long-Term Rates

- Product Consistency Test (PCT) (ASTM C1285)
  - Ground glass soaked in DIW at temperature
  - Glass component concentrations measured in solution after test

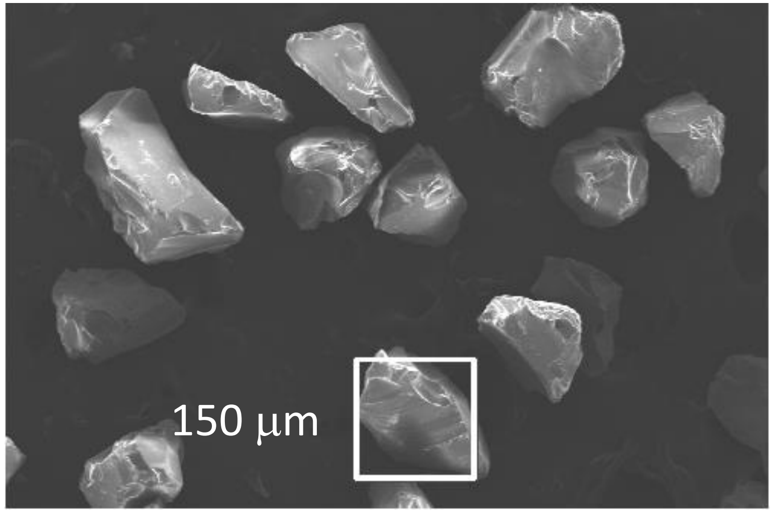

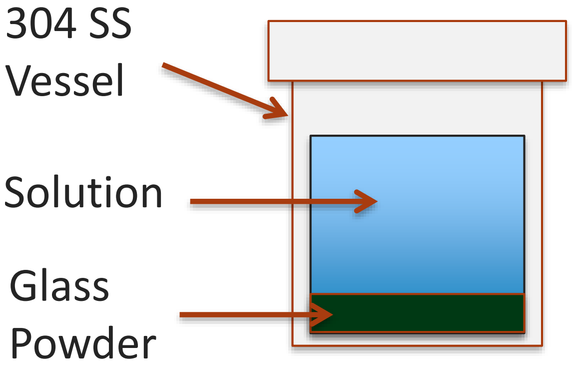

- MCC-1 (ASTM C1220)
  - Glass soaked in DIW at temperature
  - Glass component concentrations measured in solution after test
- Different solution compositions (e.g., pH, [H_4SiO_4], counter ions, etc.), temperatures, times, and isotopic tracers are also used

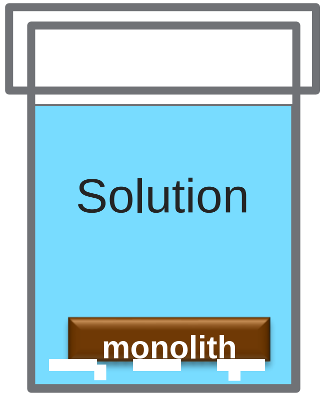

Residual Rate

- Corrosion rate is observed to slow to a nearly linear, residual, rate
- What causes rate to drop (and ultimately determines r_r)?

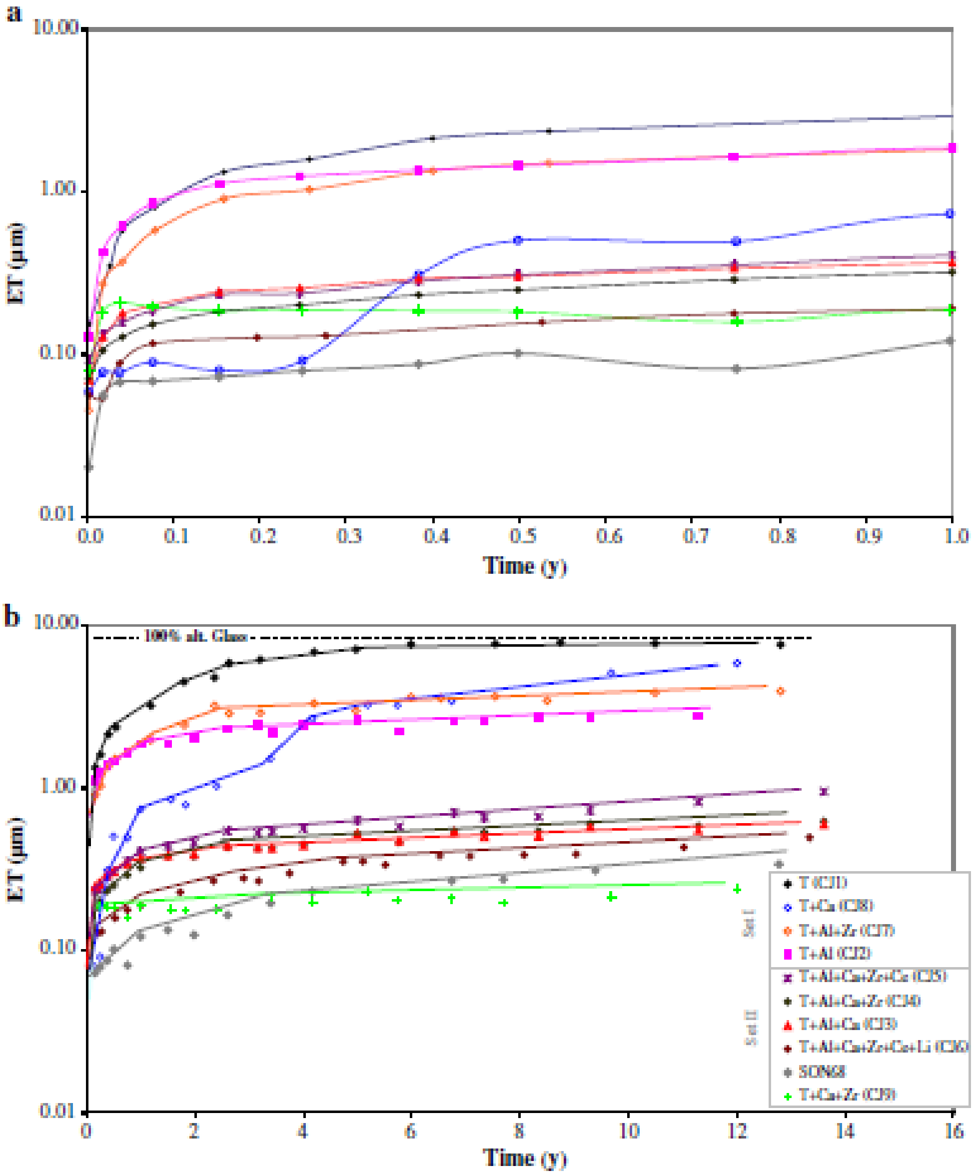

Fig. 1. Altered glass thickness, ET(B) as a function of time during the static test at 90 °C. a) from 0 to 1 year. b) up to 14 years.

Gin et al. 2012

Residual Rate, cont.

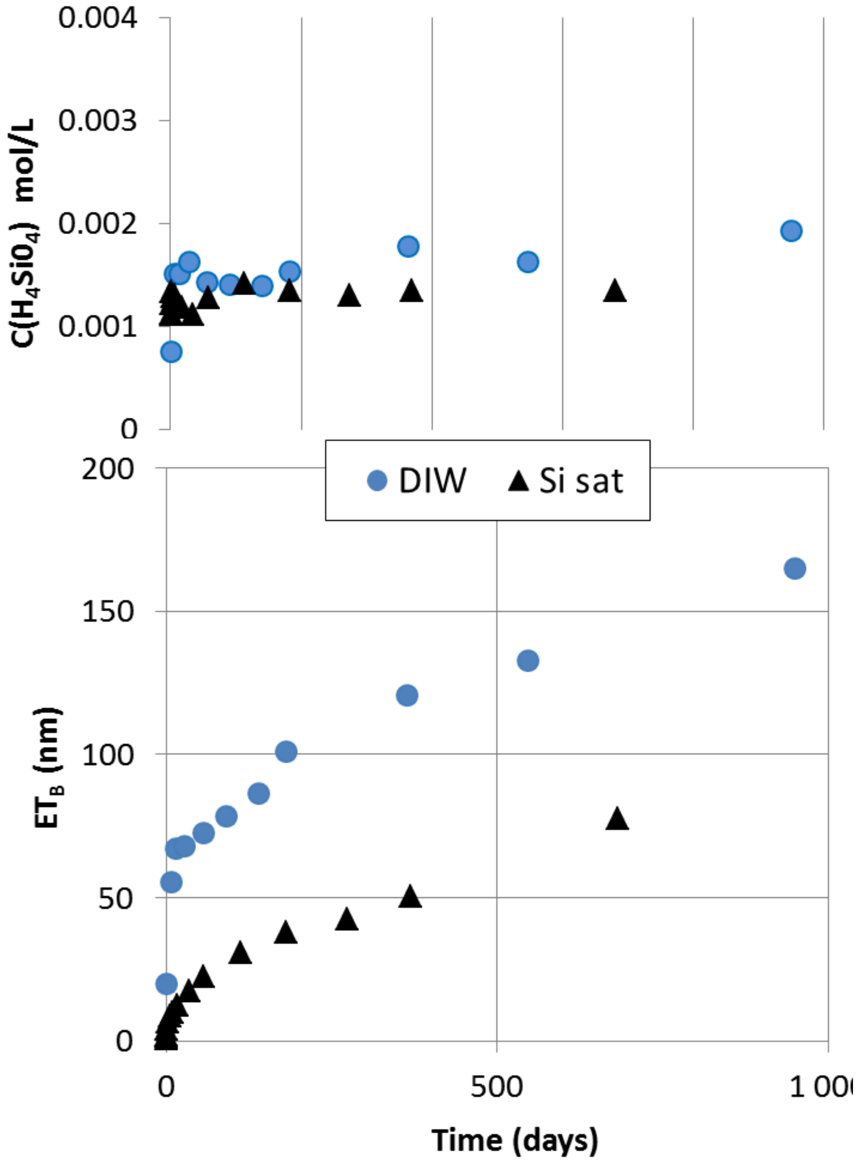

1. Thermodynamic driving force drops

- $[H_4SiO_4]$ (and other glass components) increase in concentration in solution
- Basis of Grambow 1987 model:

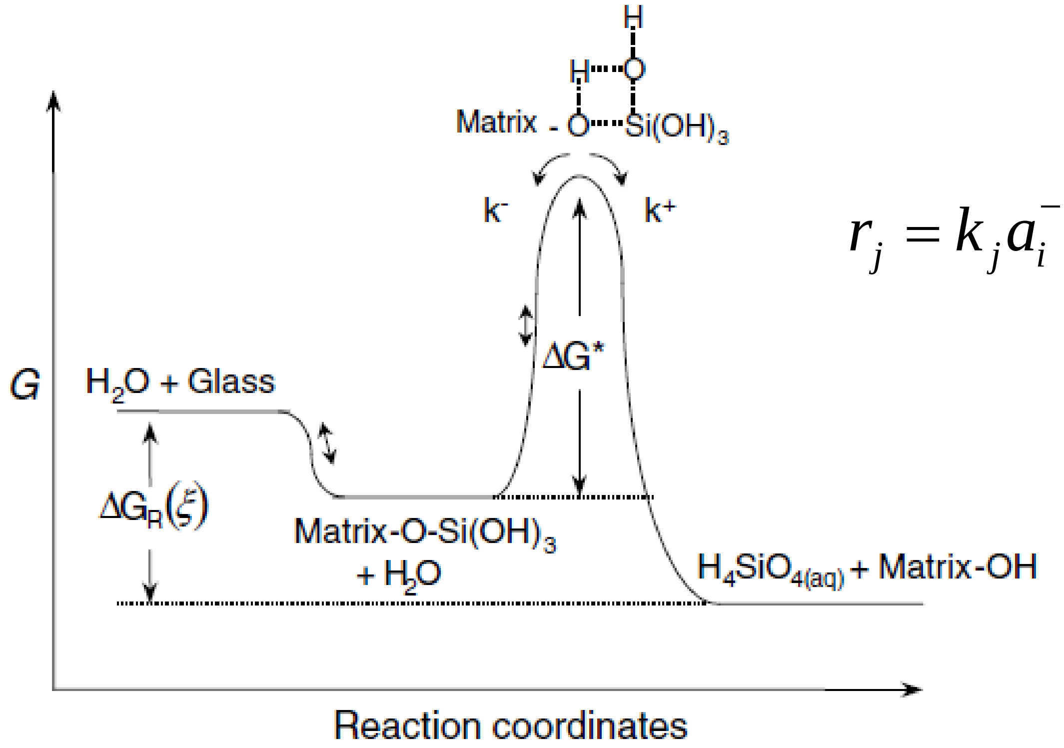

$$r_j = k_j a_i^{-\nu_{i,j}} \left[1 - \exp\left(\frac{-A_j}{\sigma_j RT} \right) \right]$$

Residual Rate, cont.

2. Formation of a passivating reactive interface (PRI)

- A high-density hydrated silicate layer close to the altering glass slows transport
- Basis of GRAAL model:

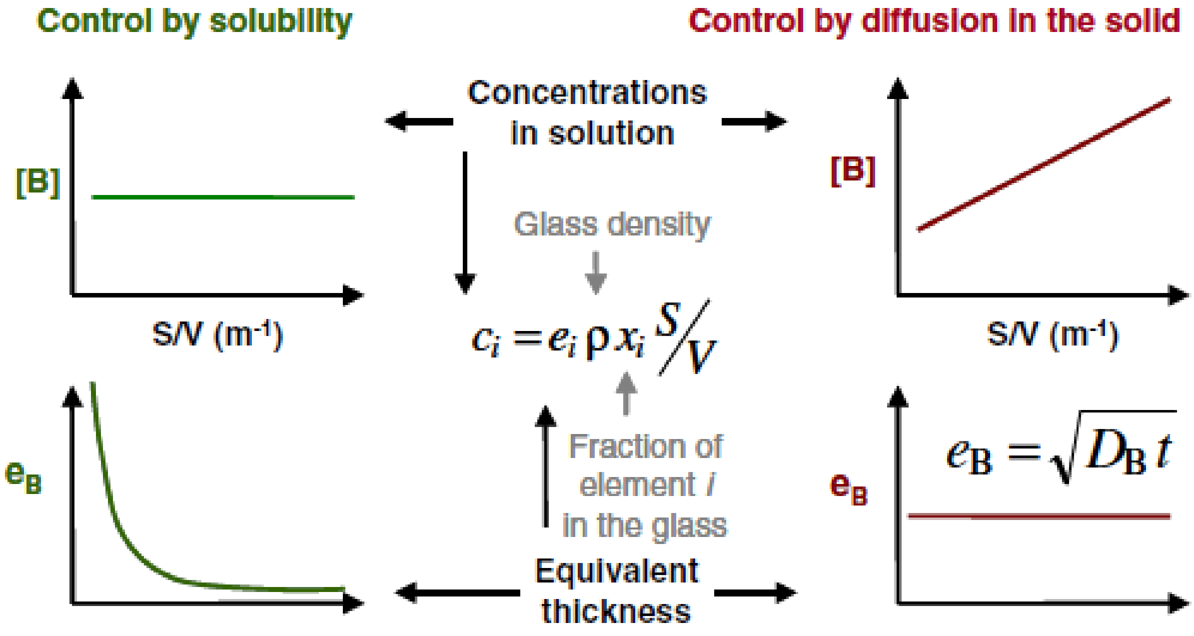

$$c_i = e_i \rho x_i \, {}^{S}\!/_{V}$$

$$e_B = \sqrt{D_B t}$$

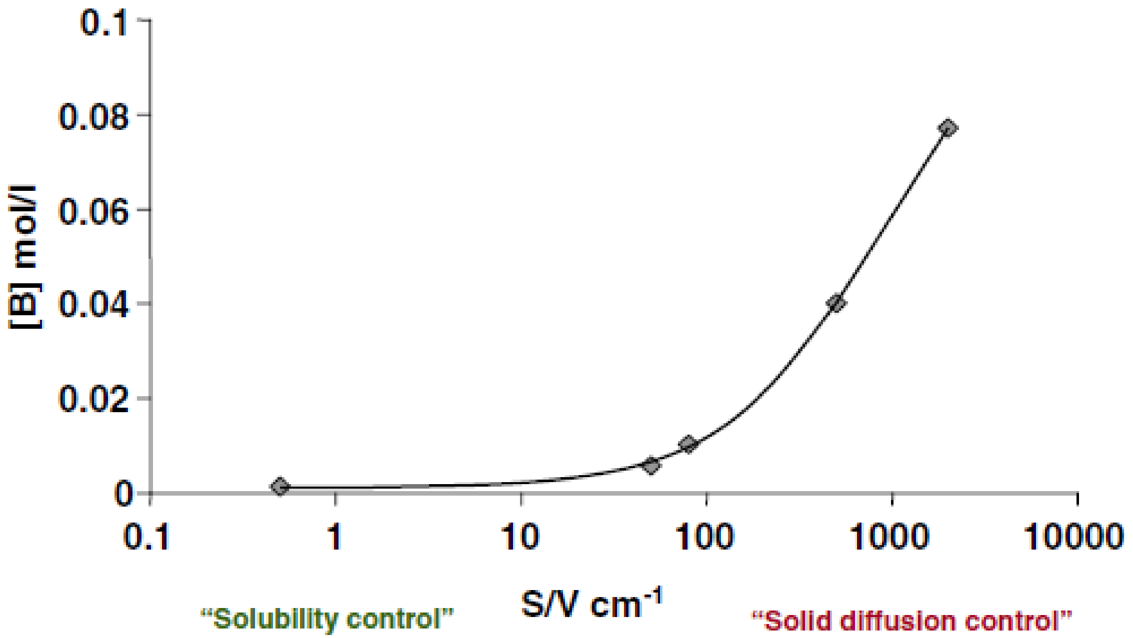

Frugier et al. 2008

Residual Rate, cont.

3. Pour “clogging”

- A high-density silica layer far from reacting interface
- High Zr limits Si reorganization

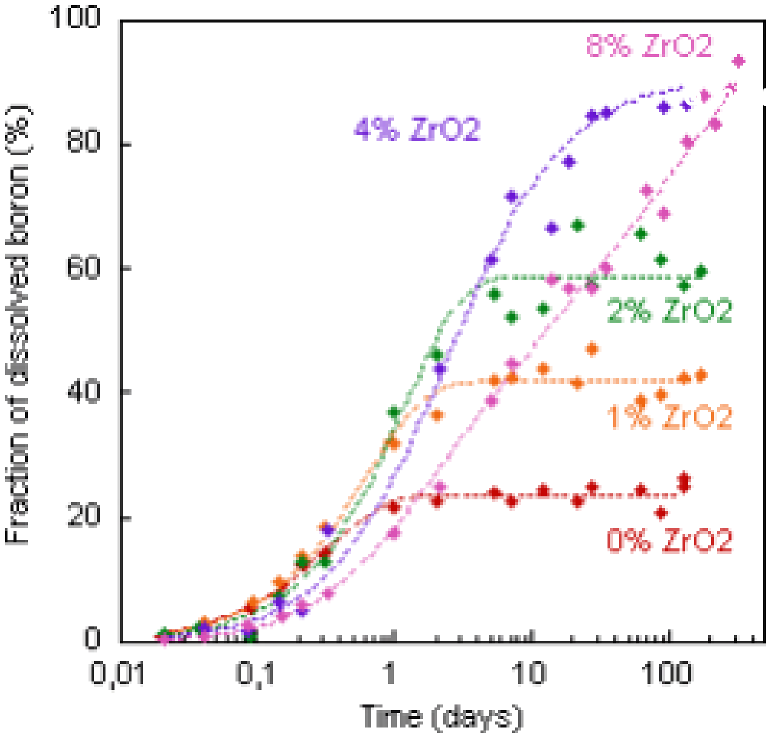

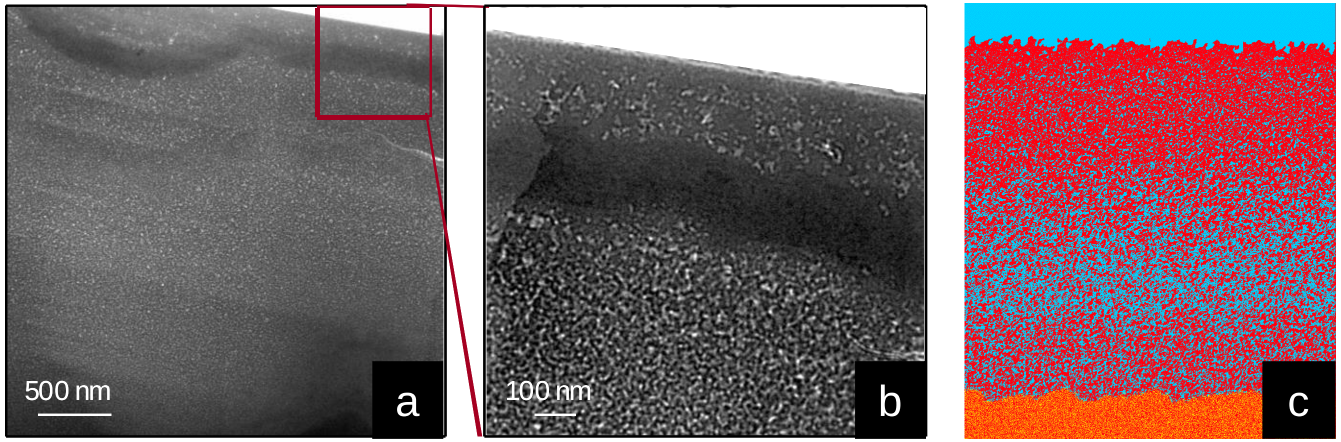

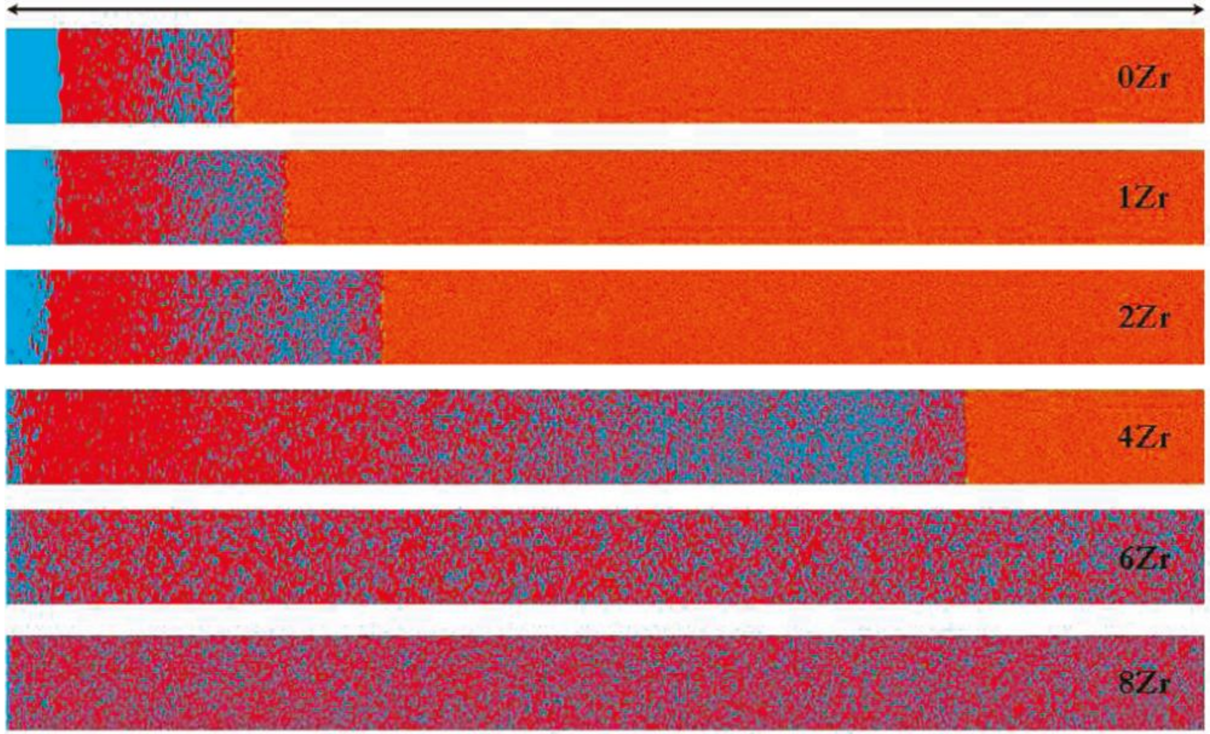

Cailleteau et al. 2008

Residual Rate, cont.

4. Dissolution/reprecipitation

- A high-density silica layer forms, glass corrodes forming a local chemical gradient, and silica deposits on this layer on the other side of the chemical gradient
- Explains layer formation seen in alteration products

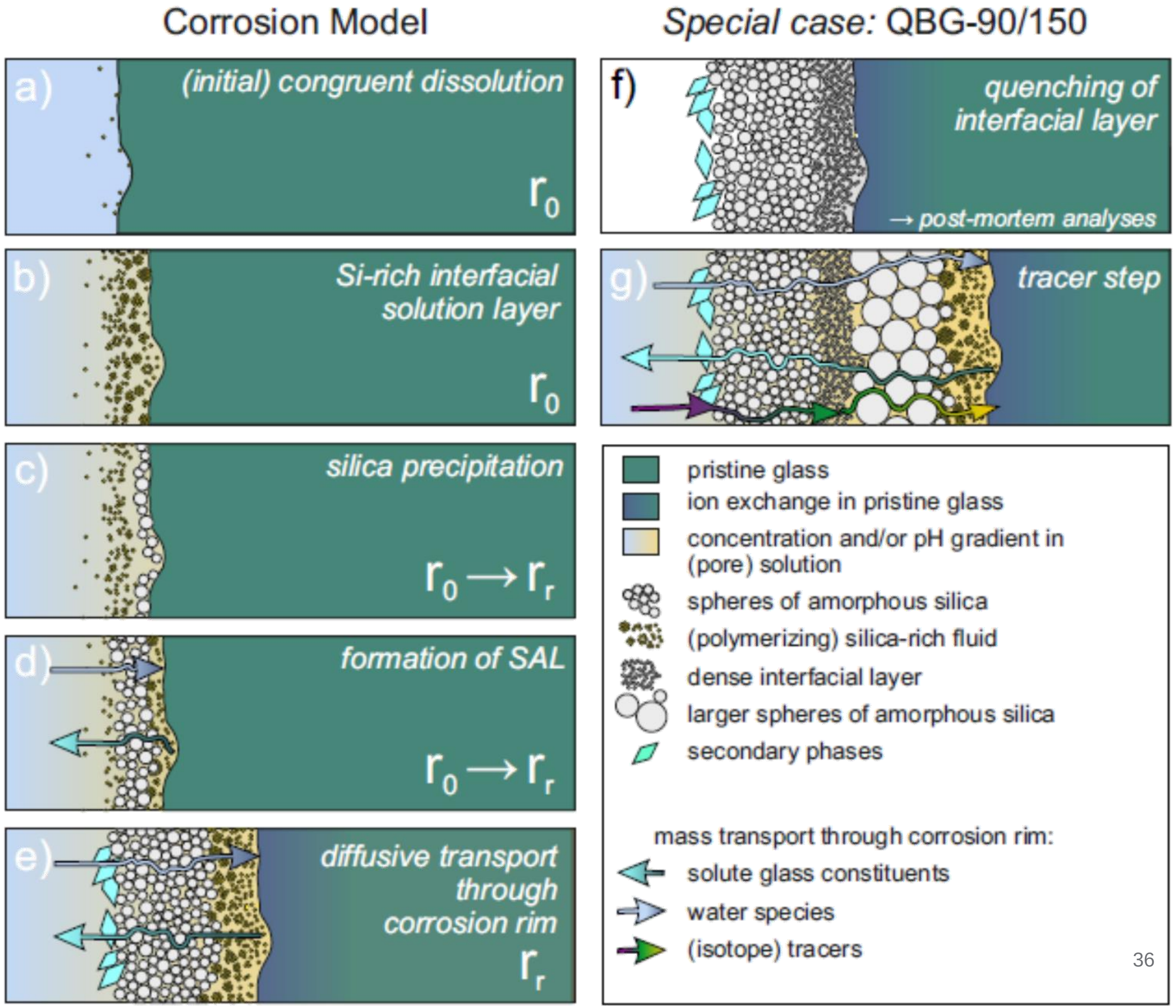

Lenting et al. 2018

What is New?

Complex Glass Structures

- Developed set of potentials for modeling multi-component waste glasses and validated the models with structural data from EXAFS and NMR:
  - First ever structural models of the ISG (international simple glass, a six component glass representing composition of waste glasses)
  - Answered questions of distribution of modifiers around $[BO_4]^-$, $[AlO_4]^-$, & $[ZrO_6]^{2-}$
  - Precisely describes how silicate network is fragmented by the borate groups → crucial for structure of altered layers

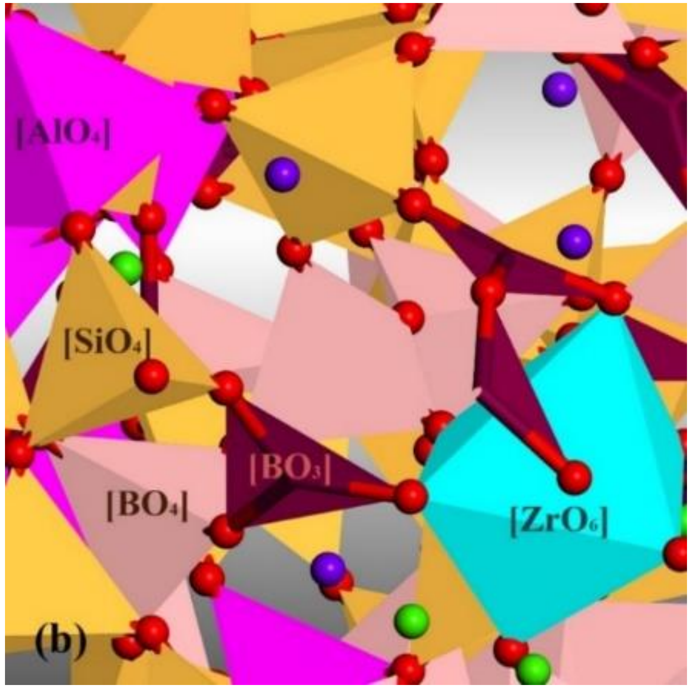

Modeled structure of ISG
Du and Rimsza 2017

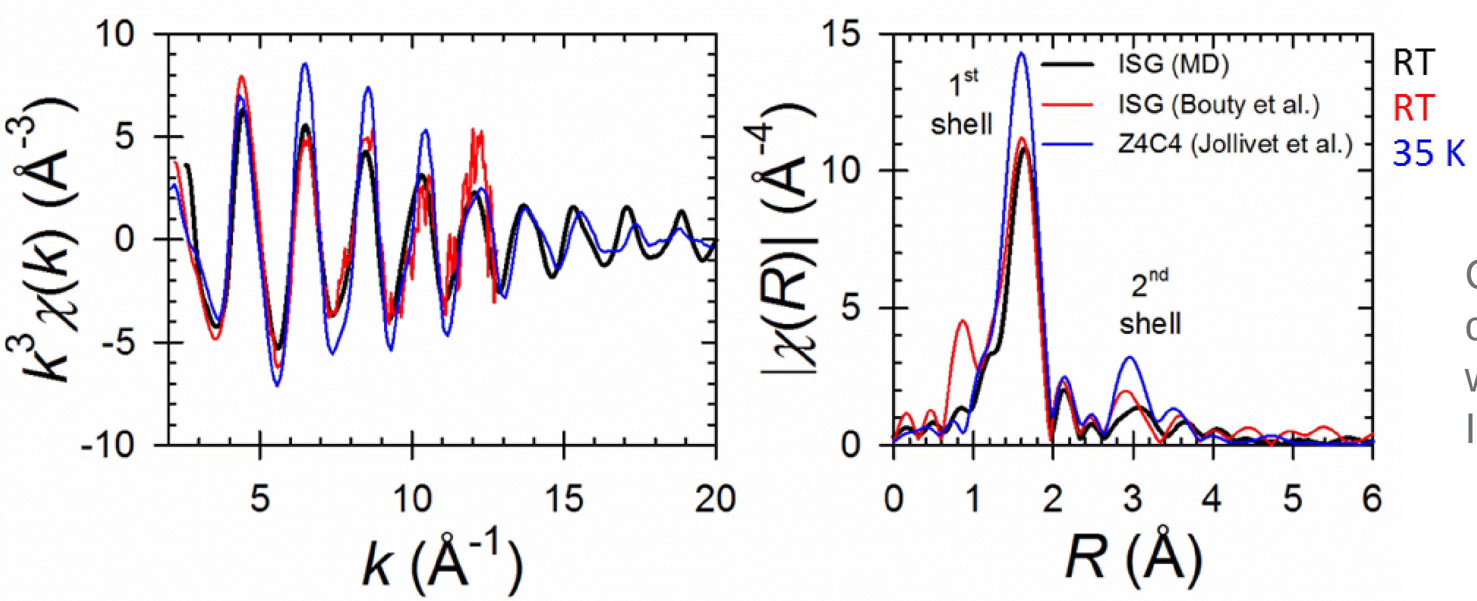

Comparison of Zr MD structure calculated (not fit) using FEFF with measured EXAFS data for ISG, Lu et al. 2018

Alteration Layer Structure/Chemistry

- Reactive potentials (MGFF) used to accurately represent interactions between water and glass surface
- Two approaches to form amorphous gel:
  - Insert porosity in predetermined pattern → allow water to interact and relax
  - Replace soluble components with OH → allow water to interact and relax
- Interconnected network of 1-4 nm pores with composition fluctuations.

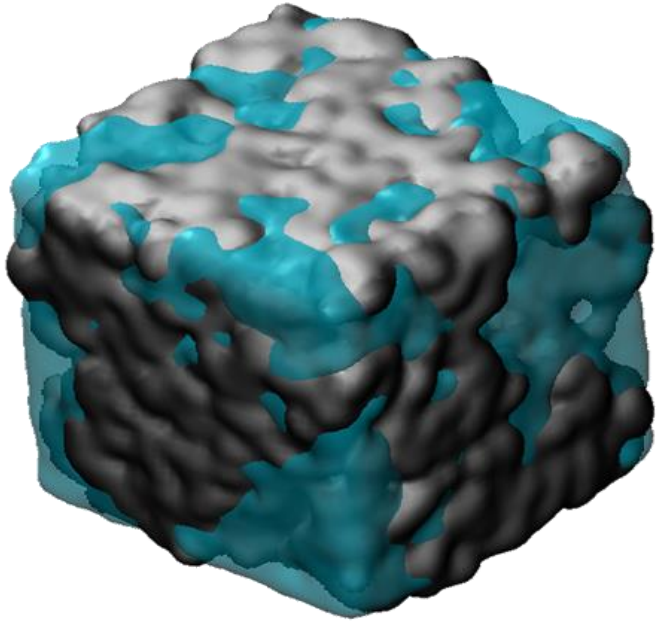

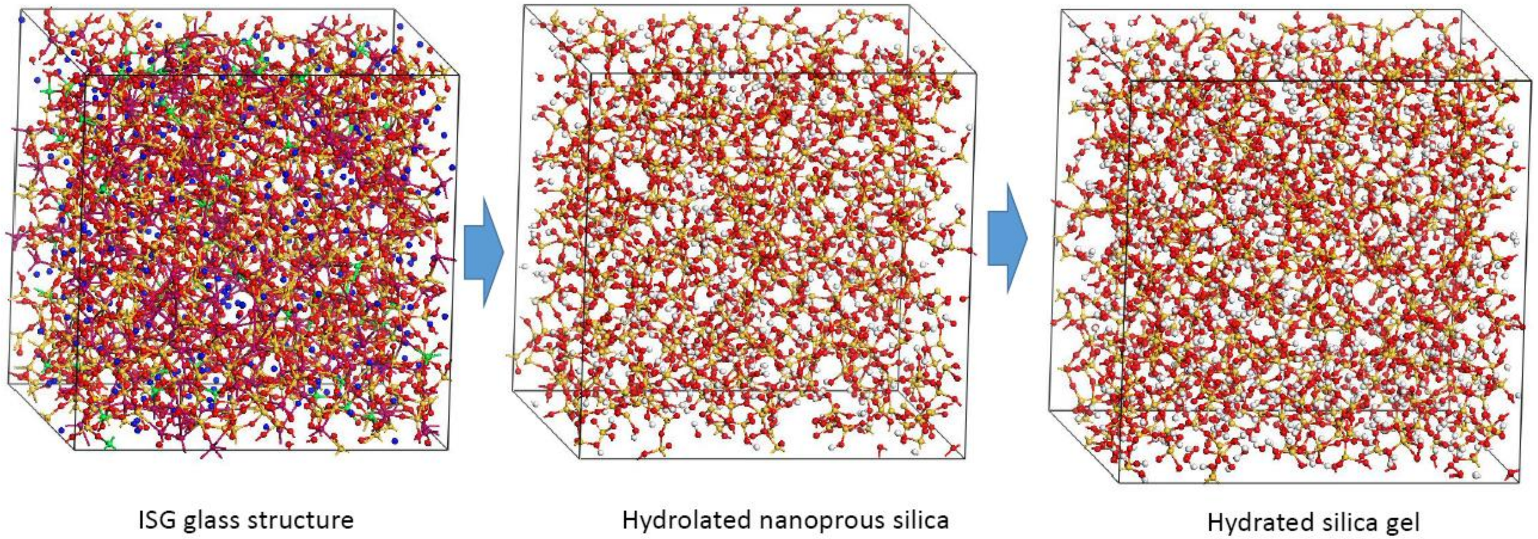

Ren et al. 2017

Alteration Layer Structure/Chemistry

- Developed method to flash-freeze, cryogenically prepare, and image surface layers using APT

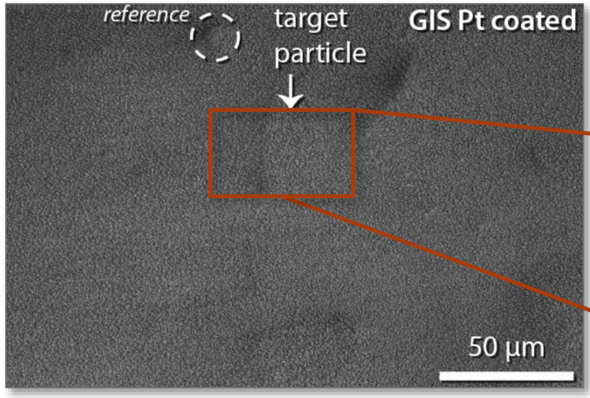

Frozen Water + Corroded Glass Particles

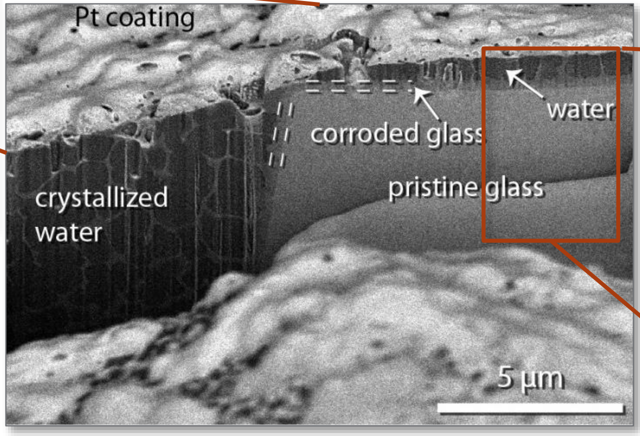

FIB Cross-Section of Corroded Glass + Water

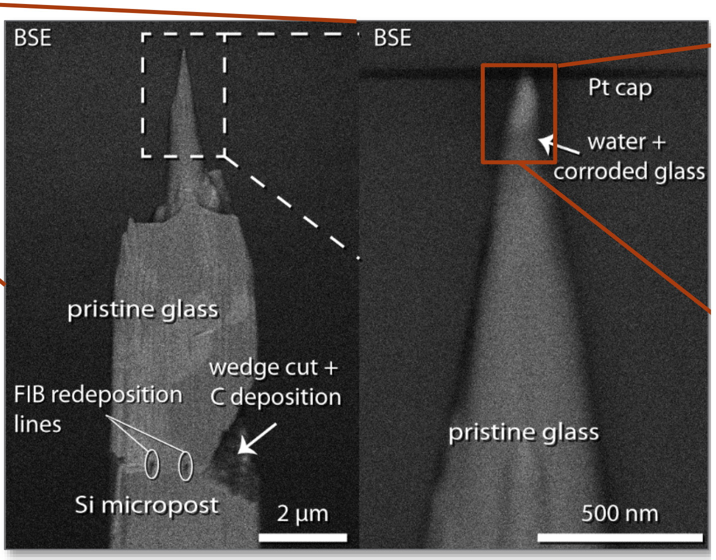

Cryo-Prepared APT Specimen

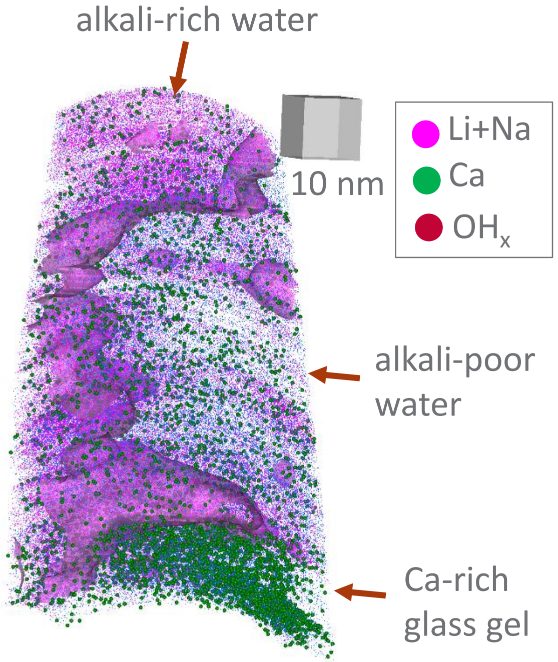

3D APT Reconstruction at Water/Gel Interface

Schreiber et al. 2018

Alteration Layer Structure/Chemistry

- Interconnected network of 1-4 nm pores with composition fluctuations.

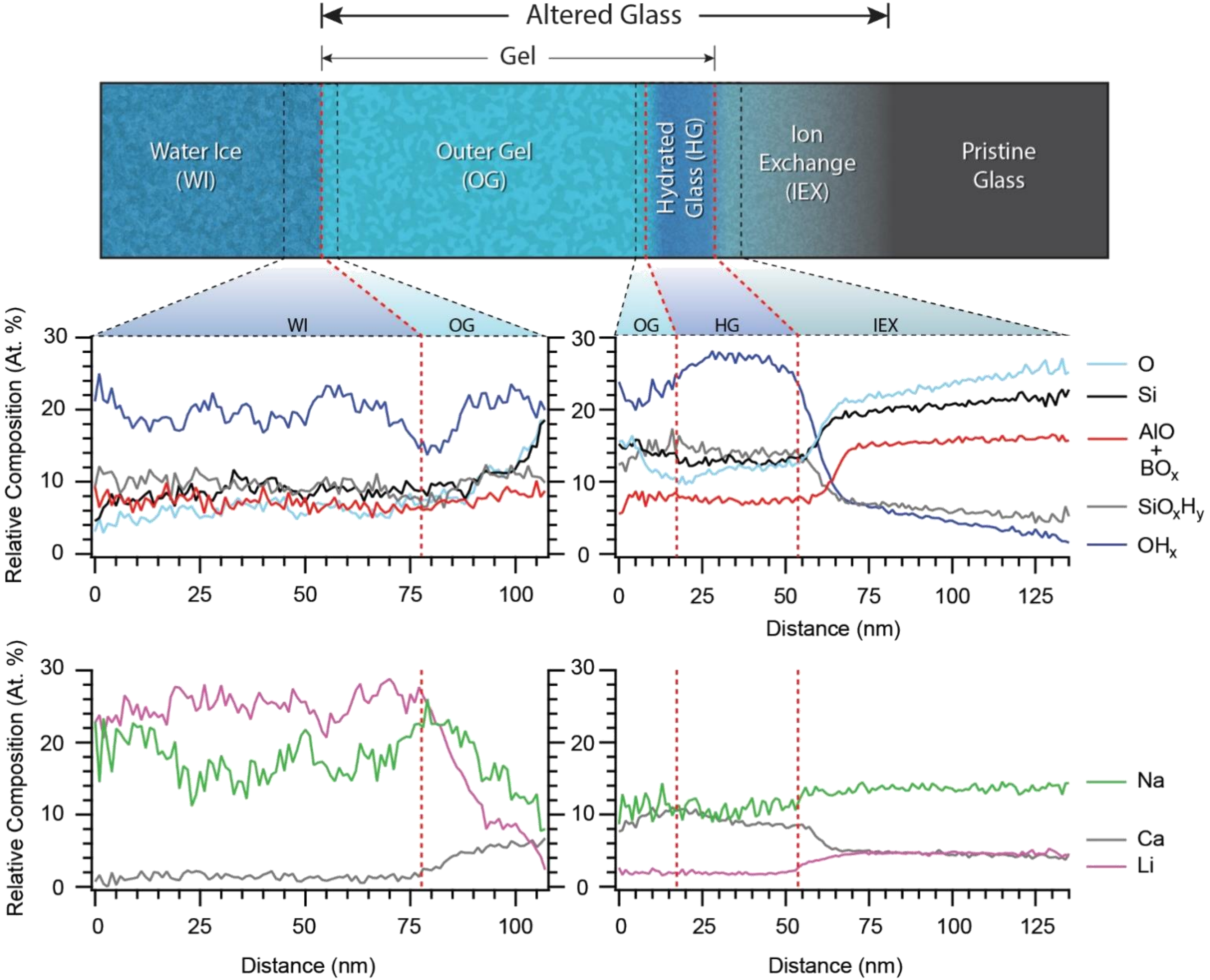

Perea et al. 2018

MD simulated

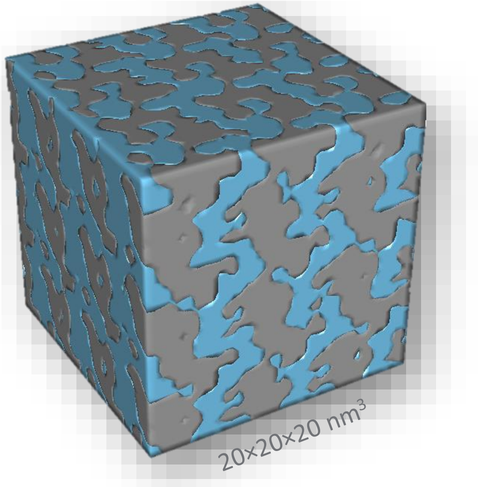

Experimental

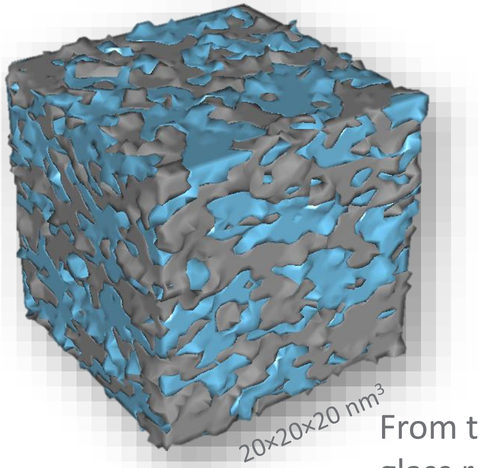

From the hydrated glass region (HG)

Alteration Layer Structure/Chemistry

- Porosity and pore size distribution in alteration layer of 1625 day-corroded ISG from spectroscopic ellipsometry (SE) to provide statistics not possible with cryo-APT → results are consistent between the two techniques

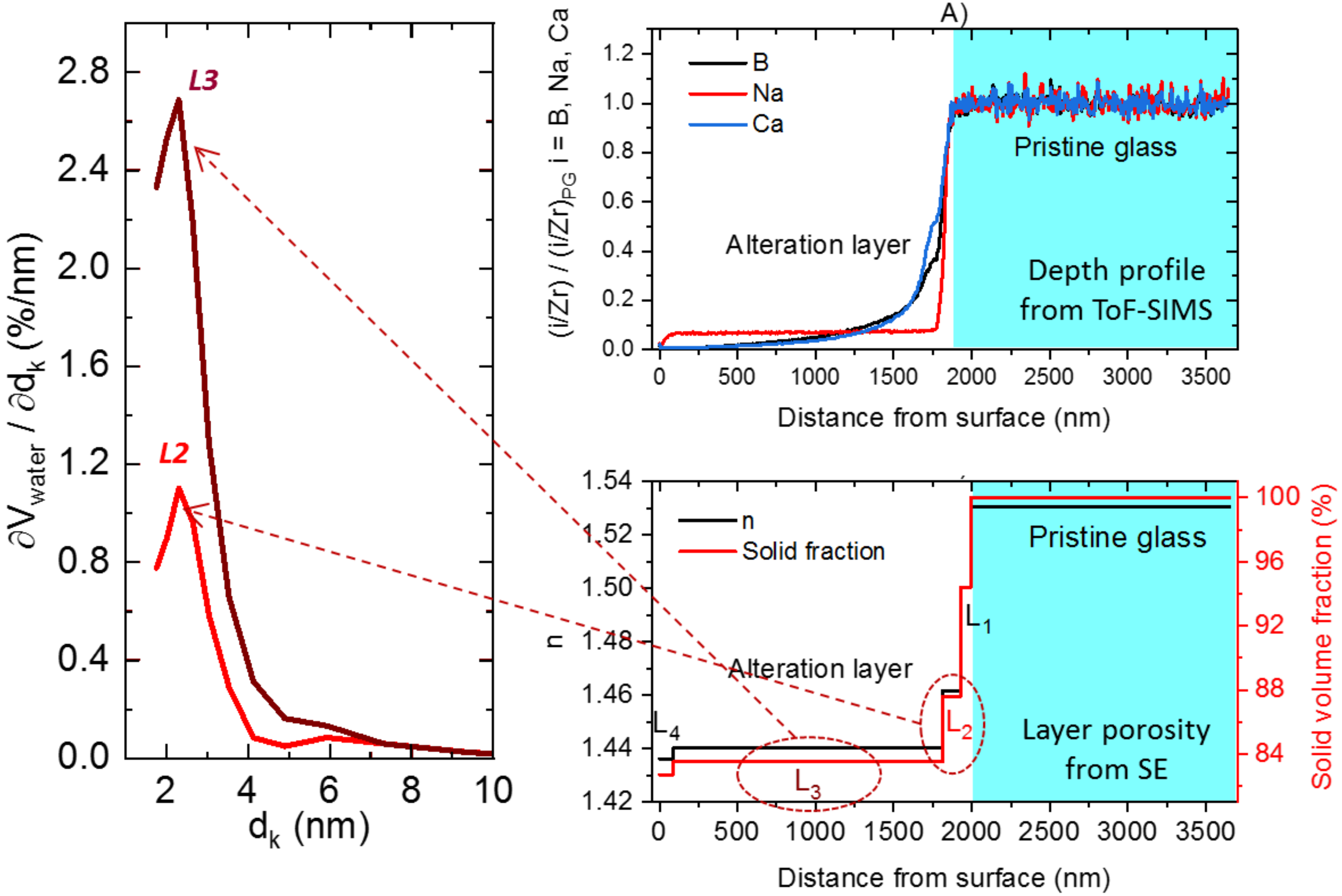

Ngo, et al. 2018

Alteration Layer Structure/Chemistry

- Water speciation within nano-pores and pore characteristics identified by NMR/TGA.

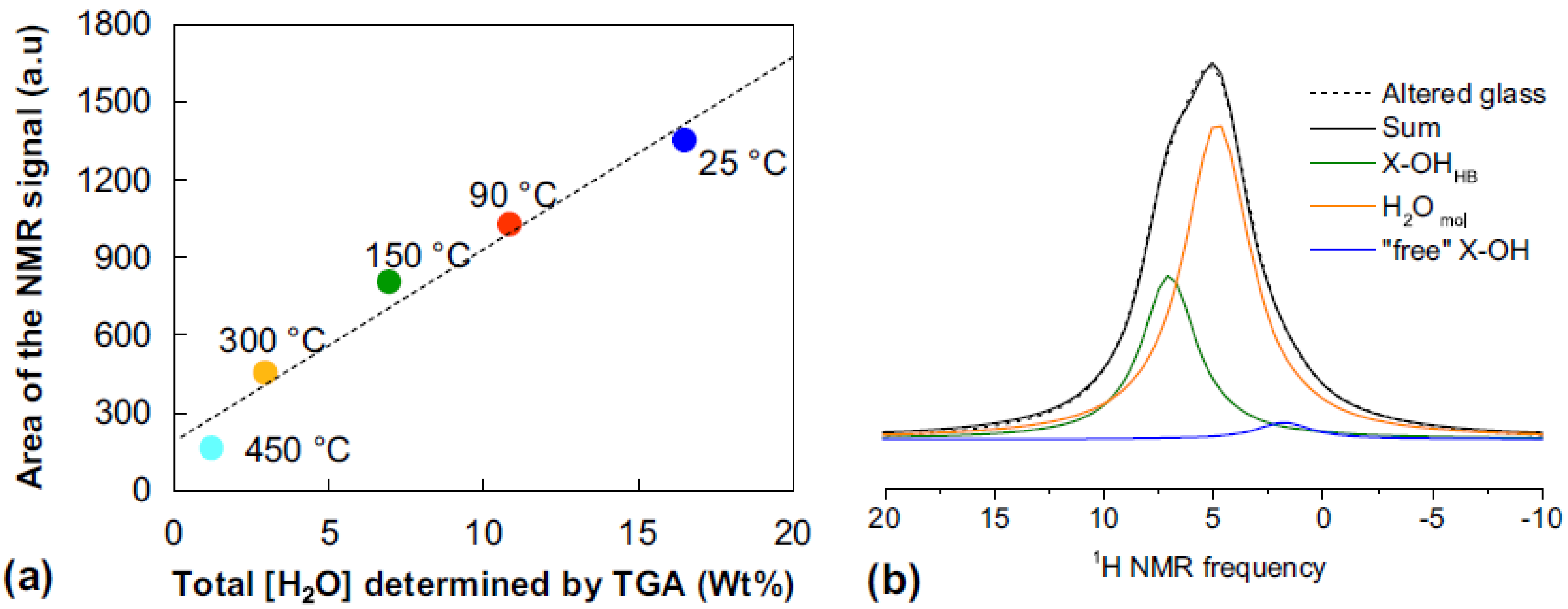

H of $-X$-OH $_{HB}$	H of H_2O_{mol}	H of "free" $-X$-OH
23.5	70.7	5.8

Collin et al. 2018

Alteration Layer Structure/Chemistry

- Spectroscopic analysis identified distinct surface structures and multiple layers → help to determine passive layer and validate models

Water uptake alters the bond length distribution of the glass network

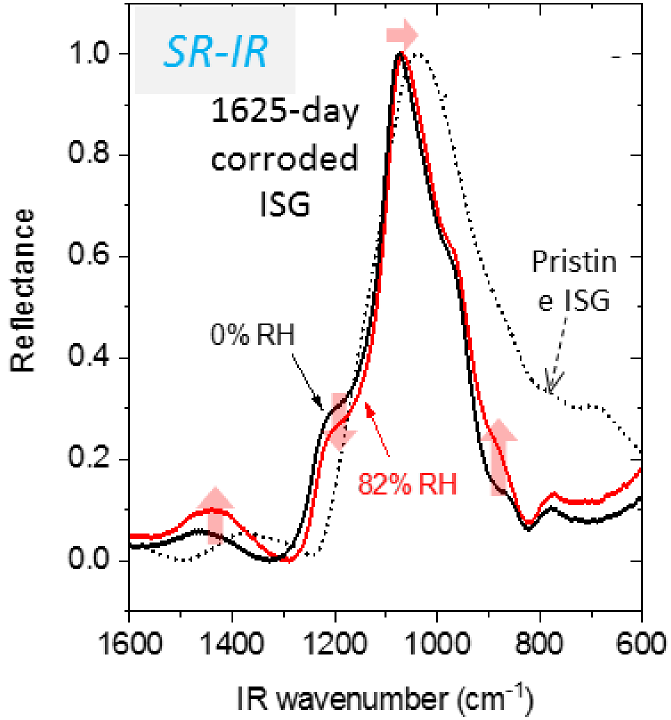

The Si-O-Si stretch peak position and shape reflect the Si-O bond length distribution (Luo, et al. J.Am.Ceram.Soc. ***2018****, 101, 178).*

Water uptake from air by the alteration layer of 1625 day-corroded ISG

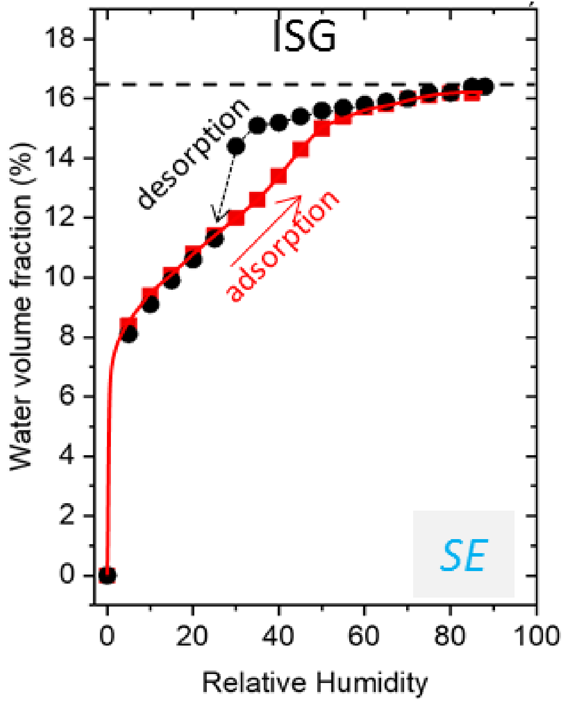

Hydrogen bonding interactions of water species in the surface region

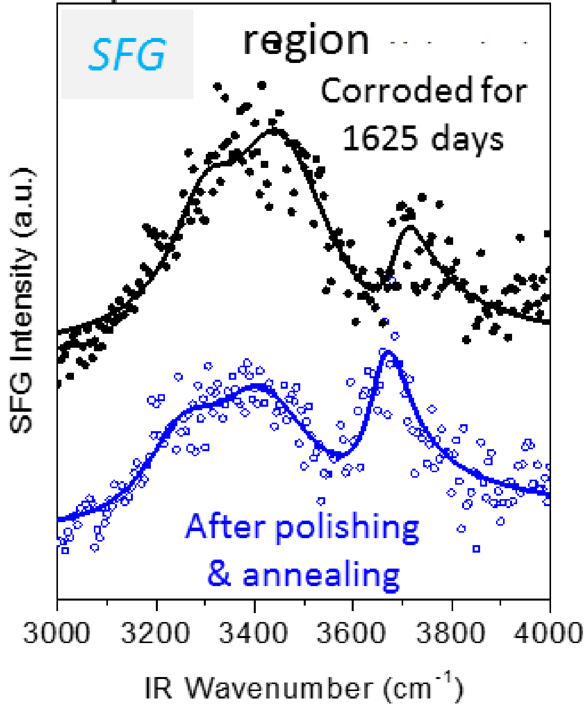

Ngo, et al. 2018

Properties of Alteration Layer

- Water transport in silica nanopores of diameters from 0.5-4 nm investigated using MD
- Transport is restricted by 1-2 orders of magnitude in confined spaces due to atomic scale roughness and reaction with pore walls.

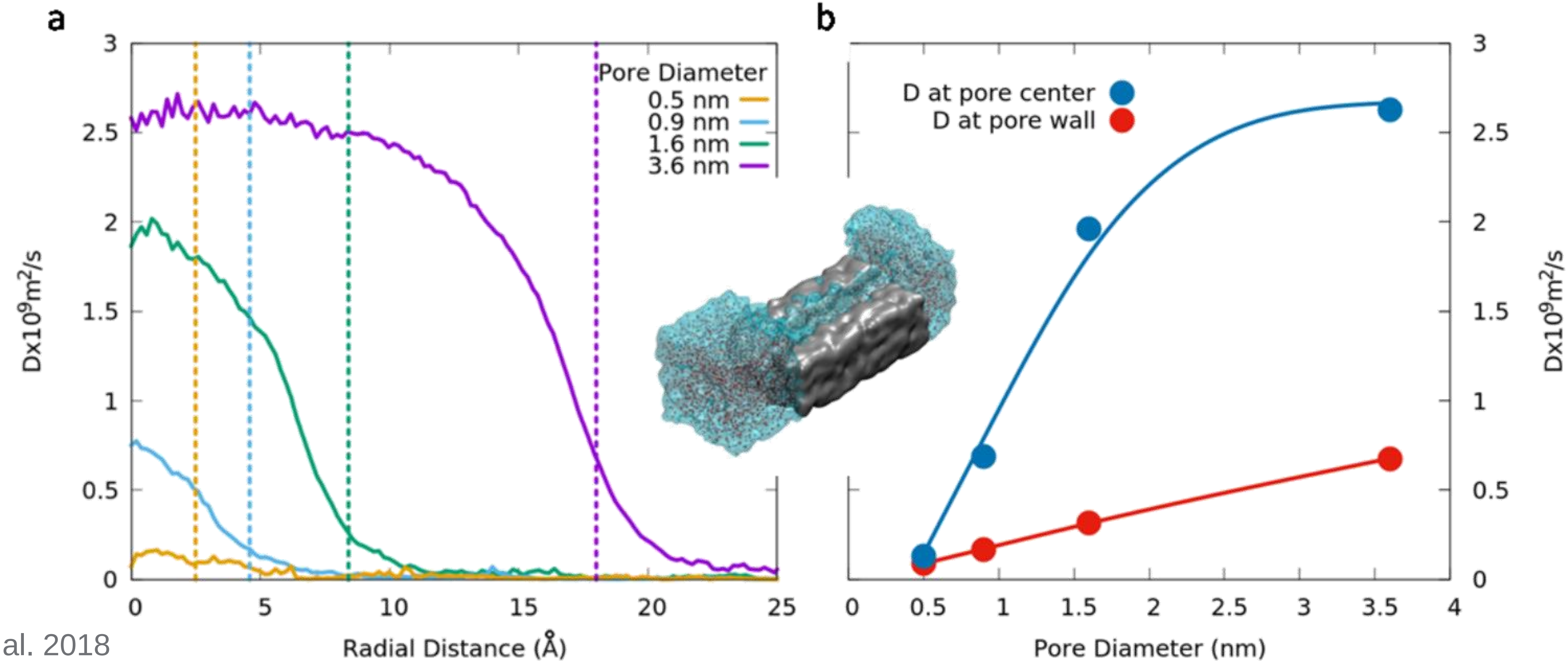

Gin et al. 2018

Properties of Alteration Layer

- Water mobility in gel recorded by time-dependent isotopic and elemental ToF-SIMS profiles
- 3D porous structure in which small fraction of water molecules diffuse quickly through micro-pores, while most are trapped in closed nano-pores.
- Gel reorganization is thus key mechanism accounting for extremely low water diffusivity (~10^{-21} $m^2 \cdot s^{-1}$), which is rate-limiting for overall reaction.

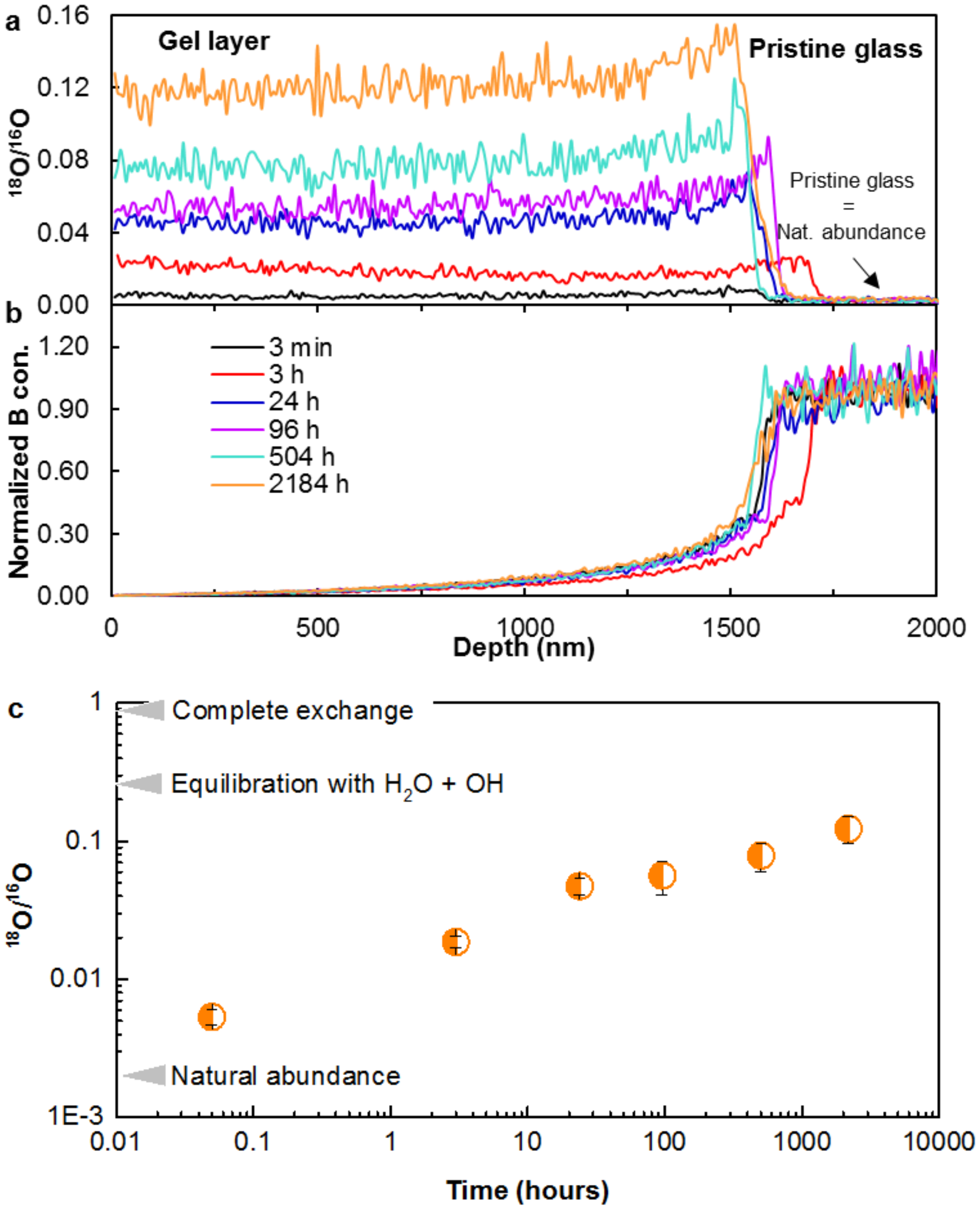

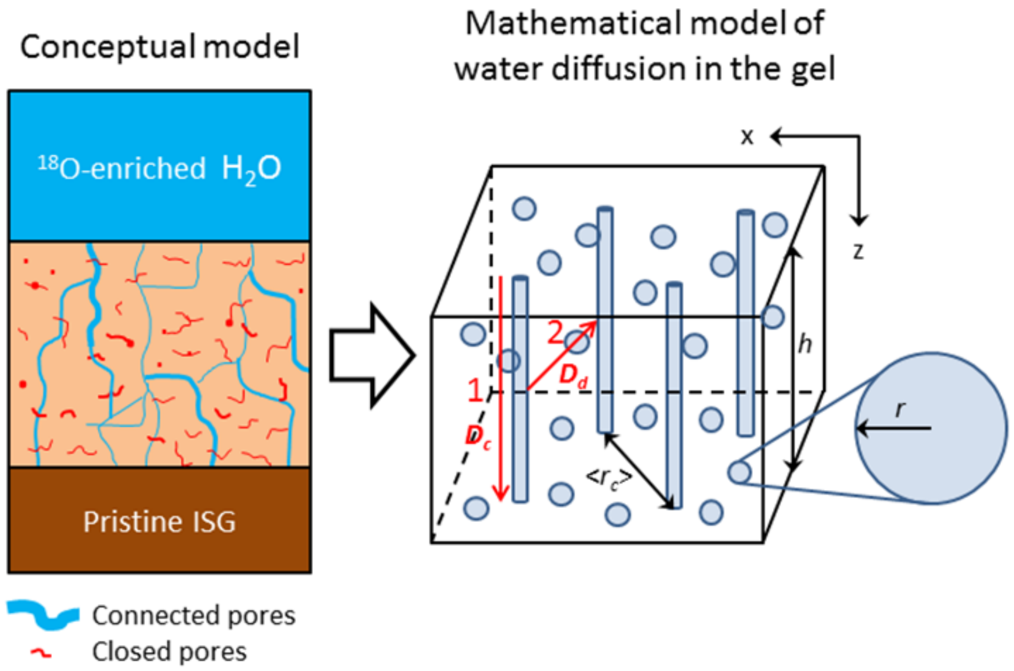

Gin et al. 2018

Acceleration (Stage III)

Empirically Measured Results Very Significantly

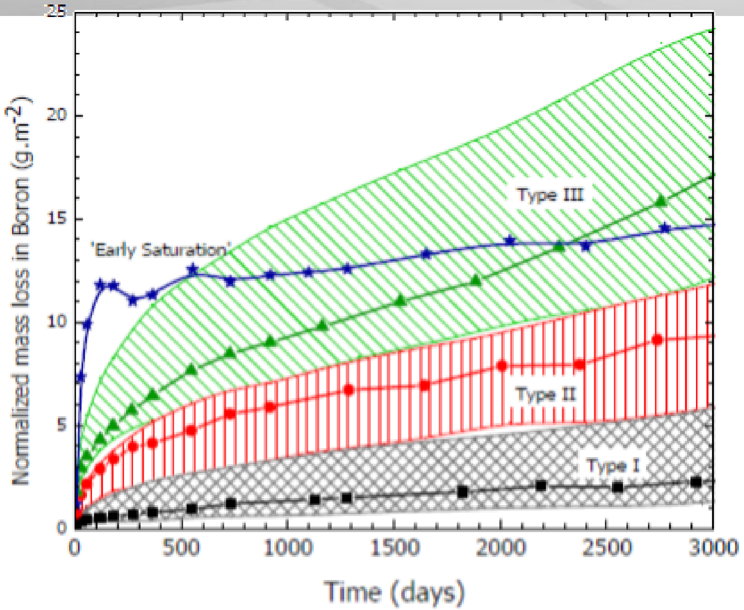

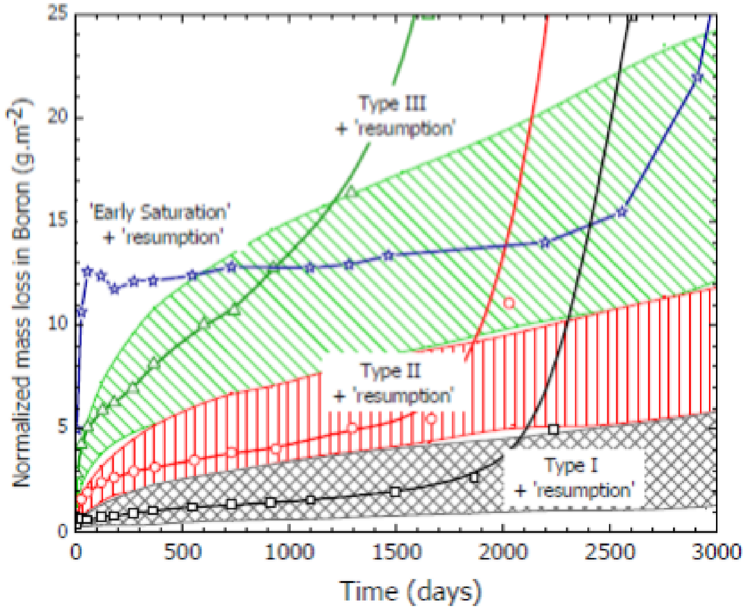

- Broad range of long-term corrosion rates observed in nearly static conditions.
- Stage III (accelerated corrosion) is particularly challenging
  - For certain glasses tested under static conditions an abrupt increase in corrosion rate is observed
    - Not all glasses and not all conditions show this rate increase
  - The rate increase is often observed coincidental with zeolite precipitation
  - Some glasses that do not display stage III in static tests can be induced to accelerate by changing conditions: e.g., pH ↑

Ribet et al. 2004

Example Disposal Environment Predictions

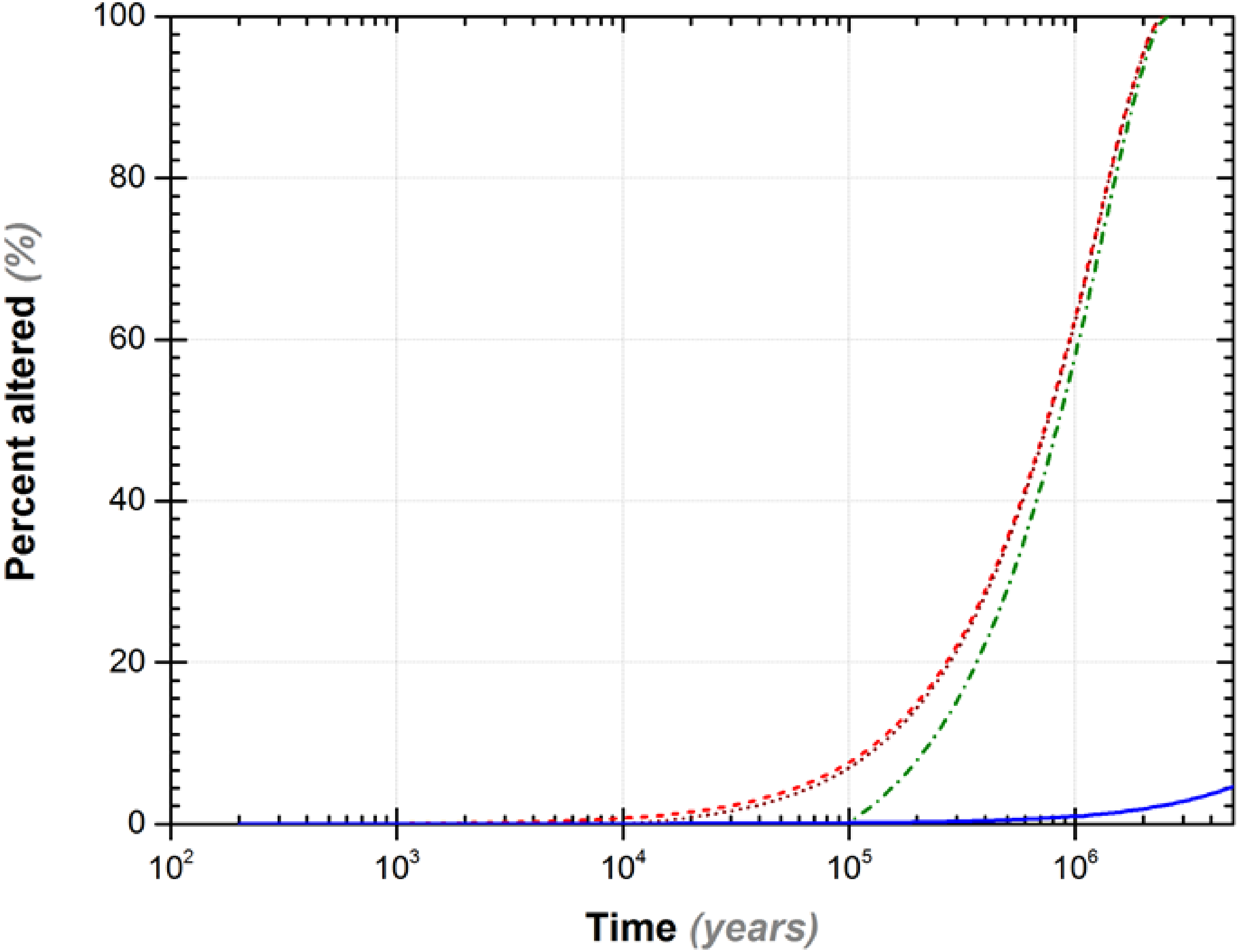

Stage III Observations

- Increasing pH of ISG glass corroding in static conditions initiates Stage III
- Stage III is often associated with higher pH conditions, but, not always
- Si, B, Na concentrations increase while Al concentration decreases
  - In unperturbed static tests, [Al] ↓ always precedes rate acceleration
- Generally, linear rate
- It’s not yet clear how the rate may vary with temperature and under what conditions it will occur
  - Not clear if it can occur in disposal environments

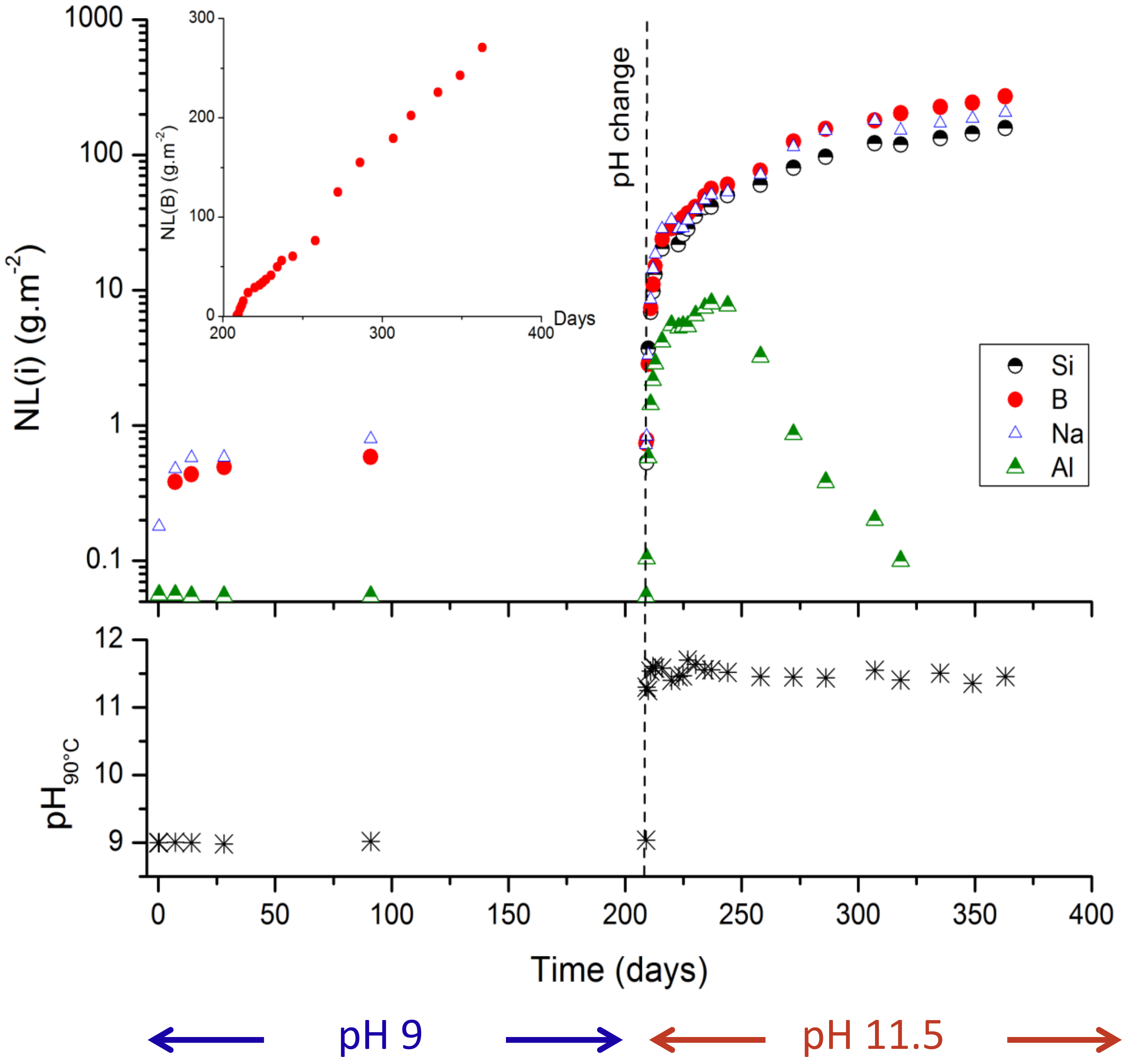

Gin et al. 2015

Stage III Observations, cont.

- Stage III can be induced (or initiated earlier) by seeding with certain zeolites
- Na-P1 and Na-P2 but not Analcime and Clinoptilolite (Crum 2017, unpub)

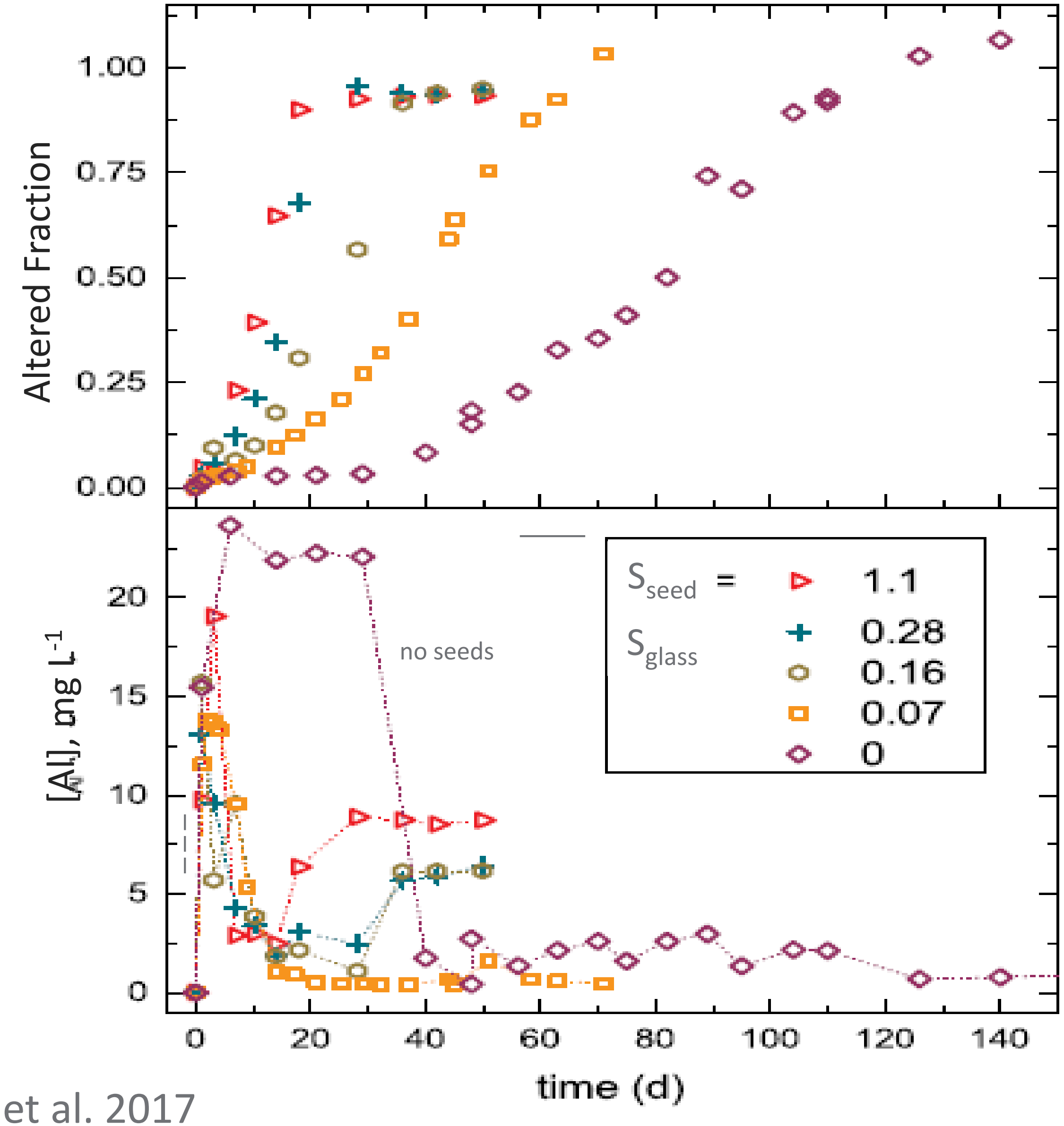

Fournier et al. 2017

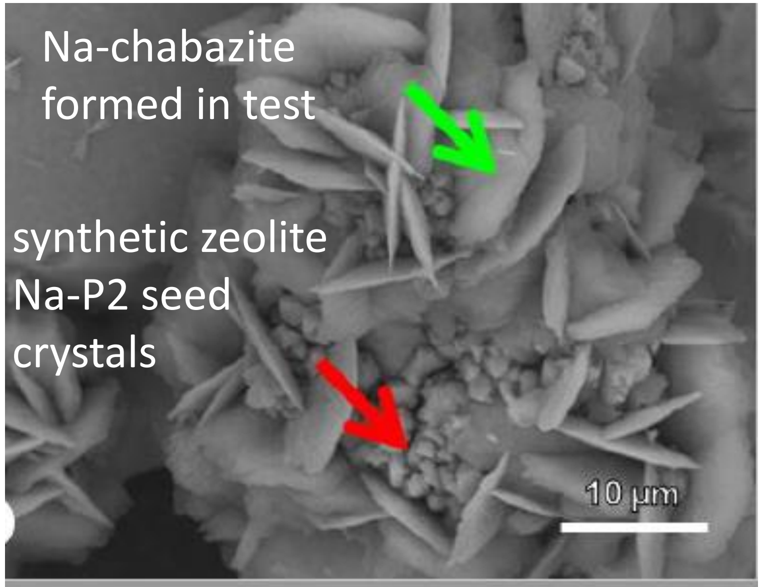
Na-chabazite formed in test

synthetic zeolite Na-P2 seed crystals

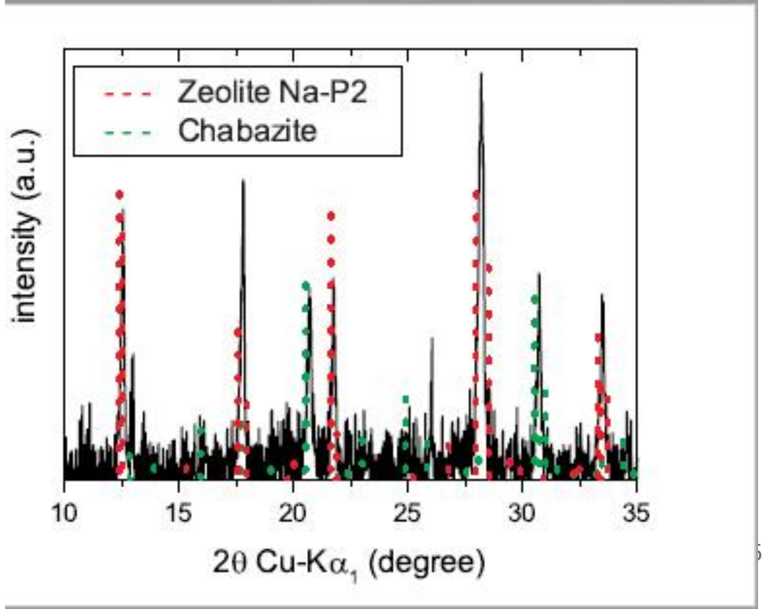

Glass as a Barrier

Glass as One of the Many Barriers in a Disposal System

- Radionuclides and hazardous components released “congruently” with glass matrix corrosion
  - Typically indicated by boron release in testing
- Available for transport and solubility control
- Near-field materials (those with chemical feedback to corroding glass)
  - Steel and steel corrosion products
  - Clay backfill
  - Cements

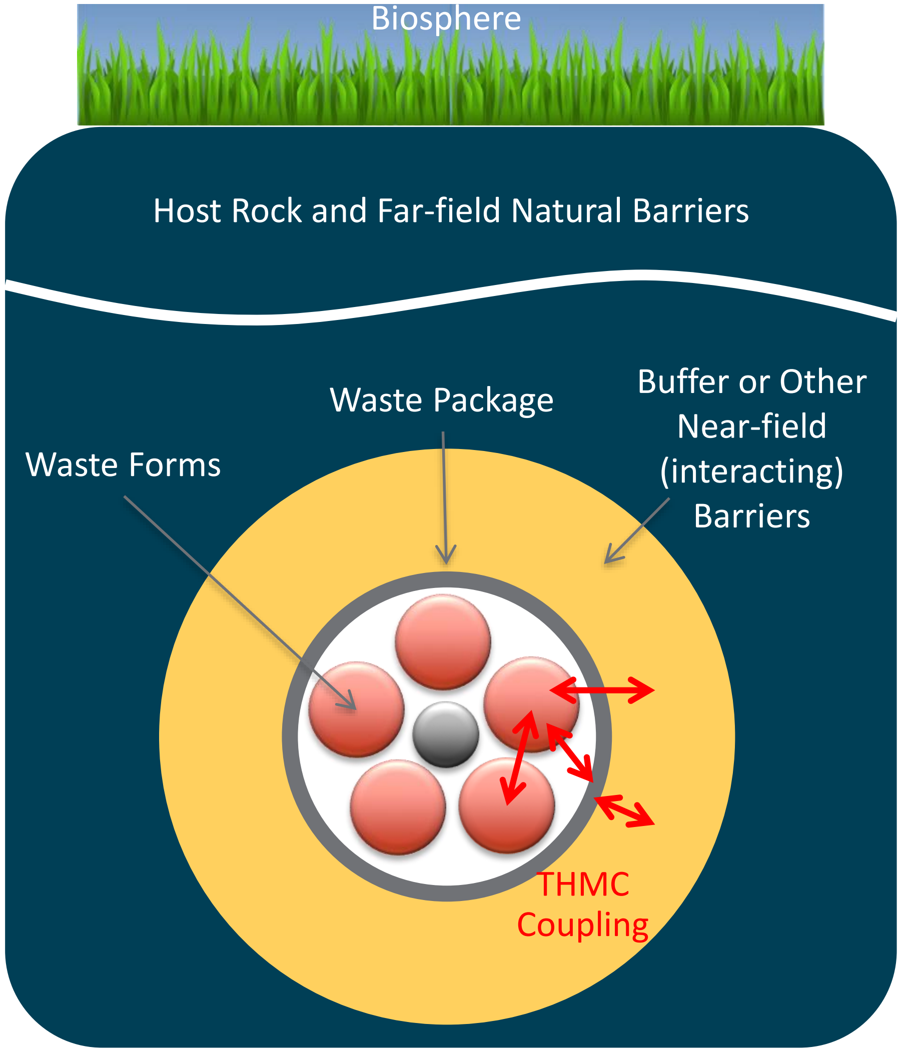

Glass as One of the Many Barriers in a Disposal System

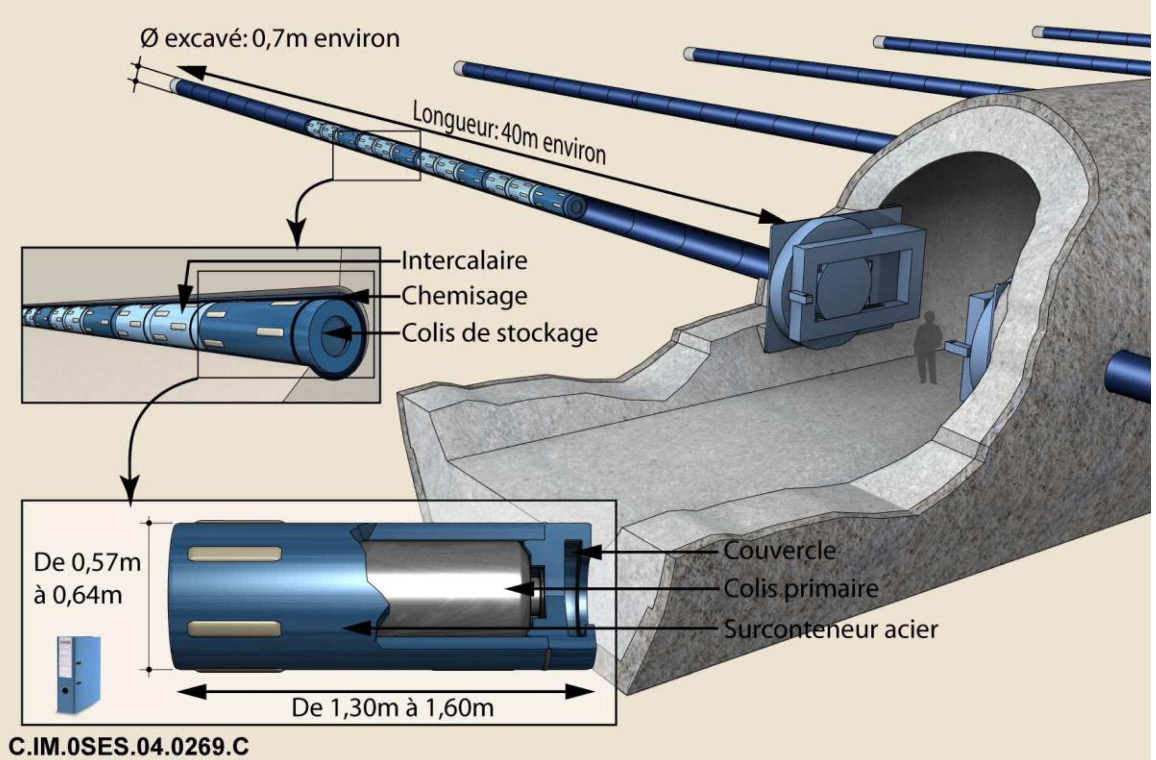

ANDRA 2005

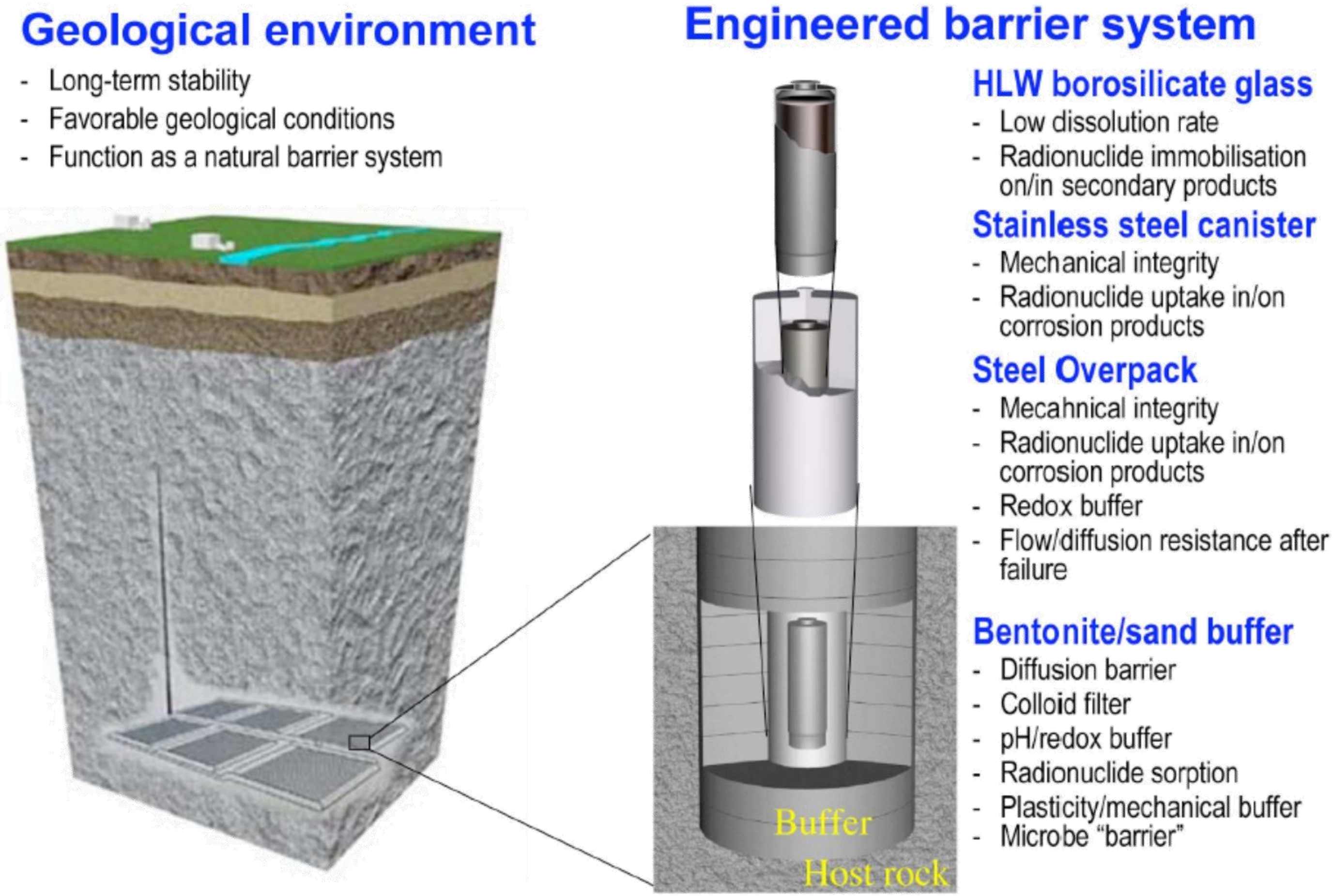

Geological environment
- Long-term stability
- Favorable geological conditions
- Function as a natural barrier system

Engineered barrier system

HLW borosilicate glass
- Low dissolution rate
- Radionuclide immobilisation on/in secondary products

Stainless steel canister
- Mechanical integrity
- Radionuclide uptake in/on corrosion products

Steel Overpack
- Mecahnical integrity
- Radionuclide uptake in/on corrosion products
- Redox buffer
- Flow/diffusion resistance after failure

Bentonite/sand buffer
- Diffusion barrier
- Colloid filter
- pH/redox buffer
- Radionuclide sorption
- Plasticity/mechanical buffer
- Microbe "barrier"

JNC 2006, *H17 Report*

Glass as One of the Many Barriers in a Disposal System

- A continuum of reliance on glass performance
  - Hanford LAW → glass performance is primary barrier
  - Belgium super-container → glass is minor barrier

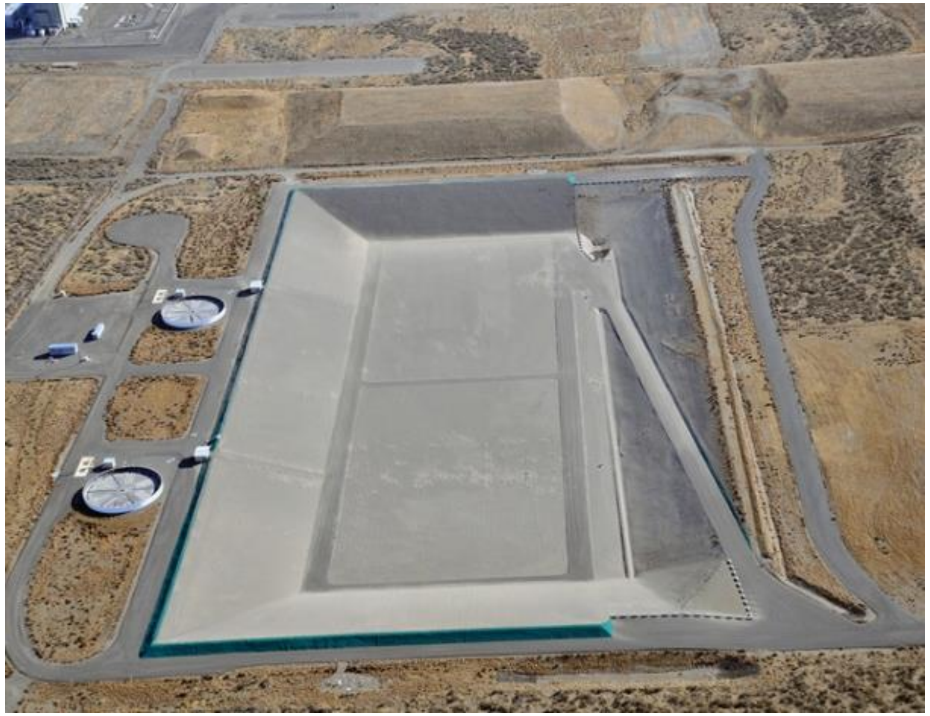

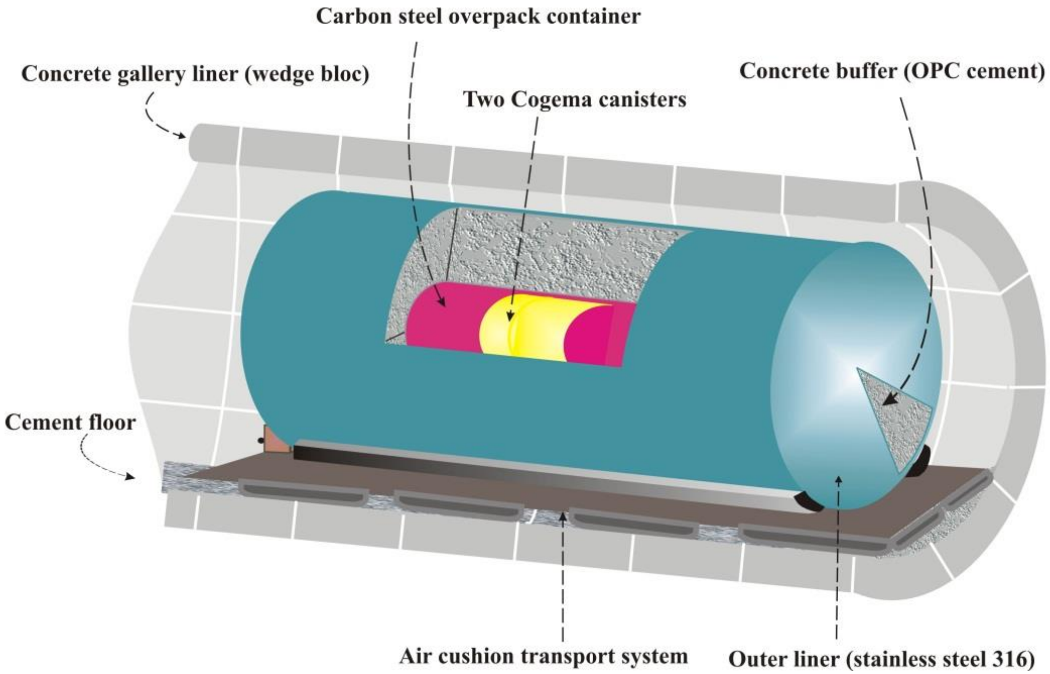

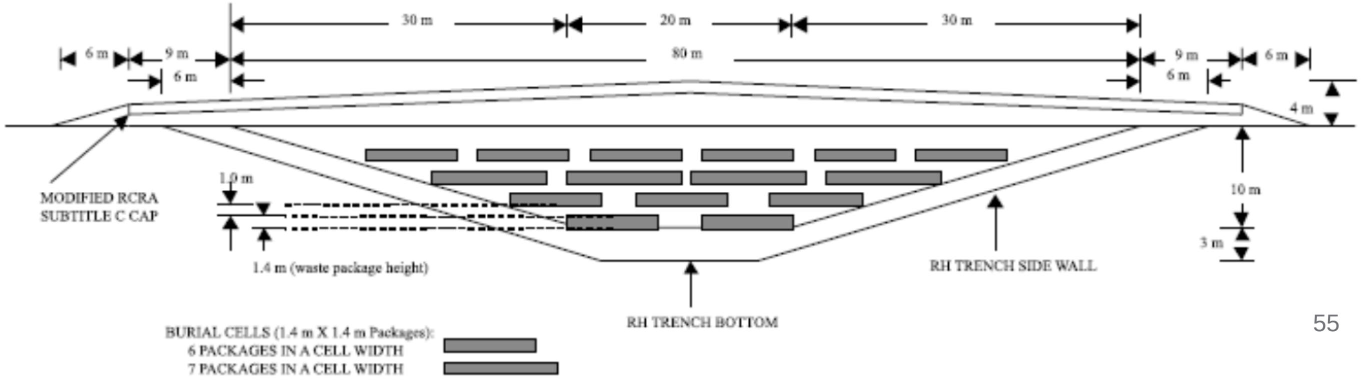

Surface Area

$$J_{RN} \propto M_{\text{algered glass}} = \iint r(t,s)dsdt$$

- Flux is proportional to reactive surface area of glass
- Glass cracking due to rapid cooling increases surface area (4 to 50× S_{geom})
- Not all cracks are accessible to corrosion

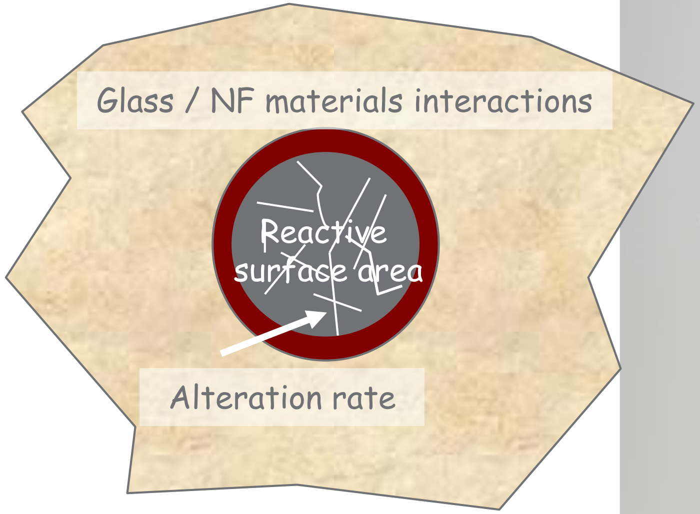

Glass / NF materials interactions

Reactive surface area

Alteration rate

ASTM Standard C1174
Poinssot and Gin, 2012

Verney Carron et al. 2010

Cross section of an inactive R7T7-type glass block

Example Glass Corrosion Models

General Modeling Approach

- Contaminant transport is modeled using the reaction-advection-dispersion equation:

$$\frac{dC}{dt} = D\frac{d^2C}{dx^2} - v_x\frac{dC}{dx} - \frac{\rho_b}{\theta}\left(\frac{dC_s}{dt}\right)_{\text{sorption}} + \boxed{\sum_{k=1}^{N_s}\left(\frac{dC}{dt}\right)}_{\text{reaction } k}$$

- Solution mass balance equation (SMBE) of species i

$$\frac{dC_i^{\text{sol}}}{dt} = \boxed{\frac{S}{V}J_i^{\text{gls}}\Big|_{x=0}} - \boxed{\frac{F_v}{V}\left(C_i^{\text{sol}} - C_i^{\text{eff}}\right)} - \boxed{\frac{dC_i^{\text{min}}}{dt}}$$

FLUX OUT
OF GLASS

FLOW IN/OUT
OF SOLUTION

MINERAL
FORMATION

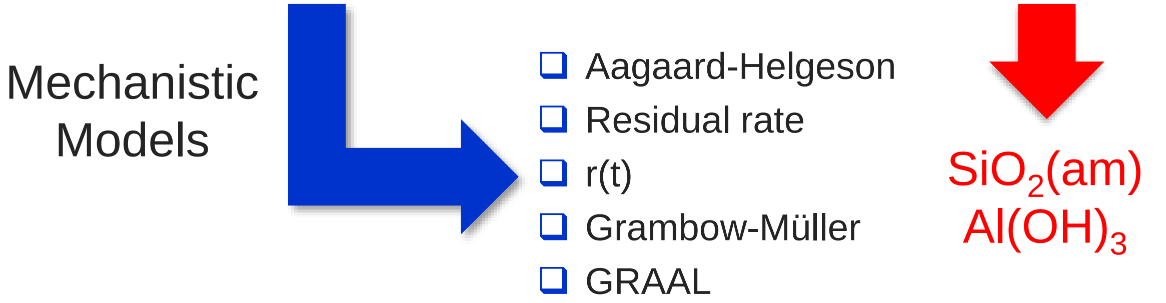

Mechanistic
Models

- ☐ Aagaard-Helgeson
- ☐ Residual rate
- ☐ r(t)
- ☐ Grambow-Müller
- ☐ GRAAL

$SiO_2(am)$
$Al(OH)_3$

C	concentration
D	dispersion coef
v	advective flow
C_s	sorbed concentration
N_s	number of sinks/sources
ρ	density of EBS
Ɵ	porosity of EBS
t	time
S	surface area
V	volume
x	depth in glass
F_v	flow
sol	solution
gls	glass
eff	effluent
min	mineral

Rieke and Kerisit 2015

Predictive Models

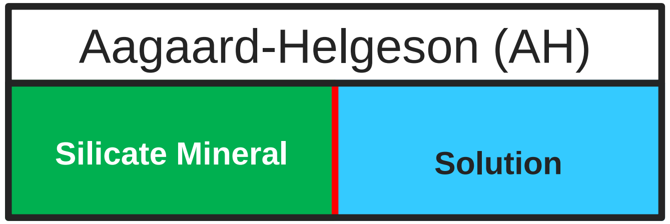
Aagaard-Helgeson (AH)

$$r_{\text{net}} = k \prod_i a_i^{-v_{i,j}} \left(1 - \left(\frac{Q}{K}\right)^{1/\sigma}\right)$$

Aagaard and Helgeson 1982
Grambow 1987

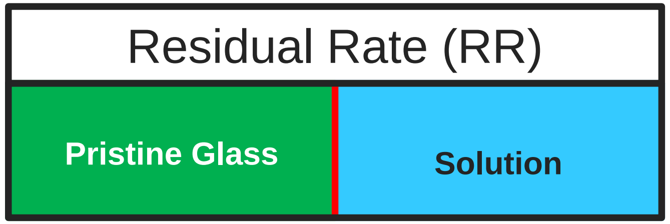
Residual Rate (RR)

$$r_{\text{net}} = k \exp\left(-\frac{E_a}{RT}\right) a_{\text{H}^+}^{-\eta} \left[1 - \left(\frac{Q}{K}\right)^{1/\sigma}\right] + r_{\text{res}}$$

Pierce et al. 2004

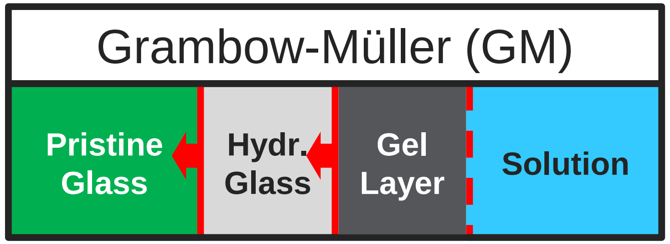
Grambow-Müller (GM)

$$\frac{dC}{dt} = D_{\text{H}_2\text{O}} \frac{d^2C}{dx^2} - r_{matrix}(t) \frac{dC}{dx}$$

Grambow and Muller 2001

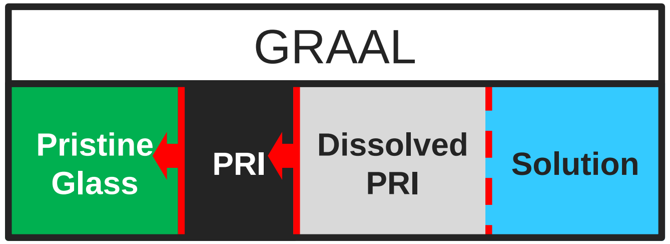
GRAAL

$$\frac{de}{dt} = \frac{r_{\text{hydr}}}{1 + \frac{e(t) r_{\text{hydr}}}{D_{\text{PRI}}}} - \frac{dE}{dt}$$

$$\frac{dE}{dt} = r_{\text{diss}} \left(1 - \frac{C_{\text{Si}}(t)}{C_{\text{sat}}}\right)$$

Frugier et al. 2008

Rieke and Kerisit 2015

Radiation Effects

Radiation Damage to Glass

- Ballistic damage due to alpha recoil is the most significant impact on glass structure and properties

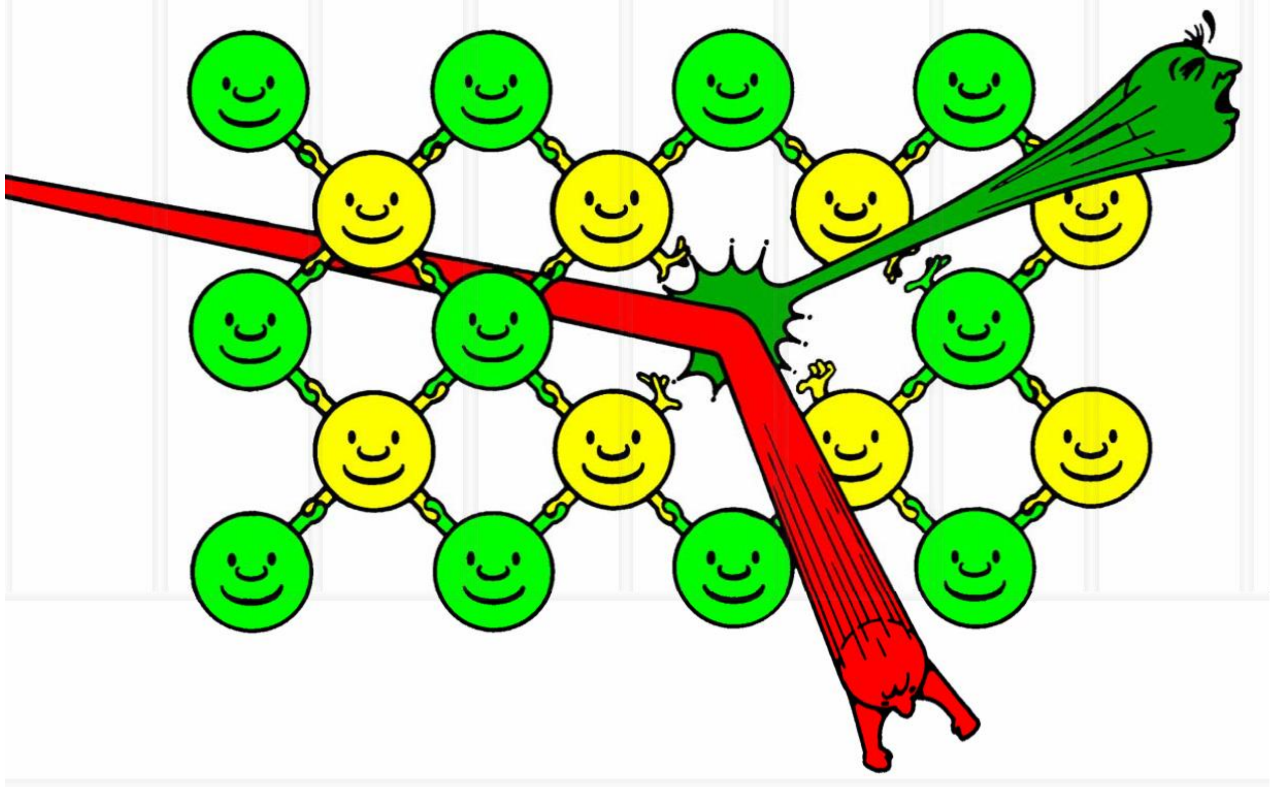

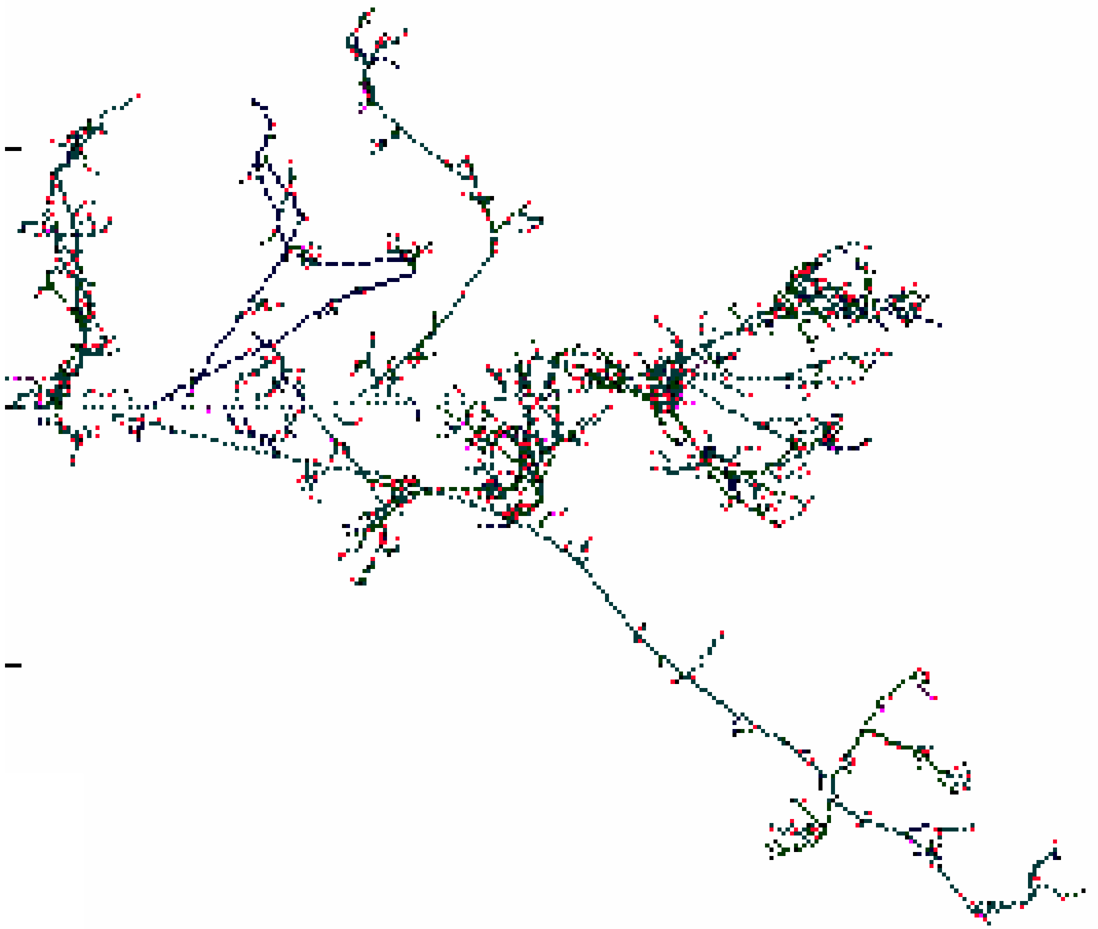

Bill Weber, personal communications

Impact of Alpha Decay

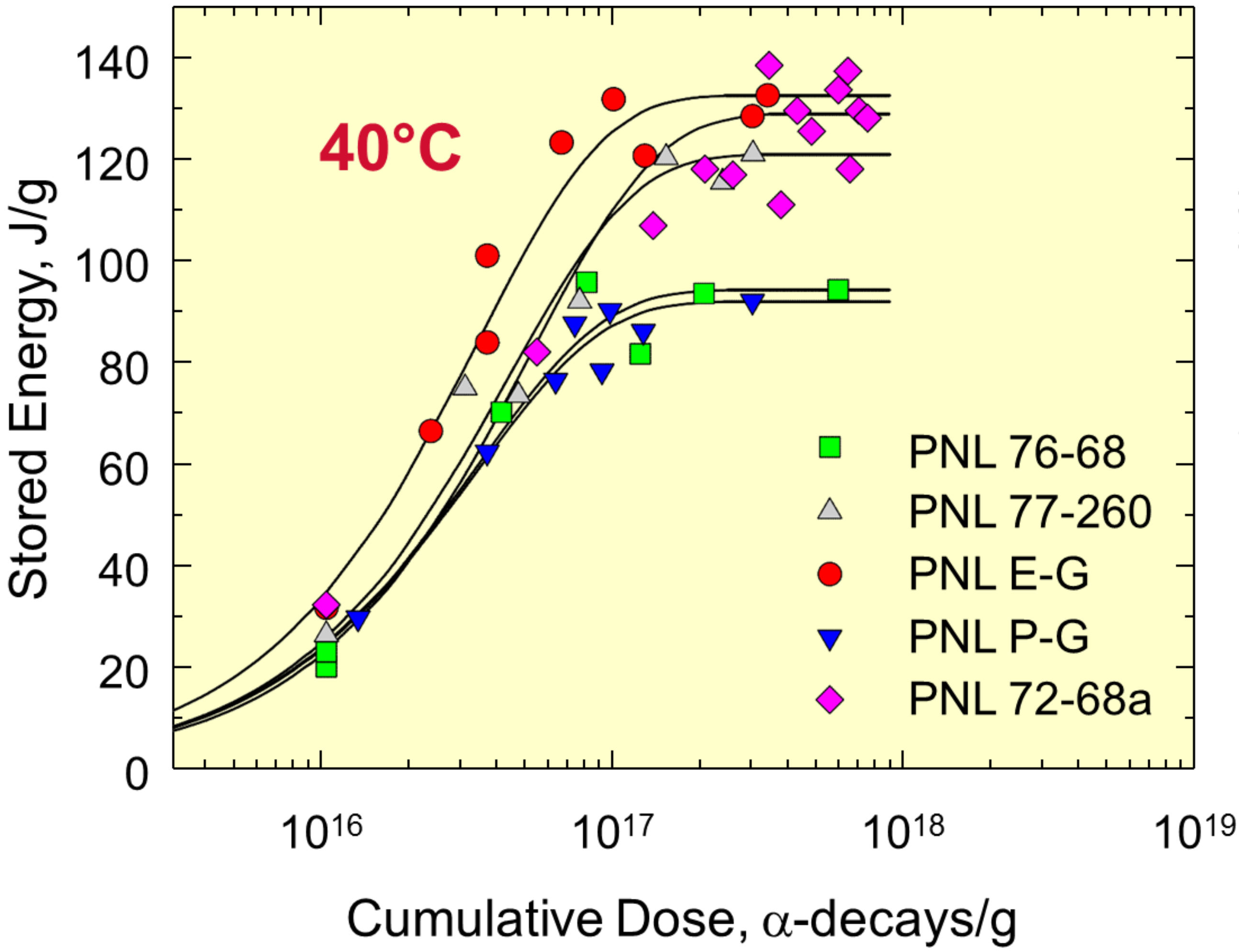

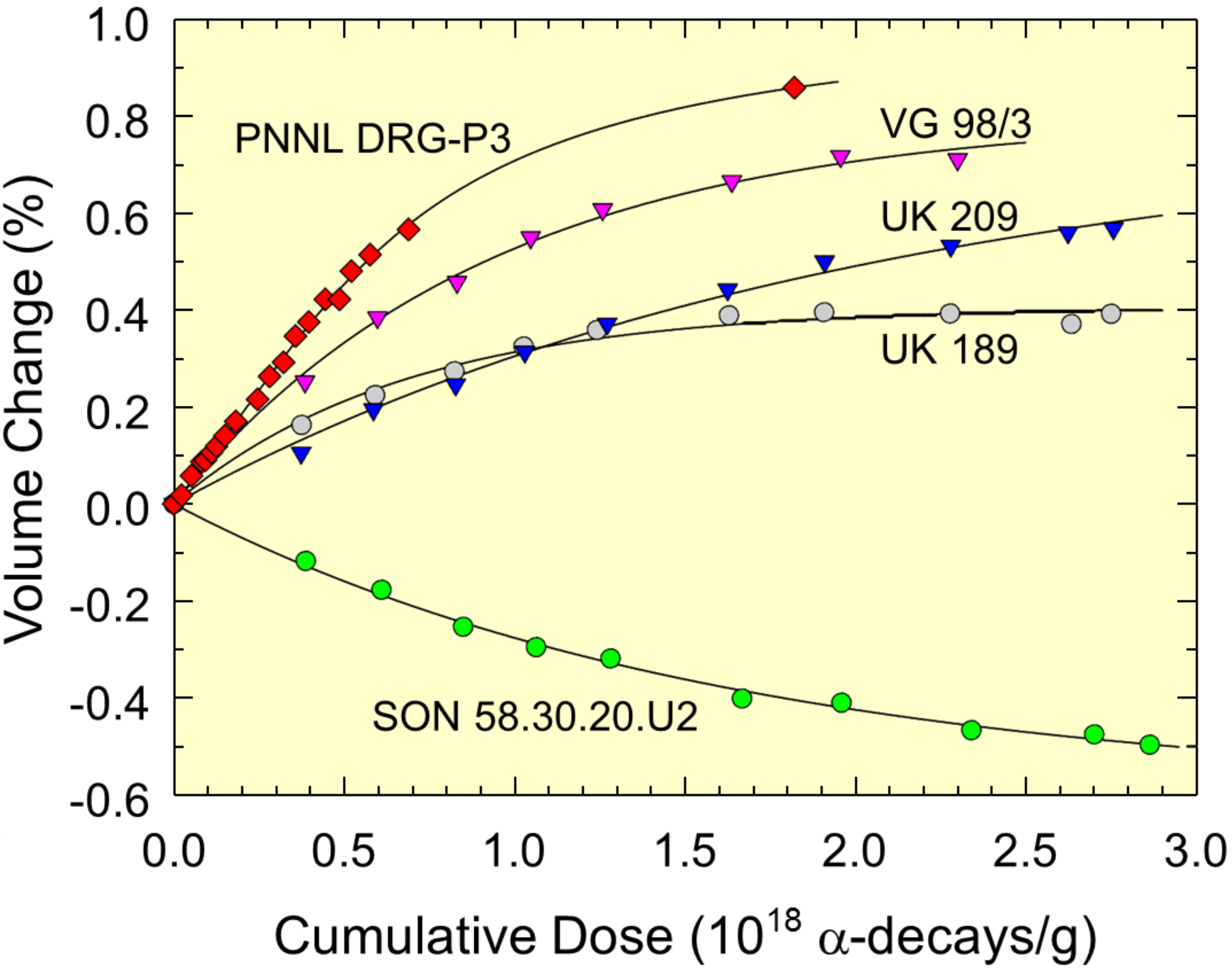

Weber 2014

Impact of Alpha Decay

- Generally alpha decay impacts saturate at ~10^{18} decay/g
- The impacts include stored energy, volume, fictive temp, NBO concentration, etc.
- Relatively small impacts have been measured on glass corrosion rates

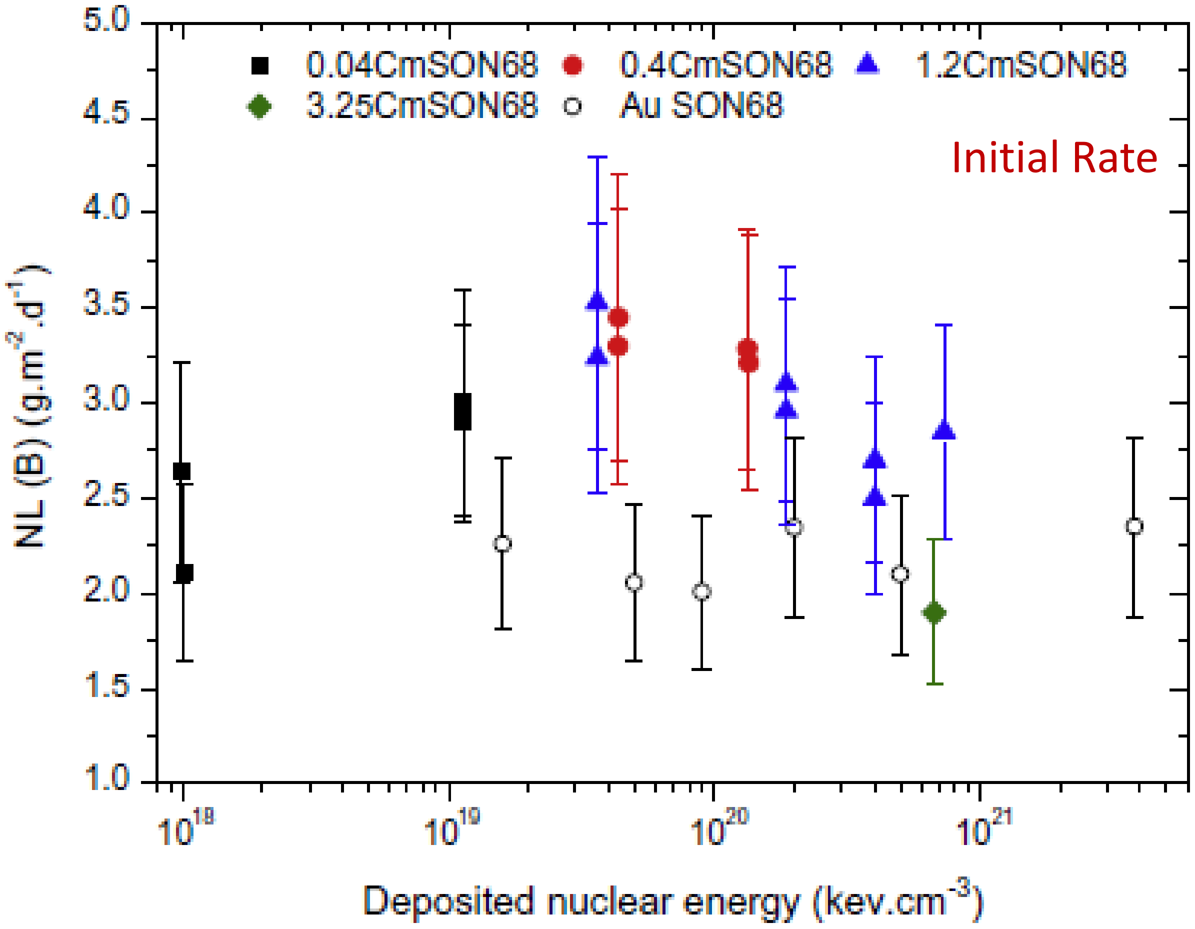

Peuget et al. 2014

Gamma Radiation Effect on Residual Rate

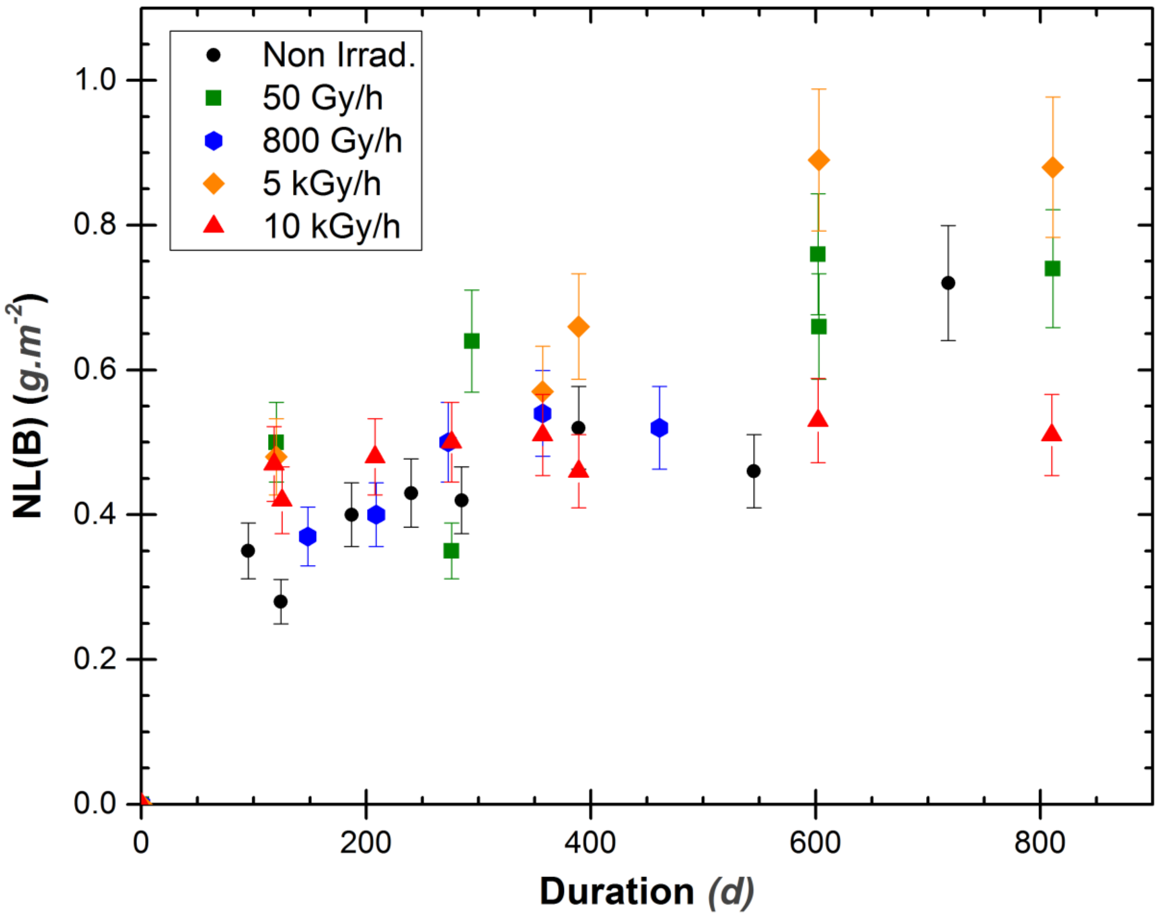

- Generally no effects measured in r_{res} for gamma radiation well in excess of those expected in disposal environments

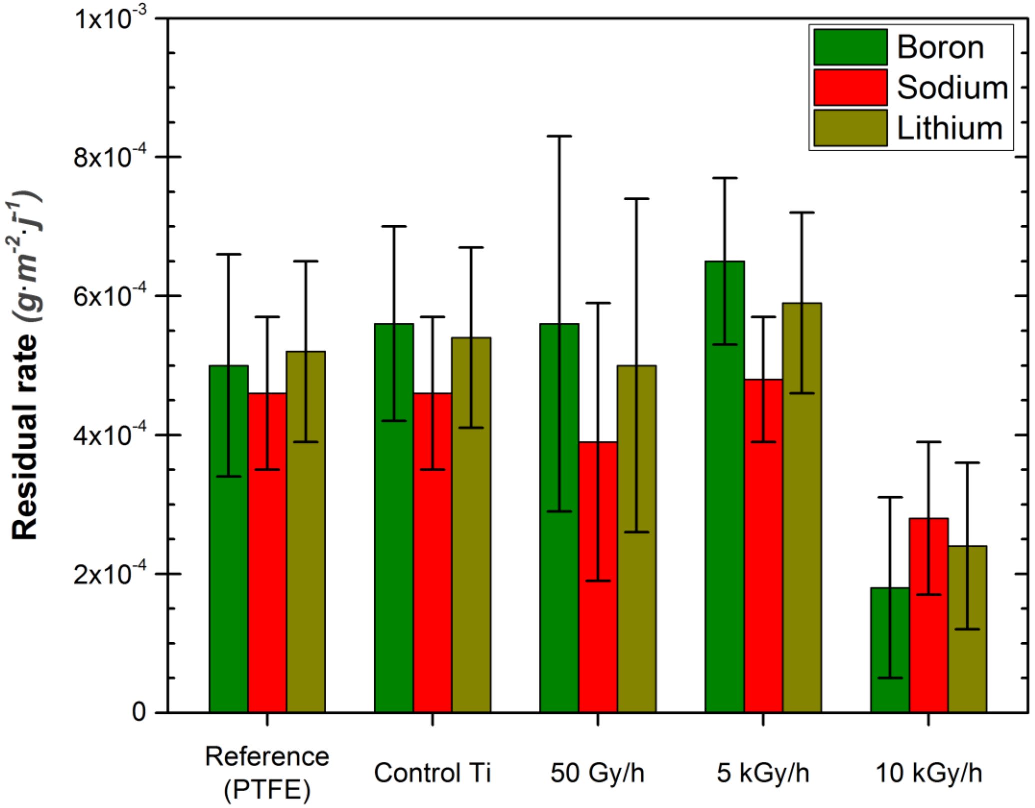

Roland et al. 2013

References Cited

References

Åagaard, P.; Helgeson, H. C., Thermodynamic and kinetic constraints on reaction rates among minerals and aqueous solutions I. Theoretical considerations. American Journal of Science 1982, 282, 237-285.

Abraitis, P. K. et al., “Single-pass flow-through experiments on a simulated waste glass in alkaline media at 40°C. I. Experiments conducted at variable solution flow rate to glass surface area ratio.” Journal of Nuclear Materials 2000, 280 (2), 196-205.

Abraitis, P. K.; et al., ‘Single-pass flow-through experiments on a simulated waste glass in alkaline media at 40 degrees C. II. Experiments conducted with buffer solutions containing controlled quantities of Si and Al.” Journal of Nuclear Materials 2000, 280 (2), 206-215.

Andra. 2005. *Dossier 2005 Argile Tome, Phenomenalogical Evolution of a Geologic Repository*, Agence Nationale pour la Destion des Déchets Radioactifs, Châtenay-Malabry, France.

ASTM. "Standard Practice for Prediction of the Long-Term Behavior of Waste Package Materials Including Waste Forms Used in Geologic Disposal of High-Level Nuclear Waste," ASTM C1174, ASTM International, West Conshohocken, PA.

ASTM. "Standard Test Method for Static Leaching of Monolithic Waste Forms for Disposal of Radioactive Waste," ASTM C1220, ASTM International, West Conshohocken, PA.

ASTM. "Standard Practice for Measurement of the Glass Dissolution Rate Using the Single-Pass Flow-through Test Method," ASTM C1662, ASTM International, West Conshohocken, PA.

ASTM. "Standard Test Methods for Determining Chemical Durability of Nuclear, Hazardous, and Mixed Waste Glasses and Multiphase Glass Ceramics: The Product Consistency Test (PCT)," ASTM C1285, ASTM International, West Conshohocken, PA.

Cailleteau, C., et al. 2008. "Insight into silicate-glass corrosion mechanisms." Nature Materials 7(12): 978-983.

Ferrand, K.; Abdelouas, A.; Grambow, B., “Water Diffusion in the Simulated French Nuclear Waste Glass SON 68 Contacting Silica Rich Solutions: Experimental and Modeling.” *Journal of Nuclear Materials* 2006, 355, 54-67.

Chick, L. A. et al. *The Effects of Composition on Properties in an 11-Component Nuclear Waste Glass System*; PNL-3188; Pacific Northwest Laboratory: Richland, WA, 1981.

Collin, M., et al. 2018. "Can alkalis improve passivation properties of amorphous layers formed on silicate glass?" *npj-Materials Degradation*

Du, J., & Rimsza, J. M. 2017. Atomistic computer simulations of water interactions and dissolution of inorganic glasses. Npj- Mat. Deg, 2017, 1-16.

Fournier, M., et al. 2014. "Resumption of Nuclear Glass Alteration: State of the Art," *Journal of Nuclear Materials*, 448:348-363.

References

Frugier, P. et al. 2005. "The Effect of Composition on the Leaching of Three Nuclear Waste Glasses: R7T7, AVM and VRZ," *Journal of Nuclear Materials*, 346(2-3):194-207

Frugier P., et al. 2008. "SON68 nuclear glass dissolution kinetics: Current state of knowledge and basis of the new GRAAL model." *J. Nucl. Mater*., 380:8-21.

Frugier, P., et al. 2009. "Application of the GRAAL model to leaching experiments with SON68 nuclear glass in initially pure water." Journal of Nuclear Materials 392(3): 552-567.

Gin, S.; Mestre, J. P., "SON 68 nuclear glass alteration kinetics between pH 7 and pH 11.5." *Journal of Nuclear Materials* 2001, 295 (1), 83-96.

Gin, S.; et al., 2013. "An international initiative on long-term behavior of high-level nuclear waste glass." *Materials Today*, 16 (6), 243-248.

Gin S., et al. 2015. "The fate of silicon during glass corrosion under alkaline conditions: A mechanistic and kinetic study with the International Simple Glass." *Geochim. Cosmochim. Acta* 151, 68-85.

Gin, S., et al. 2017. "Atom-Probe Tomography, TEM and ToF-SIMS study of borosilicate glass alteration rim: a multiscale approach to investigating rate-limiting mechanisms." *Geochimica Et Cosmochimica Acta* 202: 57-76.

Gin, S., et al. 2018. "Dynamics of self-reorganization explains passivation of silicate glasses." *Nature Communications* 9: 2169.

Gordon, N., et al.. 2013. "SON68 Glass Alteration Enhanced by Magnetite," Water Rock Interaction [WRI 14], Vol. 7, 300-303 pp. *Procedia, Earth and Planetary Science*, Avignon, France.

Grambow B. (1987) *Nuclear Waste Glass Dissolution: Mechanism, Model, Application*. JSS Technical Report 87-02.

Grambow B. and Müller R. (2001) First-order dissolution rate law and the role of surface layers in glass performance assessment. *J. Nucl. Mater*. 298, 112-124.

Hammond G.E. and Lichtner P.C. (2010) Field-scale model for the natural attenuation of uranium at the Hanford 300 Area using high-performance computing. Water Resour. Res. 46, W09527.

Hrma, P. et al. 1994. *Property/Composition Relationships for Hanford High-Level Waste Glasses Melting at 1150°C*; PNL-10359; Pacific Northwest Laboratory: Richland, WA.

Inagaki, Y., et al. 1998. "Effects of Water Redox Conditions and Presence of Magnetite on Leaching of Pu and Np from HLW Glass," *Scientific Basis for Nuclear Waste Management XXI*, Vol. 506, 177-184 pp. Materials Research Society, Warrendale, PA.

References

Inagaki, Y. et al. 2012. "Initial Dissolution Rate of a Japanese Simulated High-Level Waste Glass P0798 as a Function of pH and Temperature Measured by Using Micro-Channel Flow-through Test Method," *Journal of Nuclear Science and Technology*, 49(4):438-449

Jollivet, P., et al. 2012. "Effect of Clayey Groundwater on the Dissolution Rate of the Simulated Nuclear Waste Glass SON68," *Journal of Nuclear Materials*, 420(1-3):508-518

JNC. 2006. *H17: Development and management of the technical knowledge base for the geological disposal of HLW*; JNC TN1400 2005-022; Japan Nuclear Cycle Development Institute: Tokai-mura, Japan.

Kaspar, T.C. and J.V. Ryan. 2015. *Summary of Experiments and Modeling of the International Simple Glass*, FCRD-MRWFD-2015-000683, Pacific Northwest National Laboratory, Richland, WA.

Knauss, K. G. et al. "Dissolution Kinetics of a Simple Analogue Nuclear Waste Glass as a Function of pH, Time, and Temperature." In *Scientific Basis for Nuclear Waste Management XIII*, Materials Research Society: Boston, MA, 1990; Vol. 176, pp 371-381.

Lenting, C., et al. 2018. "Towards a unifying mechanistic model for silicate glass corrosion." npj Materials Degradation 2(1): 28.

Liu, S.H. et al. 2015. "Transport- and Surface Reaction-Controlled SON68 Glass Dissolution at 30 Degrees C and 70 Degrees C and pH=13.7," *Applied Geochemistry*, 61:302-311

Liu, H., D. Ngo, J. Luo and S. H. Kim. 2018. "Effect of initial surface conditions on aqueous corrosion of International Simple Glass." Langmuir

Michelin, A., et al. 2013. "Effect of Iron Metal and Siderite on the Durability of Simulated Archeological Glassy Material," *Corrosion Science*, 76(0):403-414.

Neeway, J. J. et al. *FY2016 ILAW Glass Corrosion Testing with the Single-Pass Flow-Through Method*; PNNL-26169; Pacific Northwest National Laboratory: Richland, WA, 2017.

Ngo, D., et al. 2018. "Spectroscopic Ellipsometry Study of Thickness and Porosity of the Alteration Layer formed at International Simple Glass (ISG) Surface in Aqueous Corrosion Conditions." npj-Materials Degradation, 2:

Peuget, S., et al. 2014. "Specific Outcomes of the Research on the Radiation Stability of the French Nuclear Glass Towards Alpha Decay Accumulation," *Journal of Nuclear Materials*, 444(1-3):76-91

Piepel, G. F. et al. *IHLW PCT, Spinel* $T_{1\%}$*, Electrical Conductivity, and Viscosity Model Development*: VSL-07R1240-4; ORP-56320; Vitreous State Laboratory, The Catholic University of America: Washington, D.C., 2008.

References

Pierce E.M. et al. (2004) Waste Form Release Data Package for the 2005 Integrated Disposal Facility Performance Assessment. PNNL-14805, Richland, WA, USA.

Poinssot, C. and S. Gin. 2012. "Long-Term Behavior Science: The Cornerstone Approach for Reliably Assessing the Long-Term Performance of Nuclear Waste," Journal of Nuclear Materials, 420(1-3):182-192

Ribet, S. et al. 2004. "Compositional Effects on the Long-Term Durability of Nuclear Waste Glasses: A Statistical Approach," *Scientific Basis for Nuclear Waste Management XXVIII*, Vol. 824, 309-314 pp. Materials Research Society, Warrendale, PA.

Rieke, P.C. and S.N. Kerisit. 2015. Modeling Tool Enhancement, PNNL-25111, Pacific Northwest National Laboratory, Richland, WA.

Rolland, S., et al. 2013. "Influence of Gamma Irradiation Effects on the Residual Alteration Rate of the French SON68 Nuclear Glass," *Journal of Nuclear Materials* 433:382-389.

Steefel C.I. et al. (2015) Reactive transport codes for subsurface environemental simulation. *Comput. Geosci*. 19, 445-478.

Trivelpiece, C.L., et al. 2016. *Accelerated Leach Testing of Glass (Altglass) Version 3.0*, SRNL-STI-2016-00527, Rev. 0, Savannah River National Laboratory, Aiken, SC.

Verney-Carron, A. et al. 2010. "Archaeological Analogs and the Future of Nuclear Waste Glass," *Journal of Nuclear Materials*, 406(3):365-370

Vienna, J. D., et al. 2001. *Hanford Immobilized LAW Product Acceptance Testing: Tanks Focus Area Results*, PNNL-13744, PNNL, Richland, WA

Vienna, J. D. et al. 2013. “Current Understanding and Remaining Challenges in Modeling Long-Term Degradation of Borosilicate Nuclear Waste Glasses.” *International Journal of Applied Glass Science*, 4 (4), 283-294.

Vienna, J.D. 2014. "Compositional Models of Glass/Melt Properties and Their Use for Glass Formulation," *Procedia Materials Science*, 7(0):148-155.

Vienna, J. D., et al. 2018. "Impacts of Glass Composition, pH, and Temperature on Glass Forward Dissolution Rate." npj, Materials Degradation 2(22): 1-12.

Weber, W.J. 2014. "Radiation and Thermal Ageing of Nuclear Waste Glass," *Procedia Materials Science*, 7:237 - 246.

Xiang, Y., et al. 2013. "Structure and properties of sodium aluminosilicate glasses from molecular dynamics simulations." *Journal of Chemical Physics,* 139(4).